Novel roles of Celf1 and Tia1 during vegetal RNA localization in *Xenopus laevis* oocytes

Doctoral thesis

Dissertation for the award of the degree
"Doctor rerum naturalium"
in the GGNB program "Genes and Development"
at the Georg August University of Göttingen
Faculty of Biology

submitted by

Diana Bauermeister

born in Uslar, Germany

Göttingen, December 2014

Thesis committee members

Prof. Dr. Tomas Pieler (supervisor & reviewer)
Developmental Biochemistry, Georg August University of Göttingen

Prof. Dr. Ernst A. Wimmer (reviewer)
Developmental Biology, Georg August University of Göttingen

Prof. Dr. Matthias Dobbelstein
Molecular Oncology, Georg August University of Göttingen

Members of the extended examination board

Prof. Dr. Ralf Ficner
Molecular Structural Biology, Georg August University of Göttingen

Prof. Dr. Ralph Kehlenbach
Molecular Biology, Georg August University of Göttingen

PD Dr. Halyna Shcherbata
Gene expression and signaling, MPI for Biophysical Chemistry, of Göttingen

Date of thesis submission: December 10, 2014
Date of oral examination: January 22, 2015

Affidavit

Herewith I declare, that I prepared the Doctoral thesis
“Novel roles of Celf1 and Tia1 during vegetal RNA localization in *Xenopus laevis* oocytes”
on my own and with no other sources and aids than quoted.

Date of submission:
December 10, 2014

_____

Diana Bauermeister

Table of contents

Acknowledgments

I would like to express my appreciation and thanks to Professor Tomas Pieler for his persistent guidance, advice and constructive feedback throughout my PhD studies. His mentoring and departmental organization provided an ideal atmosphere for progressive learning and scientific development.

I sincerely thank Dr. Maike Claußen for the provision of my thesis project and for her permanent addressability. Her competent advice was invaluable for the enjoyment of my work and the success of my study.

I thank my thesis committee members Professor Ernst Wimmer and Professor Matthias Dobbelstein for their continuous interest in my work, useful comments and reasonable suggestions.

Special thanks go to Marion Dornwell for her excellent technical assistance, to Andreas Nolte for his help in all cases of technical problems, to Eva Hesse for her efficient support in *Xenopus* handling and to Manuela Manafas for her commitment to all administrative issues.

Sincere thanks are also given to Dr. Roland Dosch, Gudrun Kracht, Stephan Riemer and Kanagaraj Palsamy for their helpful comments and support regarding zebrafish treatment.

I also thank all members of the Transport Group and of my lab. Juliane Wellner, Dr. Aliaksandr Dzemetsei, Anita Smarandache, Dr. Susanne Koch, Maja Gere, Dr. Juliane Melchert, Patrick Bernd, Katja Ditter and Sven Richts were always addressable in various issues and contributed significantly to the enjoyment of my work.

For steady support and encouragement, I am indebted to my husband Jan and to my family.

Abbreviations

°C	degree centigrade
%	percent
µg	microgram
µl	microliter
µM	micromolar
µm	micrometer
aa	amino acid
A	adenine
AP	alkaline phosphatase
as	anti sense
BCIP	1-bromo-3-chloropropane
bp	base pairs
BSA	bovine serum albumin
C	cytosine
C-terminus	carboxy-terminus
C_T	cycle threshold
cDNA	complementary DNA
D	phenylalanine
DIG	digoxigenin
Celf1	CUG and ELAV-like family member 1
del	deletion
DNA	deoxyribonucleic acid
DNase	desoxyribonuclease
dnd1	dead end1
dNTP	deoxynucleoside triphosphate
DTT	dithiothreitol
E. coli	*Escherichia coli*
e.g.	exempli gratia
EDTA	ethylene diamine tetraacetic acid
EMSA	electrophoretic mobility shift assay
et al.	*et alii*
Flu	fluorescein
G	guanine
GFP	green fluorescent protein
GST	glutatione S-transferase
h	hours
hCG	human chorionic gonadotropin
his	histidine
K_D	dissociation constant

kDa	kilodalton
LB	Luria-Bertani
LE	localization element
M	molar
MAB	maleic acid buffer
MBS	modified Barth solution
min	minute(s)
ml	milliliter
mM	millimolar
miR	micro RNA
MOPS	3-(N-morpholino)propanesulfonic acid
mRNA	messenger RNA
mut	mutant
MZT	maternal to zygotic transition
N-terminus	amino-terminus
NBT	nitro-blue tetrazolium
od	oligomerization domain
ORF	open reading frame
PAGE	polyacrylamid gel electrophoresis
PBS	phosphate buffered saline
PCR	polymerase chain reaction
PGC	primordial germ cell
pH	power of hydrogen
qRT-PCR	quantitative real-time PCR
RBP	RNA binding protein
RNA	ribonucleic acid
RNP	ribonucleoprotein
rNTP	ribonucleoside triphosphate
rpm	revolutions per minute
RRM	RNA recognition motif
RT	reverse transcriptase
S	serine
sec	second(s)
SDS	sodium dodecyl sulfate
SSC	standard saline citrate
T	thymine/threonine
T7E1	T7 endonuclease I
Taq	*Thermus aquaticus*
Tia1	T-cell internal antigen 1
Tris	tris(hydroxymethyl)aminomethane
U	uracil

UTR	untranslated region
WMISH	whole mount *in situ* hybridization
wt	wild-type
Y	tyrosine

Abstract

The localization of certain mRNAs to the vegetal cortex of *Xenopus* oocytes is of crucial importance for germ cell development and germ layer formation of the future embryo. Vegetal RNA localization is mediated by signal sequences within the RNA. These so-called localization elements recruit certain proteins that direct transport to the vegetal cortex. Although numerous localization ribonucleoprotein (RNP) components have been identified, their full composition is yet unknown. The *Xenopus* RNA binding proteins Celf1 (CUGBP, Elav-like family) and Tia1 (T-cell internal antigen 1) are novel components of vegetal localization RNPs that we identified in an RNA affinity purification approach, using the *dead end 1* (*dnd1*) RNA localization element.

Both Celf1 and Tia1 are detected as parts of an RNP complex together with other known vegetal localization proteins and show specific interactions with localization elements from several vegetally localizing RNAs. Immunostaining experiments reveal co-localization of Celf1 and Tia1 with vegetally localizing RNA and with known localization factors. Inhibition of Celf1 protein binding by localization element mutagenesis as well as Celf1 overexpression interfere with vegetal RNA localization, suggesting an active role for Celf1 during vegetal RNA transport in *Xenopus* oocytes. Ectopic expression of Celf1 and Tia1 in *Xenopus* embryos counteracts somatic degradation of *dnd1* localization element reporter RNAs. Furthermore, Tia1 protects several other localizing and germ cell specific mRNAs from somatic degradation and synergizes with the germ cell specific protein Dnd1. These results suggest that Celf1 and Tia1 are components of vegetal localization RNPs in oocytes that could have additional functions in the protection of germ cell specific RNAs in early embryos. Furthermore, Celf1 is enriched at the vegetal cortex in zebrafish oocytes and thus may play a conserved role in vegetal RNP complexes of fish and frogs. Celf1 loss of function approaches in zebrafish result in the primary development of males, indicating a role of Celf1 during zebrafish sex determination or female viability.

Our results reveal *Xenopus* Celf1 and Tia1 as novel components of vegetal localization complexes. While Celf1 actively participates in vegetal RNA localization in oocytes, both Celf1 and Tia1 seem to act in germ cell specific RNA protection in embryos. These findings support the idea that both mechanisms share the same proteins and they highlight the functional link between RNA localization and germ cell formation.

1. Introduction

1.1. RNA localization is a conserved mechanism with primary importance for different biological processes

A key feature of eukaryotic cells is their organization into compartments with different molecular compositions. These intracellular asymmetries are essential to determine cell polarity and are required for cell fate specification, embryonic patterning or specialized cell functions. Cell asymmetries can be established by selective localization of proteins to distinct cell regions based on signals in their peptide sequence. Another strategy to localize proteins is to spatially restrict their synthesis by localizing their encoding mRNAs. This mechanism known as mRNA localization is documented in a wide range of organisms including bacteria, fungi, plants and various animals (Okita and Choi, 2002; Blower et al., 2007; Mili et al., 2008; Martin and Ephrussi, 2009; Zarnack and Feldbrügge, 2010; Nevo-Dinur et al., 2012). Many proteins involved in RNA localization are conserved in different animal species, suggesting an evolutionary ancient mechanism that has been adapted in various contexts. Indeed, localized RNAs are important for many aspects of eukaryotic life, including cell motility (Lawrence and Singer, 1986), synaptic plasticity (Kang and Schuman, 1996), cell fate determination (Long et al., 1997; Jedrusik et al., 2008) and embryonic development (Berleth et al., 1988; Tannahill and Melton, 1989; Figure 1.1).

Extensive improvements of RNA detection methods have led to the identification of an increasing number of localized transcripts (Poon et al., 2006; Cuykendall and Houston, 2010; Sharp et al., 2011). In particular, a genome-wide analysis of mRNA distributions in *Drosophila* embryos revealed about 70 % of the expressed transcripts to be subcellularly localized (Lécuyer et al., 2007). This observation strikingly emphasizes the relevance of mRNA localization as mechanism for post-transcriptional gene regulation and highlights the importance of this process in animal development.

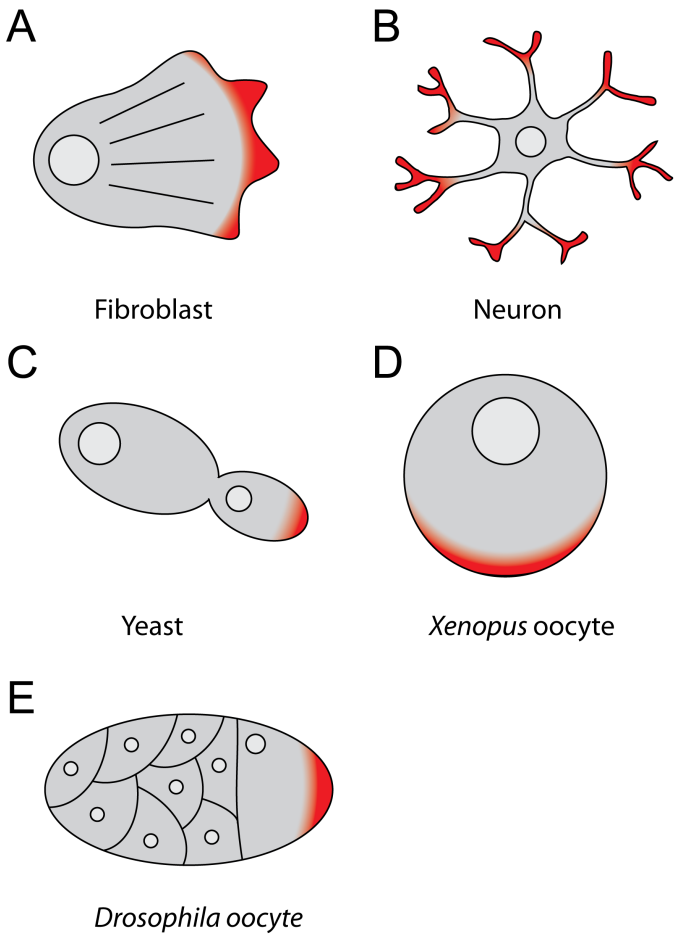

Figure 1.1. Examples of RNA localization in different biological systems. A) *ß-actin* mRNA localizes to the leading edge of chicken fibroblasts and local translation leads to high concentrations of Actin, which is required for cell motility. B) Localization of mRNA encoding the α subunit of calcium/calmodulin Kinase II (α-CaMKII) to dendrites of mouse neurons mediates modulation of synaptic plasticity. C) *ASH1* mRNA localizes to the tip of the daughter cell in budding yeast, where ASH1 protein suppresses mating type switching. D) *gdf1* mRNA localizes to the vegetal cortex of *Xenopus* oocytes and Gdf1 protein participates in early embryonic patterning. E) *oskar* mRNA localizes to the posterior pole in *Drosophila* oocytes, where Oskar protein acts in germ plasm assembly. Image adapted from Bauermeister et al. (2014).

1.1.1. Localizing RNAs define cell compartments with specialized functions

In differentiated cells, RNAs that are localized within subcellular compartments encode proteins with specialized functions. In fibroblasts, ß-actin mRNA localizes to the leading edges, where its encoded protein mediates cell motility (Katz et al., 2012; Figure 1.1). Localization of the mRNA encoding myelin basic protein directs the local formation of myelin in the distal parts of oligodendrocytes (Ainger et al., 1993; Smith, 2004). Similarly, the local translation of mRNAs that are localized to synapses act in synaptic plasticity in the mature brain (Kang and Schuman, 1996; Martin and Zukin, 2006; Figure 1.1).

1.1.2. Localizing RNAs act in cell fate determination during differentiation and embryonic development

The yeast *ASH1* mRNA is an example for a localizing RNA in yeast that acts in cell fate determination. *ASH1* mRNA localizes to the daughter cell during yeast budding and localized translation of ASH1 protein inhibits mating type switching (Long et al., 1997). In several invertebrate (e.g., ascidians, insects, echinoderms) and vertebrate species (e.g., anuran amphibians, teleost fish) the asymmetric distribution of certain RNAs during oogenesis is essential for the formation of the primary body axis and the development of the germline in embryos (reviewed in Bashirullah et al., 1998). In *Drosophila*, a number of mRNAs localize to different regions of the oocyte and direct embryonic development (reviewed in St Johnston and Nüsslein-Volhard, 1992; Lasko, 1999; Figure 1.1). Well studied examples include *bicoid* and *nanos* mRNAs, which localize to the anterior and posterior pole of *Drosophila* oocytes, respectively. After fertilization, Bicoid protein is involved in formation of anterior structures, while Nanos promotes formation of the posterior body segment and the germline (Berleth et al., 1988; Wang and Lehmann, 1991). Similarly, *oskar* mRNA localizes to the posterior pole of *Drosophila* oocytes and embryos (Kim-Ha et al., 1991) and Oskar protein plays a pivotal role in the formation of posterior structures (Ephrussi et al., 1991; Vanzo and Ephrussi, 2002). In *Xenopus* oocytes, several mRNAs localize either to the animal or to the vegetal pole and are asymmetrically inherited by subsets of cells during early cleavage stages (reviewed in King et al., 2005). For instance, *dazl* mRNA is localized to a narrow region at the vegetal cortex of oocytes together with other germ cell determinants that are referred to as the germ plasm. After cell cleavage, germ plasm mRNAs are restricted to a few cells and expression of Dazl protein supports the specification of germ cells (Houston and King, 2000; Figure 1.2). In contrast, *gdf1* mRNA is localized to a broad region at the vegetal pole and is inherited by the vegetal blastomeres during cleavage, where the encoded TGFß signaling molecule directs mesoderm and endoderm specification during early development (Weeks and Melton, 1987; Figure 1.2).

Recent studies revealed some localized RNAs to function already in oocytes rather than in embryos. Depletion of the vegetally localized RNAs *acsl1b* and *rbpms*2 (*hermes*) in *Xenopus* oocytes leads to abnormal acceleration of oocyte maturation (Zearfoss et al., 2004; Wang et al., 2012), suggesting functions of their protein products in regulation of oocyte G2 arrest.

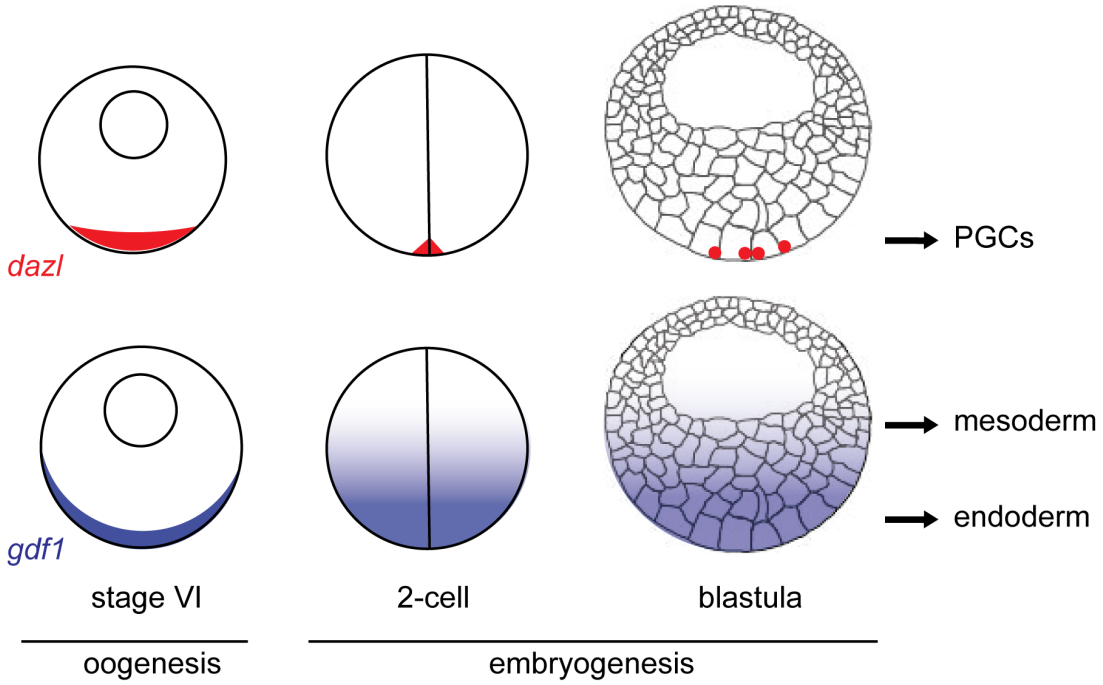

Figure 1.2. Vegetally localized RNAs in *Xenopus* oocytes function differentially in embryonic development. *dazl* mRNA (red) is restricted to the vegetal pole in oocytes and localized in the germ plasm after cleavage, where Dazl protein acts in PGC development. *gdf1* mRNA (blue) is localized to the entire vegetal cortex in oocytes and distributed in the vegetal cytoplasm after cleavage. Inheritance of *gdf1* mRNA by the vegetal blastomeres leads to restricted Gdf1 protein expression and specification of endo- and mesoderm.

1.2. RNA localization can be achieved by different mechanisms

Three distinct mechanisms are known to account for asymmetric distribution of mRNAs: selective RNA stabilization, diffusion-coupled entrapment and active transport (Figure 1.3). Selective RNA stabilization is based on general degradation but local protection of RNAs (Figure 1.3A). For instance, maternal *Hsp83* mRNA is first homogeneously distributed in early *Drosophila* embryos, but then it becomes specifically localized to the posterior pole. This localization is based on the general degradation of *Hsp83* transcripts in the embryo, whereas pole plasm components protect it from degradation at the posterior pole (Ding et al., 1993).

RNA localization can also be achieved by entrapment of diffusing RNA molecules at specific sites in the cell (Figure 1.3B), as it has been shown for several RNAs (Kloc et al., 1996; Zhou and King, 1996; Forrest and Gavis, 2003; Chang et al., 2004). *Drosophila nanos* mRNA is entrapped and anchored in an Actin-dependent manner at the posterior pole of *Drosophila* oocytes (Forrest and Gavis, 2003). Similarly, *nanos1* mRNA is entrapped in the Balbiani body

of early *Xenopus* oocytes. Life confocal imaging and photobleaching experiments showed that injected *nanos1* mRNA is freely diffusing in the cytoplasm of early oocytes and then becomes progressively immobilized in the Balbiani body (Chang et al., 2004). However, localization of *nanos1* to the Balbiani body seems to require energy and motor proteins and thus, might be at least partially mediated by active transport (Heinrich and Deshler, 2009). Certainly, the different localization mechanisms are not mutually exclusive and their combination is likely.

The third and most intensely studied mechanism for RNA localization is the active transport by motor proteins along cytoskeletal elements (Figure 1.3C). Examples are described in a wide range of cell types (Gagnon and Mowry, 2011b). The best studied actively transported mRNA is the yeast *ASH1*, which is localized by Myosin motor proteins along Actin filaments from the mother cell to the distal tip of the daughter cell, where ASH1 protein suppresses mating type switching (Long et al., 1997). Another example is the microtubule-dependent localization of *oskar* mRNA to the posterior pole of *Drosophila* oocytes, where restricted expression of Oskar protein is required for anterior-posterior polarity in the embryo (Ephrussi et al., 1991; Kim-Ha et al., 1991; Ephrussi and Lehmann, 1992). A well-studied model for active RNA localization are *Xenopus* oocytes, where motor proteins actively localize several RNAs along microtubules to the vegetal cortex during mid-oogenesis.

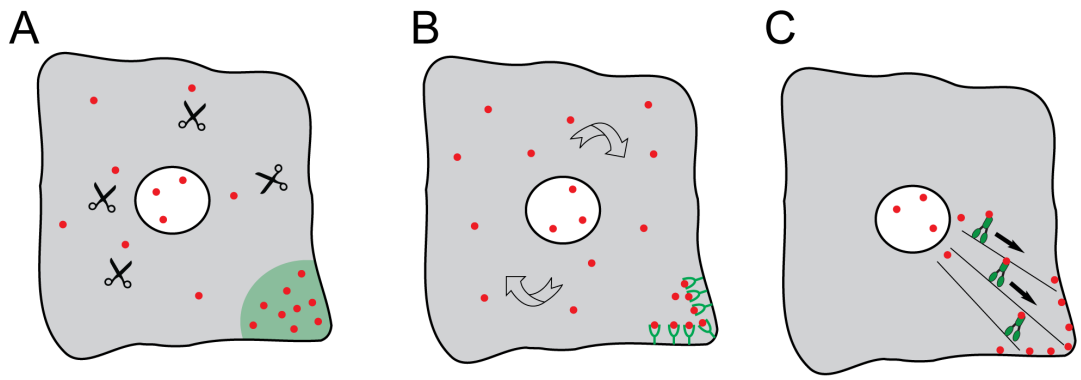

Figure 1.3. RNA localization is achieved by three different mechanisms. A) RNAs are localized by general degradation, but protection at distinct cell regions. B) RNA localization can be achieved by cytoplasmic diffusion and local entrapment by anchors. C) RNAs can be localized to distinct cell regions by active transport via motor proteins along cytoskeletal elements.

1.3. *Xenopus* oocytes as model system to study RNA localization

The oocytes of the African clawed frog *Xenopus laevis* have emerged as an important model system to study RNA localization for several reasons. The oocytes are produced in high numbers during adult frog life and are large cells of about 1 mm in diameter, facilitating micro-injection experiments. The nuclei of oocytes make up a large proportion of the whole cell volume, which allows for their manual isolation at any stage of oogenesis. The animal and vegetal poles are easy to distinguish due to a sharp transition in pigmentation at the animal/vegetal axis. Moreover, oocytes obtained from albino frogs allow for pigment-free visualization of expression patterns using whole mount *in situ* hybridization (WMISH). Finally, the possibility to generate large amounts of cell-free oocyte extracts enables biochemical purification of molecules and intermolecular interaction studies.

1.4. *Xenopus* oogenesis and the establishment of polarity

Xenopus laevis oocytes derive from a female primordial germ cell (PGC), which first undergoes mitotic divisions and forms the oogonia. Four more mitotic divisions produce 16 pear-shaped cells which are still connected by intercellular bridges. These sites of conjunction are assumed to give the first polarity cues (Hausen and Riebesell, 1991). The 16 cells synchronously enter prophase of the first meiotic division and start to aggregate mitochondria around the nucleus, which then accumulate to a mass flanking the nucleus at the vegetal side (Heasman et al., 1984; Kloc et al., 2004). This structure (called Balbiani body or mitochondrial cloud) also accumulates Golgi, endoplasmatic reticulum and germ plasm components and is the first obvious sign of oocyte polarity. In late pachytene stage, the oocytes become separated and surrounded by follicular cells before they asynchronously enter the diplotene stage. During a prolonged growth phase of 6-8 months, the oocytes increases 10,000 fold in size and accumulate all materials for later use in embryogenesis (Nieuwkoop and Faber, 1967). Dumont (1972) divided the growth phase into six stages based on morphological characteristics (Figure 1.4). Stage I oocytes are transparent, 50-300 µm in diameter and have a centrally placed germinal vesicle with a vegetally attached Balbiani body. At stage II, the oocytes become opaque due to the uptake of vitellogenin from the blood by pinocytosis (Gilbert, 2000). In stage II oocytes the Balbiani body dissociates into fragments which move towards the vegetal pole within a wedge-shaped area and are anchored at the cortex by stage III. Although it has been shown that the vegetal movement of the Balbiani body fragments is independent of cytoskeletal elements (Kloc and Etkin, 1995), the underlying mechanism is still unknown. At this stage, melanin production leads to a slight

pigmentation of the oocytes. Stage IV oocytes show a sharp contrast between the dark, pigmented animal half and the slightly pigmented vegetal half. During this stage, vitellogenin platelets translocate to the vegetal pole, which causes a shift of the nucleus to the animal hemisphere (Danilchik and Gerhart, 1987). At stage V, the oocytes pigmentation gets darker, and stage VI oocytes are fully grown with a diameter of 1100-1300 µm. The oocytes can remain in this immature state until progesterone release induces maturation to a fertile egg. During the reproductive life of *Xenopus*, oocytes are produced continuously and asynchronously, leading to a contemporaneous presence of all oocyte stages in the ovary.

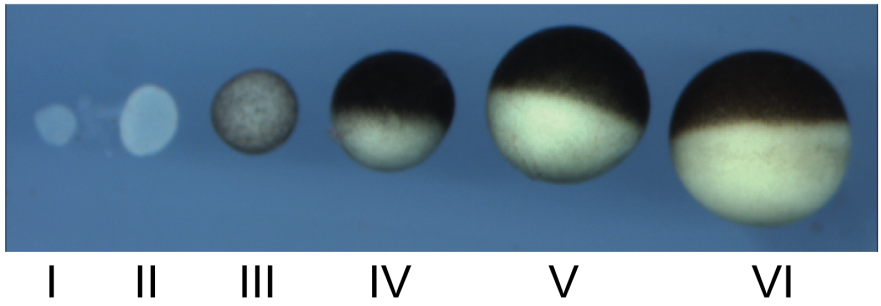

Figure 1.4. The six stages of *Xenopus* oogenesis (after Dumont, 1972). Stage I oocytes are clear and become opaque in stage II. Pigmentation starts at stage III and a contrast in animal and vegetal pigmentation is visible from stage IV onwards. During stages V and VI, oocytes grow in size and develop a sharp pigmentation contrast. Image is modified according to Horvay, (2005).

1.5. RNAs localize via different pathways in *Xenopus* oocytes

During *Xenopus* oogenesis, the localization of RNAs contributes to a high degree of polarization and is required for later development and patterning of the embryo. Different populations of RNAs are targeted to at least two destinations in the oocyte: the animal or the vegetal pole (reviewed in King and Zhou, 1999). Animally localizing RNAs show only little enrichment and are diffusely distributed in the animal hemisphere. However, the mechanism of animal RNA localization is largely unknown.

Temporal expression analysis of vegetally localizing RNAs in *Xenopus* oocytes by *in situ* hybridization revealed different localization pathways, which localize certain RNA subsets in overlapping regions (Forristall et al., 1995; Kloc and Etkin, 1995; Figure 1.5). A subset of RNAs localizes in stage I oocytes to the Balbiani body by diffusion and entrapment. In stage II oocytes, they are co-transported with Balbiani body fragments to the vegetal cortex and anchored in a small disc-like area forming the germ plasm. Many of these "early localizing"

RNAs encode RNA-binding-proteins essential for germ cell development, for example Pgat (formerly known as Xpat) (Hudson and Woodland, 1998), Dazl (Houston and King, 2000) or DeadSouth (Yamaguchi et al., 2012; Figure 1.2). However, although it was reported that Kinesin 2 and the ER are involved in RNA localization to the Balbiani body (Chang et al., 2004; Heinrich and Deshler, 2009), proteins that mediate the entrapment in the Balbiani body by functioning as adapters or anchors are unknown.

The other subset of RNAs is homogeneously distributed in stage I oocytes and accumulates in a wedge-shaped region in the vegetal hemisphere of late stage II oocytes. In stage III-IV oocytes, these RNAs are actively transported in a microtubule and motor protein dependent manner to the vegetal pole and anchored in a broad region of the cortex (Yisraeli et al., 1990). Many of these so-called late localizing RNAs encode germ layer determinants such as Gdf, a TGFß-like signaling molecule involved in early patterning events, or VegT, a T-box transcription factor essential for endoderm formation (Joseph and Melton, 1998; Zhang et al., 1998; Figure 1.2). However, *dnd1* mRNA is an example illustrating that the RNA localization pathway does not determine protein function in embryonic development. Although *dnd1* mRNA is vegetally localized by the late pathway in oocytes, after fertilization it is restricted to germ plasm structures and involved in PGC migration and specification (Horvay et al., 2006).

Other RNAs are not restricted to one pathway and have multiple functions after fertilization, for example *plin2* (formerly known as *fatvg*), *otx1* and *rbpms2* (Chan et al., 1999; Pannese et al., 2000; Zearfoss et al., 2004). These RNAs are enriched in the Balbiani body of early oocytes, but accumulate in the wedge-shaped structure and localize to a broad region at the vegetal cortex of late stage oocytes. It is not known whether these RNAs localize through a third pathway or if they are able to use both the early and the late pathway. Interestingly, early pathway RNAs are also able to localize by the late pathway, if injected into later stage oocytes. This indicates that the localization machinery of the late pathway is able to recognize early localizing RNAs. Indeed, protein compositions of early and late localization complexes overlap (Claussen et al., 2004). Thus, although the biological relevance of this phenomenon is unclear, both pathways appear to share mechanistic features and are to a certain degree linked.

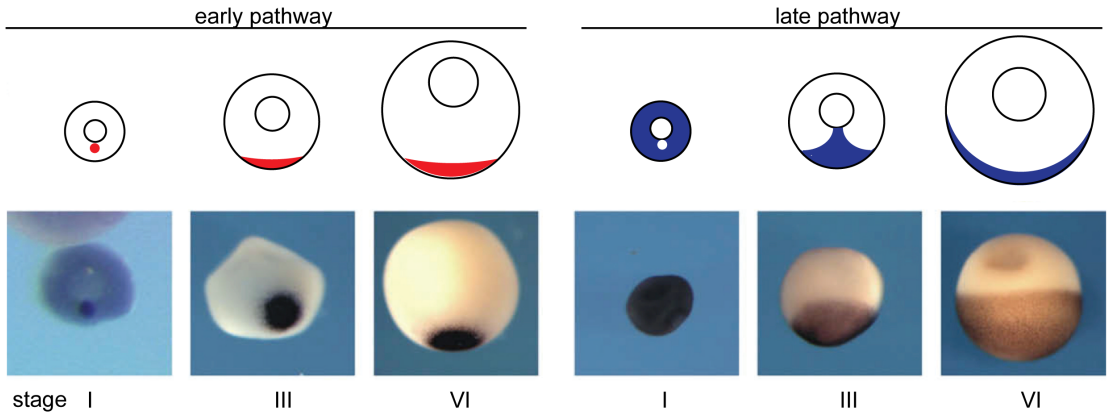

Figure 1.5. Localization to the vegetal cortex of *Xenopus* oocytes is mediated by two main pathways. Schematic presentation of *pgat* and *gdf1* mRNA localization during oogenesis, as revealed by *in situ* hybridization (depicted below). The early localizing *pgat* mRNA (red) accumulates in the Balbiani body of early oocytes and gets restricted to a narrow region at the vegetal cortex until late stages of oogenesis. The late localizing *gdf1* mRNA (blue) is homogeneously distributed in early oocytes, localizes in a wedge-shaped region during mid-oogenesis, and is located at the entire vegetal cortex until stage VI. Image adapted from Claussen and Pieler (2010).

1.6. RNA localization is mediated by *cis*-acting elements

Sorting of RNAs assigned for vegetal localization depends on *cis*-acting signal sequences called zipcodes or localization elements (LE). LEs are required and sufficient for localization and are assumed to provide binding sites for RNA binding proteins which mediate localization (reviewed in King et al., 2005; Jambhekar and DeRisi, 2007; Bauermeister et al., 2014). LEs of vegetally localizing RNAs mapped so far reside mostly in the mRNA 3'UTR and their lengths can vary from few nucleotides to several hundred bases (Mowry and Melton, 1992; Chan et al., 1999). In general, localization elements do not share primary sequence conservation. Hence, the features within the LE that mediate recognition by the localization machinery are unclear. Several localizing RNAs contain multiple or bipartite LEs (Chartrand et al., 1999; Gonzalez et al., 1999; Chao et al., 2010; Ghosh et al., 2012). In *Xenopus*, the LEs of *gdf1* and *vegt* mRNAs contain several clustered short "CAC"-containing sequence elements which are required for localization (Bubunenko et al., 2002; Kwon et al., 2002). The same sequence elements are found in several early and late localizing RNAs (Betley et al., 2002). However, the localizing RNAs *velo1* and *bicc1* lack such motifs (Betley et al., 2002; Claussen and Pieler, 2004), indicating that also other RNA motifs can mediate vegetal RNA localization.

The diversity in LE sequences might also reflect the relevance of RNA secondary structure rather than sequence. Indeed, in *Drosophila*, several LEs were predicted to form stem loops

(Serano and Cohen, 1995; Bullock and Ish-Horowicz, 2001; Bullock et al., 2003; Snee et al., 2005; Van De Bor et al., 2005), and localization of *bicoid* in *Drosophila* oocytes was shown to require a helical stem loop structure (Macdonald and Kerr, 1998). Furthermore, NMR spectroscopy revealed a stem loop with two double-stranded A'-form helices in the *Drosophila fs(1)K10* RNA localization signal, which is required for transport from the nurse cell to the anterior pole of the oocyte (Bullock and Ish-Horowicz, 2001; Bullock et al., 2010). Recently, it was shown that a stem-loop in the *oskar* 3'UTR mediates both the transport from the nurse cell to the developing oocyte and hitchhiking on endogenous RNA to the posterior pole of the oocyte (Jambor et al., 2011, 2014). Furthermore, posterior localization of *oskar* mRNA in *Drosophila* oocytes requires splicing of the first intron, thereby creating a stem-loop structure that serves as spliced *oskar* localization element (Ghosh et al., 2012). In *Xenopus* oocytes, the LE of the vegetally localizing *velo1* mRNA is predicted to form a stem-loop structure (Claussen and Pieler, 2004). While single point mutations disrupting the stem loop reduced the localization efficiency, a recovery of this structure by secondary point mutations could not restore localization (Claussen and Pieler, 2004). It has not been clarified yet whether the primary sequence or the secondary structure of RNA has an influence on RNA localization and both options are not mutually exclusive.

1.7. *Trans*-acting localization factors - generation of specific RNPs

RNA LEs are recognized by specific *trans*-acting protein factors that are thought to mediate the assembly of RNP complexes and direct their localization. One of the best characterized localization RNP mediates localization of *ASH1* mRNA to the tip of the daughter cell in budding yeast. In the nucleus, *ASH1* mRNA associates with She2p (Shen et al., 2010), an unusual RNA-binding protein that forms a symmetric homodimer with a basic helical hairpin as RNA recognition site (Niessing et al., 2004). After nuclear export, the cytoplasmic protein She3p assembles the complex (Böhl et al., 2000). In turn, She3p mediates the interaction with the motor protein Myo4p, which enables active transport along the Actin cytoskeleton. *In vitro* binding studies revealed that She2p binds *ASH1* with rather low specificity and affinity. But, in synergism with She3p, a specific interaction with high affinity is established (Müller et al., 2011). This study led to the first detailed understanding of how a specific localization RNP forms. However, localization RNP formation in higher organisms seems to be more complex, and mechanistic insights are limited.

Most localization factors identified in vertebrates contain classical RNA binding motifs (Figure 1.6). However, single RNA binding motifs can only bind short RNA sequences and thus bind

with high affinity but rather low specificity (Auweter et al., 2006). Localization factors might establish a higher target specificity by a modular arrangement of multiple RNA binding motifs (Lunde et al., 2007; Figure 1.6). Indeed, pentatricopeptide repeat (PPR) containing proteins bind specific nucleotides via a combinatorial arrangement of amino acids (Barkan et al., 2012).

Zipcode binding protein 1 (ZBP1), a factor involved in localization of *ß-actin* mRNA to the leading edges of chicken fibroblasts and neuron growthcones (Lawrence and Singer, 1986; Bassell et al., 1998), contains two RNA recognition motifs (RRM) and four hnRNP K homology (KH) domains. The third and fourth KH domains (KH34) form an anti-parallel pseudodimer (Patel et al., 2012) and, upon binding to the bipartite *ß-actin* zipcode element, they induce an approximate 180° looping of the RNA (Chao et al., 2010). This modulation of RNA structure is proposed to facilitate the assembly of further localization factors and to thus enable complex formation. ZBP1 proteins are structurally and functionally conserved (Yisraeli, 2005). The *Xenopus* homolog Igf2bp3 (formerly called Vg1RBP) is involved in *gdf1* and *vegt* mRNA localization in oocytes (Deshler et al., 1997; Kwon et al., 2002). Similar to ZBP1, all four KH domains of Igf2bp3 mediate RNA-binding (Git and Standart, 2002; Figure 1.6). Interestingly, the third and fourth KH domains were shown to promote self-association of Igf2bp3, suggesting a role in multimerization of RNP complexes (Git and Standart, 2002). However, structural details of Igf2bp3 function in RNA binding, as shown for ZBP1, are unknown.

Staufen was the first identified factor required for RNA localization in *Drosophila* (Schupbach and Wieschaus, 1986). Staufen is involved in localization of *bicoid* and *oskar* mRNAs in oocytes and *prospero* mRNA in neuroblasts (St Johnston et al., 1989; Kim-Ha et al., 1991; St Johnston et al., 1991; Li et al., 1997; Broadus et al., 1998). The identification of Staufen 1 (Stau1) as localization factor for vegetal localization of *gdf1* and *vegt* in *Xenopus* oocytes revealed its functional conservation between vertebrate and invertebrate species (Yoon and Mowry, 2004b). Staufen proteins contain several double stranded RNA binding motifs and bind RNAs with double stranded structure unspecifically *in vitro* (St Johnston et al., 1992; Figure 1.6). However, *in vivo* experiments in *Drosophila* revealed that Staufen specifically associates with *bicoid* RNPs (Ferrandon et al., 1994). Apparently non-specific RNA binding proteins might gain specificity *in vivo* through interactions with proteins that pre-assembled their target RNAs. Indeed, *Drosophila* and *Xenopus* Staufen proteins are recruited to preformed localization RNPs in the cytoplasm (Kress et al., 2004; Mhlanga et al., 2009).

Heterogeneous nuclear ribonucleoproteins (hnRNPs) are implicated in RNA localization in different systems. Several of them are nuclear-cytoplasmic shuttling proteins and implicated in initiating RNA localization in the nucleus or mediating nuclear export (Piñol-Roma and Dreyfuss, 1992; Lee et al., 1996; Hoek et al., 1998). The *Drosophila* hnRNP A1 ortholog Squid is required for localization of *gurken* mRNA in oocytes (Norvell et al., 1999). Mammalian hnRNP A2 mediates localization of *myelin basic protein* mRNA in rat oligodendrocytes (Hoek et al., 1998). In *Xenopus* oocytes, Ptbp1 (also known as VgRBP60) binds to *gdf1* and *vegt* LEs and seems to be essential for their vegetal localization (Cote et al., 1999; Bubunenko et al., 2002). Similarly, *Xenopus* Hnrnpab (formerly called 40LoVe), an RRM-type hnRNP D family protein (Figure 1.6), seems to act in vegetal localization of *gdf1* and *vegt* mRNAs (Czaplinski et al., 2005; Czaplinski and Mattaj, 2006).

Elavl1 and Elavl2 (formerly called ElrA and ElrB), *Xenopus* orthologs of the RRM-type Hu/ELAV proteins (Figure 1.6), bind specifically to a number of LEs including the *dnd1*-LE. Blocking of Elavl-protein binding interferes with vegetal localization in *Xenopus* oocytes. However, certain mRNAs seem to localize independently of Elavl proteins, indicating that localization RNP compositions might differ and depend on the transported RNA (Arthur et al., 2009).

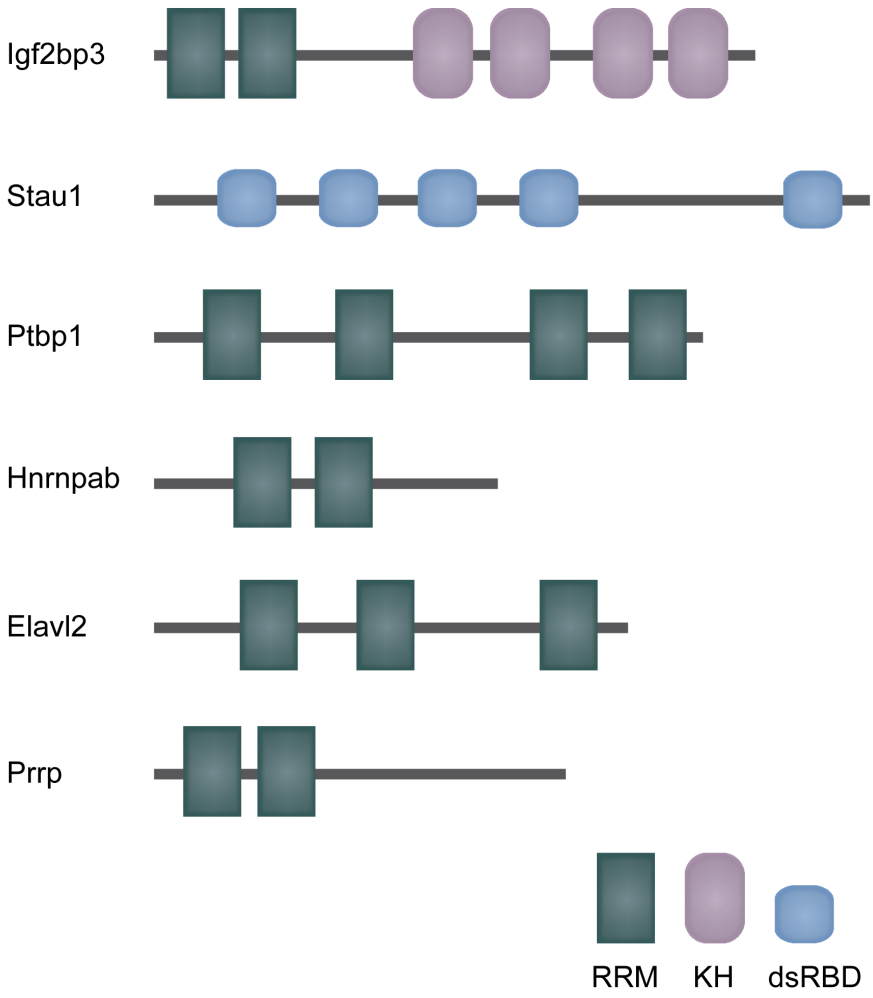

Figure 1.6. Modular arrangement of RNA binding domains of *Xenopus* localization factors. Schematic protein structures of the *Xenopus* localization factors Igf2bp3, Stau1, Ptbp1, Hnrnpab, Elavl2 and Prrp, which contain known RNA binding domains including RNA recognition motifs (RRM), K homology domain (KH) and double-stranded RNA-binding domains (dsRBD). Proteins and domains were drawn to scale as predicted by the ScanProsite domain detection tool (De Castro et al., 2006).

1.8. Motor-dependent RNA localization in *Xenopus* oocytes - a multistep process

Motor-dependent RNA localization involves multiple steps including nuclear recognition and export, cytoplasmic remodeling, coupling to motor proteins and active transport as well as anchoring at sites of destination (Figure 1.7). The molecular mechanisms underlying these different steps of active RNA localization in *Xenopus* oocytes will be introduced in the following.

1.8.1. Nuclear initiation of RNA localization

Several factors that are required for cytoplasmic RNA localization bind their target mRNAs already in the nucleus and are able to shuttle between nucleus and cytoplasm. Thus, these proteins might initially determine the destination of localizing RNAs in the nucleus (reviewed in Farina and Singer, 2002). The finding that Igf2bp3 binds *gdf1* and *vegt* mRNAs in the cytoplasm and nucleus suggests a role for this protein in nuclear initiation of RNA localization in *Xenopus* oocytes (Kress et al., 2004). Similarly, Ptbp1 binds *gdf1* and *vegt* in the nucleus and the cytoplasm. Strikingly, tagged versions of Igf2bp3 and Ptbp1 directly interact in the nucleus. Thus, both proteins might associate with each other before binding to the target RNA (Kress et al., 2004; Figure 1.7). Hnrnpab is another protein that associates with *gdf1* mRNA in the nucleus and it is distributed in the nucleus and the cytoplasm of *Xenopus* oocytes (Czaplinski and Mattaj, 2006). Although Hnrnpab interacts with Igf2bp3 and Ptbp1, it was not found to bind to VM1 or E2 motifs of the *gdf1*-LE. Czaplinski and Mattaj (2006) found that the depletion of Hnrnpab from oocyte extracts does not affect binding of Igf2bp3 and Ptbp1. Thus, Hnrnpab might assemble the nuclear localization complex after pre-assembly of Igf2bp3 and Ptbp1 (Figure 1.7). However, despite these strong indications for an initial step of RNA localization in the nucleus, LE RNAs injected in the oocyte cytoplasm localize properly to the vegetal pole, arguing for a certain degree of redundancy of nuclear complex assembly. Thus, the mechanistic purpose of nuclear localization complex assembly is not yet fully understood.

1.8.2. Cytoplasmic complex remodeling

After nuclear export, the localization RNP complex undergoes several steps of remodeling, including incorporation into larger granules, coupling to motor proteins, translational repression, and anchoring at sites of destination. In order to coordinate these steps, structure and composition of localization RNPs are suggested to change during the localization process (Lewis and Mowry, 2007). The dynamic composition of *Xenopus* localization RNPs gives compelling evidence for a cytoplasmic remodeling. Strikingly, tagged versions of Igf2bp3 and Ptbp1 directly interact in the nucleus of *Xenopus* oocytes, but in the cytoplasm the interaction is sensitive to RNase (Kress et al., 2004). This indicates that *gdf1* and *vegt* containing RNPs are remodeled during or after nuclear export and thereby Igf2bp3 and Ptbp1 get physically separated. Such RNP remodeling may be triggered by altered protein-protein interactions due to the assembly of cytplasmic localization factors. Indeed, Stau1 and proline-rich RNA binding protein (Prrp) assemble the localization RNP in the cytoplasm

(Kress et al., 2004; Figure 1.7). Stau1 might be recruited by Ptbp1, as they were shown to interact directly (Kress et al., 2004). Furthermore, expression of a mutant Stau1, which is reduced in binding Ptbp1, abolishes vegetal RNA localization (Yoon and Mowry, 2004a).

RNP remodeling might also be mediated by post-translational modifications. Indeed, Ptbp1 is found to be phosphorylated in the nucleus and unphosphorylated in the cytoplasm (Xie et al., 2003). However, the role of Ptbp1 phosphorylation in vegetal RNA localization is still unclear and it is likely that several different molecular mechanisms account for the dynamic nature of localization RNPs.

1.8.3. Recruitment of motor proteins and active transport

Localization RNPs are coupled to motor proteins and transported along the cytoskeleton (reviewed in Gagnon and Mowry, 2011b; Figure 1.7). RNP components might function as adaptors to directly or indirectly recruit motor proteins to the complex. Transport of RNPs that contain *gdf1* is mediated by Kinesin-1 and -2 towards the plus ends of a microtubule subpopulation in *Xenopus* oocytes (Messitt et al., 2008). A recent study suggests an initial Dynein-dependent step, similar to the transport of *Drosophila oskar* mRNA from the nurse cells to the oocyte (Gagnon et al., 2013). This Dynein-dependent step localizes the RNA to the upper vegetal cytoplasm of the oocyte in a uni-directional manner. A second Kinesin-dependent step is bi-directional and ultimately transfers the RNA to the posterior cortex. Stau1 is implicated to mediate directional RNA transport in *Xenopus* oocytes, as it co-precipitates with Kinesin (Yoon and Mowry, 2004a). Interestingly, animally and vegetally localizing RNPs share protein components, including Igf2bp3, hnRNP I and Hnrnpab, whereas Stau1 is a specific component of vegetally localizing RNPs (Snedden et al., 2013). However, a direct interaction of Stau1 and Kinesin has not been described so far, and other potential adaptor proteins that mediate interactions of *Xenopus* localization RNPs with Kinesin or Dynein are not yet known.

1.8.4. Anchoring at sites of destination

In order to prevent a diffusion back into the cell lumen, the final step in RNA localization is the anchoring of the RNA at the cortex (Figure 1.7). Cortical Actin-filaments were shown to be essential for RNA anchoring in vertebrates and invertebrates (Yisraeli et al., 1990; Suzuki et al., 2000; Jankovics et al., 2002). However, proteins mediating the transfer of localizing

RNAs from the microtubule to the Actin cytoskeleton are largely unknown. In *Xenopus* oocytes, Prrp might be involved in the anchoring of RNAs at the vegetal cortex, as it was shown to bind *gdf1* and *vegt* mRNAs as well as the microfilament-associated proteins Mena and Profilin (Zhao et al., 2001). Furthermore, Igf2bp3 seems to be involved in vegetal anchoring, as its phosphorylation upon egg maturation correlates with a release of Igf2bp3 itself as well as *gdf1* mRNA from the vegetal cortex (Git et al., 2009). A recent study by Mei et al., (2013) suggests that the protein product of the vegetally localizing *dnd1* mRNA in involved in the anchoring of *trim36* mRNA at the vegetal cortex . Thus, localized translation of *dnd1* might reinforce anchoring of other RNAs. Vegetal anchoring might also be mediated by RNAs, as depletion of *vegt* mRNA or the non-coding RNA *Xlsirts* leads to a cortical release of *gdf1* mRNA (Kloc and Etkin, 1994; Heasman et al., 2001). Furthermore, cytokeratin filaments appear to play a role in vegetal anchoring, as their interruption by antibodies causes a release of several localized mRNAs, whereas disruption of Actin or microtubules does not affect their vegetal localization (Heasman et al., 2001).

1.8.5. Translational regulation of localizing RNAs

To ensure a local protein synthesis, RNAs have to be transported in a translationally repressed state until they reach their destination. *Xenopus gdf1* translational repression is mediated by a *cis*-acting region downstream of the LE, named translational control element (TCE) (Wilhelm et al., 2000; Otero et al., 2001). The *Xenopus* HuR ortholog Elavl2 mediates translational repression by binding to the TCE (Colegrove-Otero et al., 2005). Interestingly, the *gdf1*-LE contains a cytoplasmic cleavage-polyadenylation site, which is able to recruit the K homology type protein Khsrp (formerly called VgRBP71) that stimulates cleavage of the TCE and thus activates translation (Kolev and Huber, 2003).

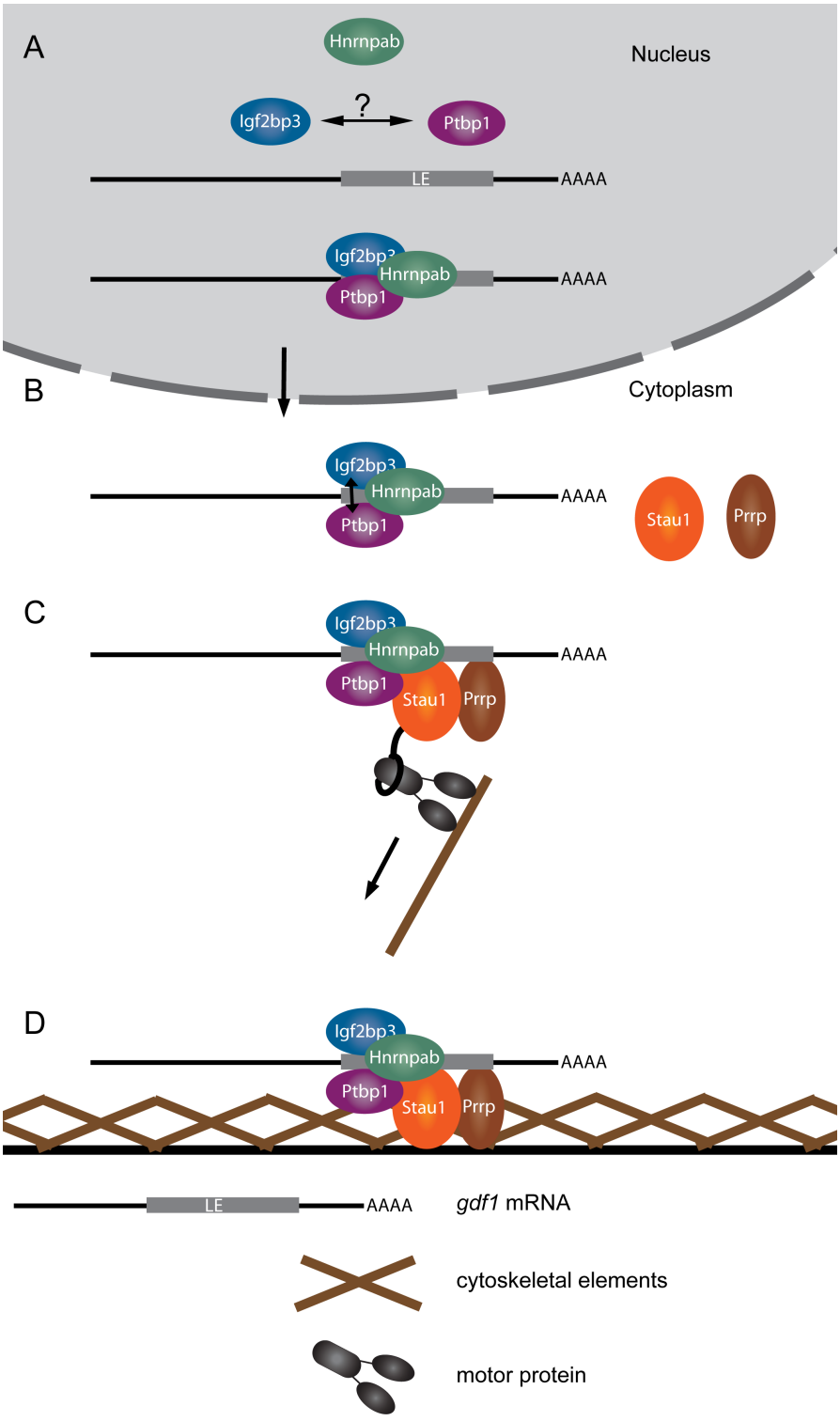

Figure 1.7. Model illustrating the mechanism of motor-dependent localization of *gdf1* mRNA in *Xenopus* oocytes. A) Nuclear initiation of RNP complex assembly. Igf2bp3, Ptbp1 and Hnrnpab bind the late localizing RNA *gdf1* in the nucleus. Igf2bp3 and Ptbp1 might directly interact before or after RNA-binding. B) After nuclear export, RNP complex remodeling includes recruitment of Stau1 and Prrp and loss of direct interaction between Igf2bp3 and Ptbp1. C) The localization complex associates with motor proteins and is transported along cytoskeletal elements to the vegetal cortex. D) The localization complex is anchored by cytoskeletal elements at the vegetal cortex. Model based on King et al. (2005), Martin and Ephrussi (2009).

1.9. A second mechanism restricts localization of vegetal RNAs after fertilization

Early embryonic development is under the control of maternal determinants deposited in the egg. During a critical period known as maternal to zygotic transition (MZT), the control of embryonic development shifts from maternally to zygotically encoded molecules. In order to prevent the interference of maternal with zygotic gene products, the MZT involves the degradation of a large fraction of maternal mRNAs (reviewed in Tadros and Lipshitz, 2009; Figure 1.8). However, certain maternal mRNAs required for germ cell formation were shown to be protected from this degradation mechanism in *Xenopus* embryos (Horvay et al., 2006).

In *Xenopus*, several early localizing RNAs remain associated with the germ plasm and are specifically inherited by prospective germ cells during cleavage stages (Hudson and Woodland, 1998; Houston and King, 2000; Horvay et al., 2006; Yamaguchi et al., 2012; Chapters 1.2; 1.5). However, although *dnd1* mRNA localizes to the entire vegetal cortex via the late pathway leading to a distribution of transcripts outside of the germ plasm, this transcript is specifically restricted to PGCs in later embryos (Horvay et al., 2006). This restriction is achieved by microRNA (miR)-mediated degradation of transcripts in the soma and selective transcript protection in PGCs during the MZT (Koebernick et al., 2010). Strikingly, the sequence that mediates somatic degradation of *dnd1* is identical to its LE and contains the target site for miR-18. Similarly, LEs of other germ cell specific RNAs contain target sites for somatic miR-mediated degradation. The localization protein Elavl2 was identified to be responsible for the protection of *dnd1* from miR-mediated decay during the MZT via binding to its LE (Arthur et al., 2009; Koebernick et al., 2010). The Dnd1 protein itself also appears to function in the stabilization of germ cell specific RNAs in the zebrafish (Kedde et al., 2007). Similarly, Dnd1 was demonstrated to cooperate with Elavl2 in protecting *dnd1* mRNA from miR-mediated degradation in the early *Xenopus* embryo (Koebernick et al., 2010). The participation of Elavl2 in RNA localization during oogenesis as well as RNA stabilization during embryogenesis suggests that certain localization factors might have a dual function in the local restriction of transcripts before and after fertilization.

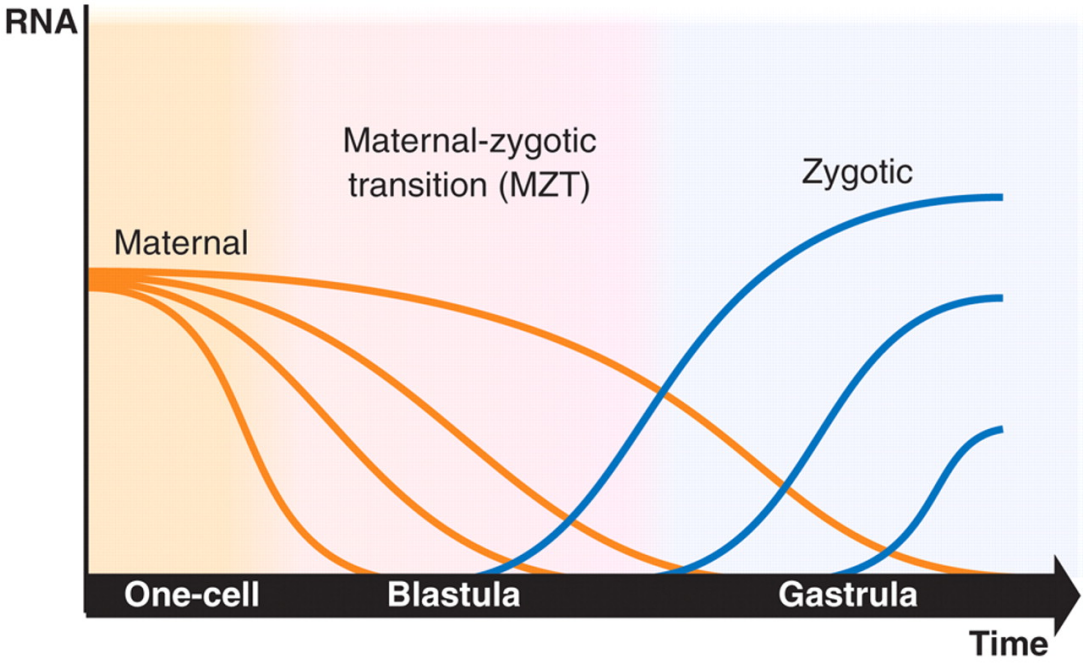

Figure 1.8. The maternal to zygotic transition in *Xenopus* embryos. Maternal transcripts (red lines) are degraded and zygotic transcription (blue lines) is activated during the maternal-zygotic transition at blastula stages. Image taken from Schier (2007).

1.10. RNA localization during zebrafish oogenesis - Parallels between fish and frog

Similar to *Xenopus* oocytes, early zebrafish oocytes contain the Balbiani body adjacent to the nucleus and it is translocated to the vegetal pole and disassembles there at late stage I. The oocyte increases in size due to yolk uptake until final stage IV. Although several RNAs initially localize to the Balbiani body, including orthologs of *Xenopus* vegetally localizing RNAs, some of them relocalize to the cytoplasm, the entire cortex or to the animal pole during progression of oogenesis (Howley and Ho, 2000; Kosaka et al., 2007; Abrams and Mullins, 2009; Figure 1.9). Thus, the existence of two distinct localization pathways, as observed in *Xenopus*, is not apparent. Nevertheless, several RNAs, including *dazl*, *syntabulin* and *celf1*, localize to the vegetal pole and remain there until late zebrafish oogenesis (Howley and Ho, 2000; Suzuki et al., 2000; Nojima et al., 2010; Figure 1.9). During egg activation, cytoplasm streams towards the animal pole and forms the yolk-free blastodiscs, leading to the accumulation of yolk at the vegetal pole (Ho, 1992; Kimmel et al., 1995; Figure 1.9). The majority of localized mRNAs then becomes passively enriched in the animal cytoplasm by cytoplasmic streaming (Howley and Ho, 2000). For example, *dazl* and *celf1* are passively translocated towards the animal pole after fertilization, whereas *syntabulin* remains at the vegetal cortex throughout early cleavage stages (Nojima et al., 2010; Figure 1.9). During cleavage stages, several RNAs become enriched in the cleavage furrows and act in germ cell formation (Figure 1.9).

The mechanism of RNA localization in zebrafish oocytes is largely unknown. However, zebrafish *vasa* 3'UTR localizes in *Xenopus* oocytes after microinjection, suggesting a conserved localization machinery between fish and frog (Knaut et al., 2002). The zebrafish ortholog of Igf2bp3 was identified to co-localize with *cyclin b1* mRNA at the animal cortex and to translationally repress this transcript (Takahashi et al., 2014). Although a role of Igf2bp3 in localization of *cyclin b1* was not described in zebrafish oocytes, this finding suggests that some localization complex components might be conserved between fish and frog.

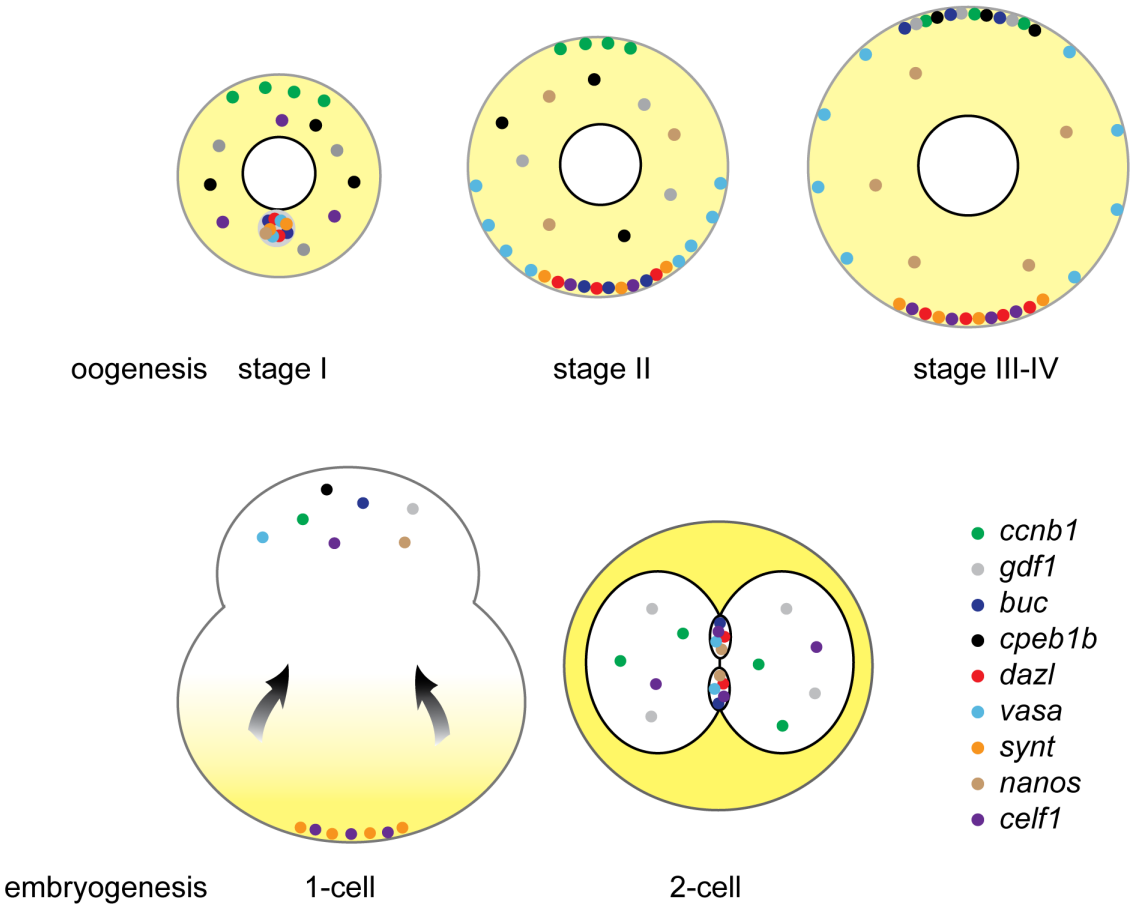

Figure 1.9. RNAs localize in diverse patterns during zebrafish oogenesis and embryogenesis. In stage I oocytes, *buckyball (buc), dazl, vasa, syntabulin (synt)* and *nanos* mRNAs are localized in the Balbiani body, while *cyclin b1* (*ccnb1*) localizes animally and *celf1* and *gdf1* are distributed within the cytoplasm. In stage II, *buc, dazl, syn* and *celf1* are localized at the vegetal cortex, while *vasa* is distributed more broadly at the vegetal cortex and *nanos* is redistributed to the cytoplasm. In stage III-IV, buc relocalizes to the animal pole, where *gdf1* and *ccnb1* are localized and *vasa* is present at the entire cortex. After fertilization (1-cell), most RNAs are passively translocated to the animal cytoplasm, while *syntabulin* and a fraction of *celf1* mRNAs remain at the vegetal cortex. During cleavage stages (2-cell, animal view) *buc, dazl, vasa* and *nanos* mRNAs localize to cleavage furrows and are involved in germ cell formation. Image based on Bally-Cuif et al. (1998), Howley and Ho (2000), Suzuki et al. (2000), Pelegri (2003), Hashimoto et al. (2004), Kosaka et al. (2007), Abrams and Mullins (2009), Abrams and Mullins (2009), Nojima et al. (2010).

1.11. Previous research

In *Xenopus* oocytes, RNA LEs recruit different protein factors which are assumed to assemble into large localization RNP complexes and mediate motor-dependent RNA localization to the vegetal cortex. A number of localization complex components has been identified to date (Deshler et al., 1997; Havin et al., 1998; Cote et al., 1999; Zhao et al., 2001; Allison et al., 2004; Yoon and Mowry, 2004a; Czaplinski et al., 2005). However, UV-crosslinking analyses of vegetal LEs in oocyte extracts revealed interactions with unknown proteins, indicating that localization complexes contain additional components (Horvay et al., 2006). In order to identify these novel components, the LE of the late localizing *dnd1* mRNA was used for the reconstitution of localization RNPs in *Xenopus* oocyte extracts and subsequent RNA affinity purification (Figure 1.10A, M. Claußen, unpublished). Analyses of purified protein preparations revealed protein bands specifically appearing in the fractions obtained with LE-RNAs (Figure 1.10B) and Western blot analyses supported purification of known localization factors in these protein fractions (Figure 1.10C). Comparative tandem mass spectrometry of purified protein preparations revealed that, in addition to the known localization factors, a number of potential novel localization complex components specifically interact with the *dnd1*-LE. Out of these novel candicates, two RNA binding proteins were chosen for further analyses in respect to RNA localization: Celf1 and Tia1.

1.11.1. Celf1

Celf1 is a member of the Celf (CUG-BP and Etr-like) family of RRM-type RNA binding proteins (Figure 1.10D). The Celf protein family is implicated in diverse aspects of RNA metabolism in the nucleus and cytoplasm, including regulation of splicing, stability and translation (reviewed in Dasgupta and Ladd, 2011). Celf proteins are conserved in diverse organisms, as they have been identified in invertebrates, vertebrates and plants (Good et al., 2000). In *Xenopus*, five Celf proteins (Celf1-5*)* have been identified*.* All Celf proteins share a similar structure of two N-terminal and one C-terminal RRM, with a divergent domain between RRM2 and RRM3. While *Xenopus* Celf1-3 are expressed in dorsal mesoderm and neuronal structures, *celf4-5* expression is restricted to neuronal structures. While the functions of *Xenopus* Celf2, -4 and -5 are largely unknown, Celf3 is implicated in the translational upregulation of *cyclin a2* mRNA and thus in stimulating proliferation (Horb and Horb, 2010). *Xenopus* Celf1 (formerly known as EDEN-BP) is involved in deadenylation of maternal transcripts in embryos by binding to GU-rich sequences called embryo deadenylation elements (EDEN) (Paillard et al., 1998). However, a function of Celf1 in

oocytes has so far been unknown.

1.11.2. Tia1

Tia1 (T cell internal antigen-1) and the highly similar protein TIA-related (TIAR) comprise the Tia1 familiy of RNA binding proteins, which possess three RNA recognition motifs (RRM) in their N-terminal region (Figure 1.10D). Tia1 proteins have multiple functions in RNA processing; they act in alternative splicing (Del Gatto et al., 1997; Förch et al., 2000; Zhu et al., 2003) and they are implicated in translational regulation of various transcripts by binding to AU-rich elements (ARE) (Piecyk et al., 2000; Dixon et al., 2003; Kandasamy et al., 2005). In addtition to regulating translation of specific transcripts, Tia1 proteins are involved in the general translational arrest that occurs in response to environmental stress, as they promote the formation of stress granules (Kedersha et al., 1999). Both Tia1 and TIAR proteins are able to shuttle between nucleus and cytoplasm of somatic cells (Kedersha et al., 1999; Zhang et al., 2005). However, in *Xenopus* oocytes they were predominantly detected in the cytoplasm (Colegrove-Otero et al., 2005). *tia1* transcripts are expressed throughout embryogenesis with highest RNA levels in neuronal tissues (Rothé et al., 2006). However, a role for Tia1 during oogenesis or embryonic development has not been described so far.

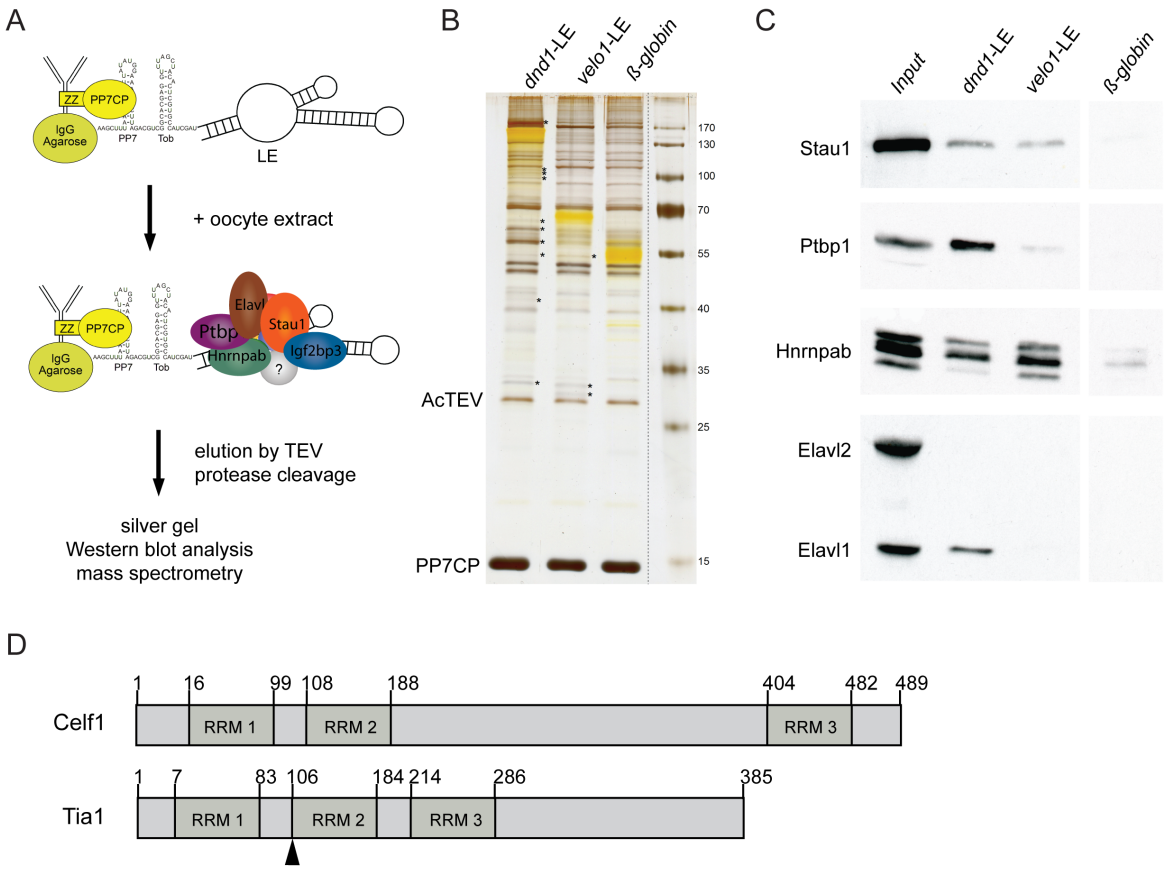

Figure 1.10. RNA affinity purification of vegetal localization complexes identified Celf1 and Tia1. A) *dnd1*-LE, *velo1*-LE or *ß-globin*-3'UTR (negative control) were fused to a *Pseudomonas aeruginosa* phage 7 (PP7) RNA stem loop and immobilized on a solid support by binding to PP7 coat protein (PP7CP) (Hogg and Collins, 2007). Incubation with oocyte extract allowed for *in vitro* assembly of localization RNP complexes, which were eluted by TEV cleavage between zz-tag and PP7CP. B) Gel-electrophoretic analysis of precipitated proteins (silver-stained). Bands that specifically appear in the protein preparations obtained with the *dnd1*-LE and/or *velo1*-LE are marked by an asterisk. Protein bands corresponding to TEV-protease and PP7CP are indicated. Co-purified RNAs appear as yellow bands. C) Western blot analysis for co-purification of known localization proteins with indicated RNAs. D) Mass spectrometric analysis revealed the RNA recognition motif (RRM)-type RNA binding proteins Celf1 and Tia1. Two isoforms of Tia1 are generated by differential splicing, which differ by the in- or exclusion of 11 amino acids in RRM2 (black arrow head). Numbers indicate amino acid positions. Images A-C were kindly provided by M. Claußen.

1.12. Aim of this study

Vegetal RNA localization in *Xenopus* oocytes is understood to be of crucial importance for the development of the embryo. The localization of RNAs involves the assembly of several RNA and protein components into RNP complexes. A number of protein components of *Xenopus* vegetal localization RNPs are known. However, the exact composition of localization RNPs as well as the functions of single components is far from a detailed understanding. Celf1 and Tia1 were identified to specifically interact with a localizing RNA in

Xenopus oocytes and thus they might be novel components of vegetal localization RNPs. The aim of this study is to analyze the functions of these proteins in RNA localization during *Xenopus* oogenesis. This includes analyses of their subcellular distribution, interactions with localizing RNAs and other localization factors, their function in active RNA transport as well as possible regulatory functions in RNA stability and translational regulation.

2. Materials and methods

2.1. Model organisms

Frog oocytes and embryos were obtained from albino or pigmented African clawed frogs *Xenopus laevis*, which were ordered from Nasco (Fort Atkinson, Wisconsin, USA). Zebrafish (*Danio rerio*) experiments were done with the wild-type strain ABxTLF and the *celf1* mutant line sa11143 obtained from the European Zebrafish Resource Center (Karlsruhe, Germany).

2.2. Bacteria strains

Escherichia coli (E. coli) strains used during this study were
XL1-Blue: recA1 endA1 gyrA96 thi-1 hsdR17 supE44 relA1 lac [F´ proAB lacIqZΔM15 Tn10(Tetr)] for cloning procedures and
BL21 (DE3): *E. coli* B F- ompT hsdS(rB- mB-) dcm+ Tetr gal λ(DE3) endA Hte [argU proLCamr] [argU ileY leuW Strep/Specr] for protein expression.

2.3. Media and buffers

The media and buffers used during this study are listed in Table 2.1. All solutions were prepared with millipore water and, if required, they were autoclaved or sterilized with membrane filters (0.2 µm pore size, Sartorius). Percentages are v/v, if not indicated differently.

Table 2.1. Buffers and media

Buffer/media name	composition
Annealing buffer 10x	400 mM Tris pH 8, 200 mM $MgCl_2$, 500 mM NaCl, 10 mM EDTA
Antibiotics	Antibiotics were dissolved in water and the following working concentrations were applied in LB-medium/-agar: ampicillin 100 µg/ml, kanamycin 50 µg/ml, carbenicillin 50 µg/ml

Alkaline phosphatase buffer (APB)	100 mM Tris-HCl pH 9.5, 50 mM $MgCl_2$, 100 mM NaCl, 0.1 % Tween 20
Bleaching solution	50 % formamide, 0.5 % H_2O_2, 5x SSC
Blocking solution (Western blot)	5 % (w/v) non-fat dry milk powder, TBST
Blocking solution (*in situ* hybridization)	1x MAB, 2 % Boehringer Mannheim Blocking reagent (BMB), 20 % horse serum
Blocking solution (immunofluorescence)	1x PBS, 2 % BSA, 2 % horse serum, 0.1 % Triton X-100
Blotting buffer	25 mM Tris, 192 mM glycine, 20 % methanol
Buffer M	150 mM NaCl, 50 mM NaH_2PO_4 pH 7.8, 1 mM DTT, 15 % glycerol, 0.1 % Triton X 100
Collagenase buffer	82.5 mM NaCl, 2 mM KCl, 1 mM $MgCl_2$, 5 mM HEPES pH 7.5
Color reaction solution (*in situ* hybridization)	80 µg/ml NBT, 175 µg/ml BCIP in APB
Coomassie staining solution	1 g/L Coomassie Brilliant Blue G-250, 50 % methanol, 10 % acetic acid
Coomassie destaining solution	40 % methanol, 10 % acetic acid
Cysteine solution	2 % L-cysteine hydrochloride in 0.1x MBSH, pH 8.0
EMSA loading dye	50 mM Tris-Cl pH 7.5, 50 % glycerol, 0.01 % bromophenol blue
Ficoll	10 % (w/v) Ficoll PM 400, sterile-filtered

HNTA buffer	1 M NaCl, 50 mM Na_2HPO_4 pH 7.8, 1 mM DTT, 1 % Triton X-100
Hybridization mix	50 % formamide, 5x SSC, 1 mg/ml torula RNA, 100 µg/ml heparin, 1x Denhards, 0.1 % Tween 20, 0.1% (w/v) CHAPS
Injection buffer	1x MBS, 2 % Ficoll
IPP145 1x	10 mM Tris pH 8, 14.5 mM NaCl, 0.1 % NP40, 5 % glycerol
L15 oocyte culture medium	50 % L-15 medium, 1 mM L-glutamine, 1 µg/ml insulin, 15 mM HEPES pH 7.8, 100 µg/ml gentamycine, 50 µg/ml tetracycline, 50 units/ml nystatin, 2.5 mg/ml vitellogenin (isolated from frog blood)
Luria-Bertani (LB)-Agar	35 g LB-Agar (Roth) in 1 l water
Luria-Bertani (LB)-Medium	20 g LB-Medium (Roth) in 1 l water
Lysis buffer (zebrafish fin clips)	100 mM Tris pH 8.4, 500 mM KCl, 15 mM $MgCl_2$, 100 µg/ml Proteinase K
MAB	100 mM maleic acid; 150 mM NaCl, pH 7.5
MBSH 1x	80 mM NaCl, 1 mM KCl, 2.4 mM $NaHCO_3$, 10 mM HEPES pH 7.5, 0.82 mM $MgSO_4$, 0.66 mM KNO_3, 0.41 mM $CaCl_2$
MEM	100 mM MOPS, 2 mM EGTA, 1 mM $MgSO_4$
MEMFA	1x MEM, 4 % formaldehyde
MNTA buffer	500 mM NaCl, 50 mM Na_2HPO_4, pH 7.8, 1 mM DTT, 1 % Triton X-100

PBS 10x	1.37 M NaCl, 27 mM KCl, 100 mM Na_2HPO_4, 20 mM KH_2PO_4, pH 7.4
PBT	1x PBS, 0.1 % Tween 20
PBT (immunofluorescence)	1x PBS pH 7.4, 0.2 % BSA, 0.1 % Triton X-100
SDS running buffer 10x (Laemmli)	250 mM Tris-base, 2.5 M glycine, 0.1 % SDS
SDS loading buffer 2x	62.5 mM Tris-HCl pH 6.8, 700 mM 2-Mercaptoethanol, 10 % glycerol, 2 % SDS (w/v), 0.05 % (w/v) bromophenol blue
SSC 20x	150 mM NaCl, 15 mM sodium citrate, pH 7.4
TAE (Tris/acetate/EDTA)	40 mM Tris-acetate pH 8.5, 2 mM EDTA
TBE (Tris/boric acid/EDTA)	89 mM Tris, 89 mM boric acid, 2 mM EDTA
TBST (Tris buffered saline with Tween 20)	20 mM Tris-HCl pH 7.5, 150 mM NaCl, 0.05 % Tween 20
TE (Tris/EDTA)	10 mM Tris-HCl pH 8.0, 1 mM EDTA
Tris-HCl	1 M Tris, pH adjusted with 37 % HCl
UV crosslinking buffer 5x	25 mg/mL heparin, 5 % glycerol (v/v), 250 mM KCl, 50 mM DTT, 26 mM Hepes pH 7, 5 mM $MgCl_2$, 0.5 mM EDTA, 200 µg/ml yeast RNA
YSS buffer	50 mM Tris pH 8, 75 mM NaCl, 1 mM $MgCl_2$, 0.05 % NP40, 100 mM sucrose, 1 mM DTT, 1/4 Proteinase inhibitor tablet per 50 ml buffer (Roche)

2.4. Oligonucleotides

Table 2.2. Sequencing oligonucleotides

Name	Sequence (5'-3')
Sp6	TTAGGTGACACTATAGAATAC
T7 (pCS2+)	TCTACGTAATACGACTCACTATAG
T7 (pGEM-T easy)	TAATACGACTCACTATAGGGCGA
T3	AATTAACCCTCACTAAAGGG
M13 rev	AGCGGATAACAATTTCACAC

Table 2.3. Oligonucleotides used for amplification and cloning of Celf1, Tia1 and GST (restriction sites are underlined)

Label	Name	Direction	Sequence (5'-3')
DO1	EDEN-BP-F NheI	forward	CTAGCTAGCATGAATGGCACAATGGACC
DO2	EDEN-BP-R Xho1	reverse	CCGCTCGAGGTAGGGTTTGCTGTCATTCTTGG
DO3	TIA-1-F NheI	forward	CTAGCTAGCATGGAGGAAGATCTACCC
DO4	TIA-1-R XhoI	reverse	CCGCTCGAGTTGTGTTTGGTATCCAGCC
DO112	FLAG GST EcoR1 F	forward	CGACGATGACAAGAATTCAATGTCCCCTATACTAGG
DO113	FLAG GST EcoR1 R	reverse	GGCCGAATTCAACAGAACTTCCAGATCCGATTTTG GAGG

Table 2.4. Modified antisense DNA oligos used for depletion of *celf1* mRNA. Phosphorothioate linkages between nucleotides are indicated by asterisks.

Label	Name	Sequence (5'-3')
DO8	Phos-EDEN-BP 4	T*T*G*GATGATGCATCCC*A*G*G
DO25	Phos-TIA-1 5	A*G*C*TGTGGGCTCCGCTC*T*G*C
DO29	Phos control	C*C*T*CTTACCTCAGTTACAATTT*A*T*A

Table 2.5. Oligonucleotides used for site-directed mutagenesis of Celf1

Label	Name	Direction	Sequence (5'-3')
DO40	EDEN Mut RRM1 RNP1 F	forward	GCAAAGGATGCTGTGCTATTACTTTCTAC
DO41	EDEN Mut RRM1 RNP1 R	reverse	GTAGAAAGTAATAGCACAGCATCCTTTGC
DO42	EDEN Mut RRM2 RNP1 F	forward	GCAGAGGTTGTGCAGCTATTACATTTACAAC
DO43	EDEN Mut RRM2 RNP1 R	reverse	GTTGTAAATGTAATAGCTGCACAACCTCTGC
DO97	EDENBP S28D F	forward	CGAAGCTGGGATGAGAAAGAGCTAAGAGAAC

DO98	EDENBP S28D R	reverse	GCTCTTTCTCATCCCAGCTTCGAGGAACCTG
DO99	EDENBP S294D F	forward	CTTCCAGCGATCCCCTCAGCATCCTAACC
DO100	EDENBP S294D R	reverse	GCTGAGGGGATCGCTGGAAGAAGTGAGTGCTG
DO101	EDENBP S302/304D F	forward	CATCCTAACCAGTGATGGTGACTCCCCCAACTC
DO102	EDENBP S302/304D R	reverse	GGGGGAGTCACCATCACTGGTTAGGATGCTGAG G
DO114	EDENBP T156D F	forward	GCATTTATTACATTTGATACTAGATCCATGGCACAG
DO115	EDENBP T156D R	reverse	GGATCTAGTATCAAATGTAATAAATGCACAACCTCT G
DO116	EDENBP T198D F	forward	GAAGCGAATGGACCAGCAACTTCAGCAGCAAATG
DO117	EDENBP T198D R	reverse	CTGAAGTTGCTGGTCCATTCGCTTCTGTTCTTTG
DO118	EDENBP S236D F	forward	CAGACCACAGACTCTGGGAACCTCAACTCC
DO119	EDENBP S236D R	reverse	GTTCCCAGAGTCTGTGGTCTGCTGGAGG
DO120	EDENBP S287D F	forward	GAGTGCAGGCGATGCACTCACTTCTTCCAGC
DO121	EDENBP S287D R	reverse	GTGAGTGCATCGCCTGCACTCTGGGTATTCTGGG
DO122	EDENBP S387D F	forward	GAGCCTTTTGGATCAACAGGGTTTGGGG
DO123	EDENBP S387D R	reverse	CCTGTTGATCCAAAAGGCTCTGGTTGTAGAGTG
DO124	EDENBP S451D/Y452D F	forward	GTTTTGGTTTCATAGATGATGACAATCCCGTTTCT GCTC
DO125	EDENBP S451D/Y452D R	reverse	CGGGATTGTCATCATCTATGAAACCAAAACATTTG CTG

Table 2.6. Oligonucleotides used to create deletions or insertions in Celf1. 5' phophorylations are indicated as P.

Label	Name	Direction	Sequence (5'-3')
DO83	EDENBP delOD(183-210) F	forward	P-GCCTCAATGTGGGGTAACCTAGCTGGAC
DO84	EDENBP delOD(183-210) R	reverse	P-CACGATTGGTGAGGAACAGCCCTCCATAG
DO92	EDENBP N-term F	forward	P-TGACTCGAGCCTCTAGAACTATAGTGAGTCG
DO93	EDENBP N-term R	reverse	P-GGATGTGGTCTGCTGGAGGAGTGCTAAATAC
DO94	EDENBP C-term F	forward	P-TCTGGGAACCTCAACTCCCTTAGTGG
DO157	GST R	reverse	P-TGAATTCAACAGAACTTCCAGATCCGATTTTGG
DO138	EDENBP del1-118 F	forward	P-TGTAATGAGAATGATATCCGGACCTTGTTC
DO141	EDENBP del1-118 R	reverse	P-CTTCTTGGAAACCATTCCAATAAAGAGCTTTCTG
DO163	EDENBP del119-188 F	forward	P-CAGAAAGACAAAGAACAGAAGCGAATGACG
DO164	EDENBP del189-236 R	reverse	P-AGTGTCTGCGAACTTGACCACGATTG
DO90	NLS insert EDENBP-C-term F	forward	P-AAGCGTAAGGTATGACTCGAGCCTCTAGAACTA TAGTGAGTCG

DO91	NLS insert EDENBP C-term R	reverse	P-CTTCTTTGGTGAGTAGGGTTTGCTGTCATTCTTGGAGC

Table 2.7. Oligonucleotides used to generate T7 promoter containing dnd1-LE deletion fragments (T7 sequence is underlined)

Label	Name	Direction	Sequence (5'-3')
DO32	dnd1-LE T7 5' F	forward	TAATACGACTCACTATAGGGCTGCCCTTGCATCCTACA
DO33	dnd1-LE T7 5'del1 F	forward	TAATACGACTCACTATAGGGTTGCATTGGTGTAAAGCT
DO34	dnd1-LE T7 5'del2 F	forward	TAATACGACTCACTATAGGGTCACTTGTTATTGCACTT
DO35	dnd1-LE T7 5'del3 F	forward	TAATACGACTCACTATAGGGTGTATCTTGCACTTAAGA
DO39	dnd1-LE 3' R	reverse	AGGTGAAAATCAAGACAG
DO37	dnd1-LE 3'del1 R	reverse	GGAAAGCCCTTTATGAAA
DO38	dnd1-LE 3'del2 R	reverse	ATCGCCTCACTTCAAAGT
DO36	dnd1-LE 3'del3 R	reverse	GCAGGGAGCAGGCAGATG
DO46	dnd1-LE 3'del4 R	reverse	TTTTCCGATCTTAAGTGC
DO47	dnd1-LE 3'del5 R	reverse	AAAGTGCAATAACAAGTG

Table 2.8. Oligonucleotides used for dnd1-LE site directed mutagenesis

Label	Name	Direction	Sequence (5'-3')
DO52	dnd1-LE Celf1 binding-site Mut1	forward	GTTTCACTTTATTTATTTTTTTCACTAGATATTGC
DO53	dnd1-LE Celf1 binding-site Mut1	reverse	GTGCAATATCTAGTGAAAAAAATAAATAAAGTG
DO54	dnd1-LE Celf1 binding-site Mut2	forward	CTTGTTATTGCACTTAATTAGAATGAGAGTATCTTGC
DO55	dnd1-LE Celf1 binding-site Mut2	reverse	CTTAAGTGCAAGATACTCTCATTCTAATTAAGTGC
DO60	dnd1-LE Celf1 binding-site Mut1+3	forward	GTTTCACTTTATTTATTTTTTTCAAAAGATATTAAAC
DO61	dnd1-LE Celf1 binding-site Mut1+3	reverse	GTTTAATATCTTTTGAAAAAAATAAATAAAGTGAAAC
DO48	dnd1-LE Tia1 binding-site Mut1	forward	GCATTGGTGTAAAGCTAATAAATGTATCAC
DO49	dnd1-LE Tia1 binding-site Mut1	reverse	ATAAAGTGATACATTTATTAGCTTTACACC
DO50	dnd1-LE Tia1 binding-site Mut2	forward	GCTAATTTTTGTTTCACTAAATAAATAATTTTCACTTG
DO51	dnd1-LE Tia1 binding-site Mut2	reverse	GCAATAACAAGTGAAAATTATTTATTTAGTGAAAC

Table 2.9. Oligonucleotides used for quantitative RT-PCR

Label	Gene/reporter (direction)	Sequence (5'-3')
DO30	*celf1* (forward)	GGGGACGGCAAGCGGGAAA
DO31	*celf1* (reverse)	CAAGGTCCGGATATCATTCTCG
	gapdh	Arthur et. al., 2009
	lmnb1	Arthur et. al., 2009
	odc	Arthur et. al., 2009
	vegt	Arthur et. al., 2009
	gdf1	Arthur et. al., 2009
	dnd1	Horvay et. al., 2006
	h4 (forward)	CGGGATAACATTCAGGGTATCACT
	h4 (reverse)	ATCCATGGCGGTAACTGTCTTCCT
DO154	*grip2* (forward)	GCCTGGTGGGCAGATAATACACAC
DO155	*grip2* (reverse)	CACTTTATTGGACAAGGCTGCAT
DO152	*trim36* (forward)	GAAACAACCAATACCAGCAAAATCCTCACAG
DO153	*trim36* (reverse)	TTAATATCAGATGCAACGCCTACTTTCACCAG
DO150	*spire1* (forward)	TGAACTTGACGGGACAAAGA
DO151	*spire1* (reverse)	GCCCAACGTTCAGGTGTAGT
	velo1	Claußen and Pieler, 2004
226	firefly (forward)	GCAACTGCATAAGGCTATG
227	firefly (reverse)	CGTGTACATCGACTGAAATC
228	renilla (forward)	GGCCAGATGTAAACAAATG
229	renilla (reverse)	CATCCCATGAATCAATCAC

Table 2.10. Three target sites in *celf1* exon 4 and respective oligonucleotides used to construct the associated single guide RNA expression vectors

Target site	Target sequence (5'-3') PAM	Oligonucleotide F (5'-3') (label)	Oligonucleotide R (5'-3') (label)
1	TTCTATAAAGATGTTTGT GGG	TAGGTTCTATAAAGATGTTT GT (DO165)	AAACACAAACATCTTTATA GAA (DO166)
2	TCCCTCGGACGTGGTCA GAGG	TAGGTCCCTCGGACGTGG TCAG (DO167)	AAACCTGACCACGTCCGA GGGA (DO168)
3	TGAGCTGTTTGAGCCCT ATGG	TAGGTGAGCTGTTTGAGCC CTA (DO169)	AAACTAGGGCTCAAACAG CTCA (DO170)

Table 2.11. Oligonucleotides used for the nested PCR amplification of CRISPR/Cas mutated regions in zebrafish *celf1* exon 4

Label	Name	Direction	Sequence (5'-3')
DO171	dr_*celf1* Exon4 F (inner)	forward	TGACTCTGTTGCACAGTTAGCA
DO172	dr_*celf1* Exon4 R (inner)	reverse	ATCCTGCATCCCAAGACAAC
DO181	dr_*celf1* Exon4 F2 (outer)	forward	AAATGTGGGCTAGTGCTCAA
DO182	dr_*celf1* Exon4 R2 (outer)	reverse	TCCCACTATGGGGACTGTTCCA

Table 2.12. Oligonucleotides used to amplify mutated regions in zebrafish *celf1* exon 10 of line sa11143

Label	Name	Direction	Sequence (5'-3')
DO188	*dr_celf1* Exon10 F T7 (inner)	forward	TAATACGACTCACTATAGGGCGATTTCG TAAAGCCCCTGAATG
DO184	*dr_celf1* Exon10 R (inner)	reverse	CTGTTCCCAGTTCCTGTGGT
DO186	*dr_celf1* Exon10 F2 (outer)	forward	CATGGGTGTGCTGTGAAAAC
DO187	*dr_celf1* Exon10 R2 (outer)	reverse	CGAAGCCACAGACAAAAACA

2.5. Constructs

Table 2.13. Expression constructs

Label	Insert	Vector	Kindly provided by
MC397	Tia1	pcS2+Flag	M. Claußen
MC401b	Celf1	pcS2+Flag	M. Claußen
MC337	VgRBP60	pcS2+MT	M. Claußen
JL103	eGFP	pcS2+Flag	J. Löber
5A5	Dead End	pcS2+Flag	K. Koebernick
DO1	His-TIA-1	pET21a	
DO2	His-Celf1	pET21a	
DO3	Celf1 Mut RRM1 F63A	pcS2+Flag	
DO4	Celf1 Mut RRM2 F152A	pcS2+Flag	
DO5	Celf1 Mut RRM1+2 F63/152A	pcS2+Flag	
DO25	Celf1 delOD	pcS2+Flag	
DO59	Celf1 S28/294/302/304D/T156/198D/S236D/ S287D/S387D/S451D/Y452D	pcS2+Flag	
MC410	GST	pcS2+Flag	
DO63	GST Celf1 del119-236 NLS	pcS2+Flag	
DO75	GST Celf1 full length	pcS2+Flag	

DO76	GST Celf1 N-term	pcS2+Flag
DO77	GST Celf1 del119-236	pcS2+Flag
DO78	GST Celf1 C-term	pcS2+Flag
DO79	GST Celf1 del1-118	pcS2+Flag

Table 2.14. Constructs for *in vitro* transcription of localization elements

Label	Insert	Vector	Kindly provided by
MC359	Xgrip-LE	pGEM-T easy	M. Claußen
MC191	vg1-LE	Blue script delta sac/sp1	M. Claußen
MC319	dnd1-LE F2	pGEM-T easy	M. Claußen
MC185	velo1-LE UTR4	Blue script delta sac/sp1	M. Claußen
MC364	ß-Globin 3'UTR	pGEM-T easy	M. Claußen
5A1	dnd1-LE +lacZ	pBK-CMV	K. Horvay

Table 2.15. Wild-type and mutant dnd1-LE constructs

Label	Insert	Vector
DO28	dnd1-LE WT F2 5'del1	pGEM-T easy
DO29	dnd1-LE 5'del1 mut TIA-1 binding-site (1+2)	pGEM-T easy
DO30	dnd1-LE 5'del1 mut Celf1 binding-site (1+2+3)	pGEM-T easy

Table 2.16. Reporter constructs for RNA stability analyses in *Xenopus* embryos

Label	Insert	Vector
DO80	mGFP dnd1-LE 5'del1 wt	pSP64
DO81	mGFP dnd1-LE 5'del1 Mut Tia1 binding-site (1+2)	pSP64

Table 2.17. Control constructs for quantitative real-time PCR

Label	Insert	Vector	Kindly provided by
DO64	velo1 RT fragment	pGEM-T easy	
DO65	pgam1 RT fragment	pGEM-T easy	
DO66	rtn3 RT fragment	pGEM-T easy	
DO67	haprin/trim36 RT fragment	pGEM-T easy	
DO68	grip RT fragment	pGEM-T easy	
DO69	spire2/eg6 RT fragment	pGEM-T easy	
MC296	gapdh	pGEM-T easy	M. Claußen
MC301	lamin b1	pGEM-T easy	M. Claußen
MC298	vegT	pGEM-T easy	M. Claußen
MC297	gdf1 (vg1)	pGEM-T easy	M. Claußen

14B4	odc	pGEM-T easy	T. Klisch

Table 2.18. Single guide RNA expression constructs

Label	Insert	Vector
DO85	dr_celf1 Exon4 target-site1 sgRNA	pDR274
DO86	dr_celf1 Exon4 target-site2 sgRNA	pDR274
DO87	dr_celf1 Exon4 target-site3 sgRNA	pDR274

Table 2.19. Constructs for luciferase assays

Label	Insert	Vector	Kindly provided by
DO34	dnd1-LE 5'del1 wt +firefly luciferase	pBK-CMV	
DO35	dnd1-LE 5'del1 mut Celf1 binding-site (1+2+3) +firefly luciferase	pBK-CMV	
DO36	dnd1-LE 5'del1 mut Tia1 binding-site (1+2) +firefly luciferase	pBK-CMV	
18G4	Renilla luciferase	pCS2	J. Souobgui
MP4	MS2BP	pCS2+MT	M. Püschel
MP5	MS2BP XPABP	pCS2+MT	M. Püschel
MC230	Firefly Luciferase	pBK-CMVluc+ polyA73	M. Claußen
MC239	Firefly Luciferase+VTE	pBK-CMVluc+ polyA73	M. Claußen
SK162	Firefly Luciferase MS2	pBK-CMV	S. Koch

Table 2.20. Constructs used to prepare *in situ* antisense probes

Label	Insert	Vector	Kindly provided by
MC353	lacZ	pGEM-T	M. Claußen
6B4	dr cyclinB1 (ISH probe)	pGEM-T	R. Dosch
6B5	dr dazl (ISH probe)	pCRII Topo	R. Dosch
DO91	dr syntabulin (ISH probe)	pGEM-T easy	

2.6. DNA methods

2.6.1. Cloning and construct preparation

Expression constructs

For expression in oocytes/embryos and *in vitro* translations, Flag-tagged Celf1, Tia1, Ptbp1 (VgRBP60) in pCS2+Flag vector were kindly provided by M. Claußen. The Celf1 open reading frame corresponds to the isoform Celf1b (NCBI accession no. Q6PF35.1) and the Tia1 open reading frame corresponds to the isoform Tia1a (NCBI accession no. NP_001167497.1). The Dead end 1 in pCS2+Flag vector was kindly provided by K. Koebernick.

For bacterial expression of recombinant proteins, Celf1 and Tia1 open reading frames were amplified from plasmid templates using oligonucleotides containing Nhe1 and Xho1 restriction sites (DO1-4, Table 2.3) and cloned into expression vector pET21a (Novagen).

Mutations in the Celf1 RRM domains or potential phosphorylation sites, as predicted by the Scansite motif scan program (Obenauer et al., 2003) and the NetPhos 2.0 Server (Blom et al., 1999), were created stepwise by site-directed mutagenesis using the QuikChange II Site-Directed Mutagenesis Kit (Agilent technologies) and oligonucleotides with base substitutions (DO97-102, DO114-125, Table 2.5) according to manufacturer's instructions.

The Celf1 oligomerization domain was deleted by whole plasmid amplifications of the Flag-Celf1 (MC401b) with non-overlapping 5' phosphorylated oligonucleotides flanking the deleted sequence in opposing directions (DO83/84, Table 2.5). For the Celf1 deletion constructs used for nuclear/cytoplasmic distribution studies, the GST sequence was amplified with EcoRI containing oligonucleotides (DO112/113, Table 2.3) from Flag-GST plasmid template (MC410) and ligated into EcoRI sites of Flag-Celf1 (MC401b). This Flag-GST-Celf1 plasmid (DO75) was used as template for whole plasmid amplifications with non-overlapping 5' phosphorylated oligonucleotides (Table 2.5) as described above. The N-terminal nuclear localization signal (NLS) was inserted into Flag-GST-Celf1 del119-236 by amplification of the whole plasmid with each oligonucleotide containing a fragment of the NLS (DO90/91, Table 2.5). Fragments with insertions or deletions were purified using Invisorb Fragment Cleanup kit (Invitek), re-ligated and transformed. All constructs described in this section are listed in Table 2.13.

Constructs for *in vitro* transcription of localization elements

For *in vitro* transcriptions of LEs, dnd1-LE, grip2-LE and ß-globin-3'UTR in pGEM-T easy (Promega) as well as gdf1-LE and velo1-LE in pBluescript KS+ (Stratagene) were kindly provided by M. Claußen. For detection of *dnd1*-LE localization by WMISH, dnd1-LE in lacZ containing pBK-CMV was kindly provided by K. Horvay. The constructs are listed in Table 2.14.

Deletion fragments and site-directed mutagenesis of *dnd1*-LE

Deletion fragments of the dnd1-LE were amplified from plasmid template (MC 319) using forward oligonucleotides that contain a T7 sequence (Table 2.7). The 5'del1 fragment was cloned into pGEM-T easy and mutant versions of 5'del1 dnd1-LE were generated by site-directed mutagenesis using the QuikChange II Site-Directed Mutagenesis Kit (Agilent technologies) and oligonucleotides with base substitutions (Table 2.3) according to manufacturer's instructions. The constructs are listed in Table 2.15.

Reporter constructs for RNA stability analyses in *Xenopus* embryos

Wild-type and mutated *dnd1*-LE 5'del1 fragments were amplified with XhoI/NotI restriction sites from plasmid templates and cloned into mgfp-psp64 (provided by E. Raz, Institute of Cell Biology, Münster, Germany). Constructs are listed in Table 2.16

Control constructs for quantitative real-time PCR

Plasmid templates used as controls in quantitative real time PCR were amplified from oocyte cDNA and cloned into pGEM-T easy. The constructs are listed in Table 2.17**.**

Single Guide RNA (sgRNA) expression vectors

The customized sgRNA expression vectors were mainly constructed as described in Hwang et al. (2013). The pDR274 plasmid (Addgene) harboring a T7 promoter upstream of a partial guide RNA sequence was digested with BsaI. A pair of oligonucleotides containing the sgRNA target sequence and overhangs that are compatible with cloning into the BsaI-digestion sites were annealed as follows: 100 µM of each oligo in a 50 µl volume containing 1x annealing buffer was heated to 95 °C and cooled (-1 °C per 30 sec) to 4 °C. 15 µM of the annealed oligos were cloned into the pDR274 vector backbone. The genomic target sites in the *celf1* gene and sequences of the oligonucleotides are listed in Table 2.10. The constructs are listed in Table 2.18.

Constructs for luciferase assays

The firefly luciferase ORF alone or with adjacent *gdf1* translational control element (VTE) in pBK-CMV was kindly provided by M. Claußen. The firefly luciferase constructs containing

5'del1 wild-type and mutant *dnd1*-LE fragments were cut out with BahmHI and NotI from DO28, DO29 and DO30 and cloned into BamHI/NotI sites of MC276. The renilla luciferase construct is described in Souopgui et al. (2008) and was kindly provided by J. Souobgui. His-MS2BP and MS2-PABP in pCS2+MT vector were kindly provided by M. Püschel. Celf1 and Tia1 were amplified from plasmid templates with oligonucleotides containing NheI and XhoI restriction sites (Table 2.3) and cloned into MS2-PCS2+MT. The firefly luciferase construct used for the MS2 tethering assay contains MS2 binding sites in its 3'UTR and was kindly provided by S. Koch. All constructs used for luciferase assays are listed in Table 2.19.

Constructs used to prepare *in situ* antisense probes

The lacZ dnd1-LE fragment in pGEM-T easy vector was kindly provided by M. Claußen. The zebrafish cyclin b1 and dazl fragments in pGEM-T were kindly provided by R. Dosch and the syntabulin fragment was amplified from oocyte cDNA and cloned into pGEM-T easy. These constructs are listed in Table 2.20.

2.6.2. Plasmid DNA isolation and purification

Plasmid DNA in analytical amounts (miniprep) was isolated using the illustraTM plasmidPrep MiniSpin Kit (GE Healthcare) and Plasmid DNA in preparative amounts (midiprep) was isolated using the Plasmid Midi Kit (Qiagen) according to manufacturer's instructions.

2.6.3. DNA restriction digestion

DNA was digested using restriction enzymes (Thermo Scientific) according to manufacturer's instructions

2.6.4. Agarose gel electrophoresis

DNA/RNA fragments were separated using standard agarose gel electrophoresis (Fisher and Dingman, 1971; Helling et al., 1974) in 1x TAE buffer and DNA/RNA was visualized using 0.5 µg/ml ethidium bromide (Sharp et al., 1973).

2.6.5. Polymerase chain reaction

DNA fragments were amplified by standard PCR reactions (Bartlett and Stirling, 2003) using DreamTaq polymerase (Thermo Scientific) or GoTaq polymerase (Promega) for analytical amplifications and High Fidelity PCR Enzyme Mix (Thermo Scientific) or *Pfu*Ultra HS II (Agilent Technologies) for amplifications with downstream cloning procedures according to manufacturer's instructions.

2.6.6. DNA ligation

DNA fragments were ligated using T4 Ligase (Thermo Scientific) according to manufacturer's instructions.

2.6.7. Transformation of bacteria

Chemical transformation of bacteria was performed according to Mandel and Higa (1970). Cells were thawed and incubated with 100 ng of plasmid DNA or 5 µl of a ligation reaction for 30 min on ice. A heat shock was performed for 90 sec at 42 °C, and cells were incubated on ice for 2 min. Cells were then supplemented with LB medium, cultivated for 30 min at 37 °C with shaking and plated on LB-agar supplemented with antibiotics.

2.6.8. DNA sequencing

DNA sequencing was performed according to Sanger et al. (1977) using the Big DyeTMTerminator Kit (Applied Biosystems) according to manufacturer's instructions and an ABI 3100 Automated Capillary DNA Sequencer (Applied Biosystems).

2.6.9. DNA extraction of zebrafish fin clips

DNA extraction of adult zebrafish tail fin clips was done by Proteinase K digestion. Fin clips were lysed in 100 µl lysis buffer at 55 °C for 1 h. Proteinase K was inactivated at 95 °C for 10 min, and the reaction was cooled down to 4 °C and centrifuged at 3000 rpm for 5 min. The DNA solution was stored at -20 °C until use.

2.6.10. Evaluation of mutation efficiency by T7 endonuclease 1 (T7E1) assay

The *celf1* mutation efficiency in CRISPR/Cas treated zebrafish was estimated using the T7 Endonuclease I assay as described before (Reyon et al., 2012; Hwang et al., 2013). In brief, the genomic target region in *celf1* (exon 4) was amplified with oligonucleotides designed to anneal approximately 200 bp up- and downstream of the expected restriction site (Table 2.11). 2 µl of gDNA from embryos or fin clips were applied in a 50 µl PCR reaction using GoTaq polymerase (Promega) according to manufacturer's instructions. The PCR program was as followed: 2 min at 95 °C followed by 33 cycles of 30 sec at 95 °C, 30 sec at 52 °C and 30 sec at 72 °C and final 2 min at 72 °C. The PCR on fin clips was done in a two step nested PCR using the outer oligonucleotides DO181/182 (Table 2.11) in a first PCR reaction. 1 µl of a 1:3 dilution of this PCR product was used as template in a second PCR with the inner oligonucleotides DO171/172 (Table 2.11). PCR products of the second PCR were purified using the Invisorb Fragment Cleanup kit (Invitek) and eluted in 20 µl of 10 mM Tris-HCl (pH 7.5). 200 ng of purified PCR product were then denatured and re-annealed in NEBuffer 2 (New England Biolabs, M0302) using a thermocycler and the following protocol: 95 °C for 5 min; 95–85 °C at −2 °C/s; 85–25 °C at −0.1 °C/s; hold at 4 °C. Hybridized PCR products were treated with 10 U of T7 Endonuclease I (New England Biolabs) at 37 °C for 1 h in a reaction volume of 20 µl and subsequently visualized on a 1 % agarose gel. Mutation efficiency was estimated by visual inspection of cleaved DNA fractions, and adult fish were divided into groups of individuals with high, intermediate, low and no detectable mutation rates.

2.6.11. Sequence confirmation of somatic *celf1* gene mutations

Two PCR products of zebrafish showing high, intermediate, low or no mutation efficiency in the T7EI assay were chosen for confirmation via Sanger sequencing. PCR products corresponding to these fish were cloned into pGEM-T easy vector and transformed into XL1-blue cells. Plasmid DNA was isolated from multiple colonies of each transformation and sequenced using T7 oligonucleotides (Table 2.2).

2.6.12. Evaluation of germline mutation efficiency in female zebrafish

Female zebrafish were anesthetized in 0.02 % tricaine, and unfertilized eggs were obtained by slightly pressing the abdomen region. From each fish, 20 eggs were used for DNA extraction using the DNeasy Blood and Tissue Kit (Qiagen) according to manufacturer's instructions. To amplify the exon 4 region in *celf1*, approximately 200 ng of genomic DNA were used in a first 12.5 µl PCR reaction using the outer oligonucleotides DO181/182 (Table 2.11), GoTaq polymerase (Promega) according to manufacturer's instructions and the PCR program as follows: 2 min at 95 °C followed by 40 cycles of 30 sec at 95 °C, 30 sec at 50 °C and 30 sec at 72 °C and a final 2 min step at 72 °C. 1 µl of a 1:3 dilution of this PCR product was used as template in a second PCR with the inner oligonucleotides DO171/172 (Table 2.11) using the PCR program described above. PCR products were purified using the Invisorb Fragment Cleanup kit (Invitek) and cloned into pGEM-T easy. From each PCR product, approximately 10 clones were sequenced.

2.6.13. Genotyping of zebrafish line sa11143

Genomic DNA was extracted from fin clips as described above. The target region in *celf1* exon 10 was amplified as described for T7E1 assay using outer oligonucleotides DO186/187 (Table 2.12). The PCR product was diluted 1:3 and 1 µl was used as template in a second PCR reaction with the inner oligonucleotides DO188/184 and the forward oligonucleotide containing a T7 sequence (Table 2.12). PCR products were purified using Invisorb Fragment Cleanup kit (Invitek), eluted in 20 µl of 10 mM Tris-HCl pH 7.5 and sequenced using T7 oligonucleotides (Table 2.2). Heterozygous fish were identified by single nucleotide polymorphisms in the sequence chromatogram.

2.7. RNA methods

2.7.1. *In vitro* transcription and labeling of RNAs

Labeled RNA transcription

Labeled RNAs for oocyte injection or co-immunoprecipitations were synthesized from linear pGEM-T easy vector (Promega) using 20 U of T7 or T3 RNA polymerase (Thermo Scientific) in a 25 µl reaction volume containing 10 nmol rATP, rCTP, rGTP, 6.4 nmol rUTPs and 3.5 nmol Cyanine-3-UTP (Perkin ELmer, NEL582) or 1 nmol Aminoallyl-UTP-ATTO-633 (Jena Bioscience, NU-821-633), 1x transcription buffer, 30 mM DTT, 40 U Ribolock RNase inhibitor

(Thermo Scientific). Reactions were incubated overnight at 37 °C. Digoxygenin- (DIG) or fluorescein- (Flu) labeled antisense RNAs for *in situ* hybridization were synthesized from linear vectors using T7 or Sp6 RNA polymerase in a 25 µl reaction volume as described above and 10 nmol rATP, rCTP, rGTP, 6.4 nmol rUTPs and 3.5 nmol DIG/Flu r-UTPs (Boehringer). Reactions were incubated at 37 °C for 3 h. DNA templates were degraded by addition of 1 µl of Turbo DNase (Ambion) and incubation at 37 °C for 15 min. Labeled RNAs were purified using the "RNeasy® Mini" kit (Qiagen) according to manufacturer's instructions.

Capped RNA transcription

In vitro transcription of capped RNAs was done from linearized vectors using mMessage mMachine Sp6 Kit (Ambion) according to manufacturer's instructions. Capped RNAs were purified using the Illustra RNASpin Mini kit (GE Healthcare).

sgRNA and *cas9* RNA transcription

sgRNAs were transcribed using the MAXIscript T7 kit (Life Technologies) from DraI-digested sgRNA expression vector templates. The *cas9* RNA was transcribed using the mMESSAGE mMACHINE T7 kit (Life Technologies) from Acc651-digested pCasX expression vector (Blitz et al., 2013). Following completion of transcription after 3-4 h, Turbo DNase (Ambion) treatment was performed at 37 °C for 15 min. Both the sgRNA and the Cas9 encoding RNA were then purified by Qiagen column and eluted in RNase-free water.

2.7.2. Co-immunoprecipitation of Cy3-labeled RNAs

Co-immunoprecipitation of Cy3-labeled RNAs was done as described in Claussen et al. (2011). In brief, 35 ng of each Cy3-labeled RNA, 11.5 µl *in vitro* transcribed protein (Chapter 2.8.2), 10 µg yeast RNA (Ambion) and 1x UV crosslinking buffer were mixed in a 20 µl reaction volume and incubated at RT for 30 min. Complexes were bound to anti-Flag M2 affinity gel (Sigma) in 500 µl YSS buffer (Kress et al., 2004) at 4 °C for 1 h. The affinity gel was washed 4 times with 800 µl YSS buffer and all reaction were supplemented with 1 µl glycogen (5 mg/ml, Ambion) and 20 µl 10 % SDS. RNAs were purified from supernatant fractions (2/5 of total binding reaction) and bound fractions by phenol-chloroform extraction and they were subsequently precipitated by adding 40 µl ammonium acetate and 500 µl ethanol and incubation at -20 °C overnight. RNAs were separated by urea-PAGE (8 % acrylamide, 7 M urea, 1x TBE) (Albright and Slatko, 2001) and fluorescence was detected using a phosphor imager (Typhoon 2400, GE healthcare).

2.7.3. Electrophoretic mobility shift assays (EMSA)

To compare binding affinities of wild-type and mutant *dnd1*-LE for different proteins, electrophoretic mobility shift assays were performed essentially as described in Claussen et al. (2011). 0.4 pmol Cy3-labeled wild-type and mutant *dnd1*-LE 5'del1 fragments were incubated with indicated concentrations of recombinant proteins in a 20 µl reaction mix containing 1x UV crosslinking buffer for 30 min at RT. 5 µl EMSA loading dye was added, and the whole volume was loaded on a 1 % agarose TAE buffer gel. The gel was run in 1x TAE buffer at 40 V for 1.5 h, and the RNA was analyzed by a phosphor imager (Typhoon 2400, GE Healthcare). The band intensities of bound and unbound fractions were quantified using ImageQuant 5.2 (Molecular Dynamics), and non-linear curve-fitting and K_D calculations were done using Prism 6 (GraphPad).

2.7.4. Total RNA isolation from *Xenopus* oocytes

Oocytes were homogenized in 400 µl peqGOLD TriFast (PEQLAB) and vortexed for 30 sec. After addition of 80 µl chloroform and further mixing, samples were centrifuged at 13,000 rpm for 10 min at 4 °C. The aqueous phase was transferred to a new tube, mixed with 200 µl chloroform and centrifuged at 13,000 rpm for 10 min at 4 °C. After an additional extraction with 200 µl chloroform the aqueous phase was transferred to a new tube and RNAs were precipitated by addition of 500 µl isopropanol and incubation at -20 °C overnight. Precipitated RNAs were pelleted by centrifugation at 13000 rpm for 30 min at 4 °C. The pellet was washed in 70 % ethanol and air-dried. RNAs were re-dissolved in 12.5 µl water and genomic DNA was digested by incubating with 1U/µl DNaseI (Thermo Scientific) at 37 °C for 1.5 h. RNAs were purified from DNase by phenol-chloroform extraction and precipitated with ammonium acetate/ethanol. After pelleting and washing the RNA as described above, it was re-dissolved in 20 µl water.

2.7.5. Reverse transcription (cDNA synthesis)

cDNA was synthesized from 50-100 ng total RNA in a 10 µl reaction containing 1x Go Flexi buffer (Promega), 5 mM $MgCl_2$, 5 mM dNTP mix, 5 ng random hexamers (Invitrogen), 8 units Ribolock RNase Inhibitor (Thermo Scientific) and 20 units MuLV Reverse Transcriptase (Roche). The reaction performed in a thermocycler using the following program: 20 min at 20 °C, 60 min at 42 °C, 5 min at 95 °C.

2.7.6. Semi-quantitive RT-PCR

For semiquantitative RT-PCR, 3 µl cDNA was used in a 25 µl reaction volume containing 1x Green Go Taq Flexi Buffer (Promega), 1.5 mM $MgCl_2$, 0.5 U Go Taq polymerase and 0.2 µM of each oligonucleotide. The reactions were incubated in a thermocycler using the following conditions: 2 min at 95 °C, 24-28 cycles of 30 sec at 95 °C, 30 sec at 56-58 °C, 30 sec at 72 °C and a final step for 2 min at 72 °C.

2.7.7. Quantitative real time PCR

2.5 µl cDNA were used in a 20 µl reaction containing 1x iQ SYBRGreen Supermix (Biorad) and 0.2 µM of each oligonucleotide. The real-time RT-PCR was performed in 96 well plates using the CFX96 Real-Time PCR Detection System with the following conditions: 3 min at 95 °C, 54 cycles of 10 sec at 95 °C, 15 sec at 56 °C and 30 sec at 72 °C. The copy numbers were calculated based on a plasmid standard dilution series.

2.7.8. Quantitative RNA Co-immunoprecipitation

5 µl anti-Celf1 (anti-CUGBP1, sc-20003, Santa-Cruz Biotechnology, Inc.) or 1 µl anti-Myc (M5546, Sigma) antibodies were bound to 15 µl slurry of gamma bind plus sepharose (GE Healthcare) for 1 h at 4 °C in 1.5 mL IPP145 buffer. The antibody bound beads were washed two times in IPP145 buffer and incubated with extracts of 200 oocytes (stage III/IV) in IPP145 buffer in a 1 ml volume for 1 h at 4 °C. After four washes in IPP145, co-precipitated RNAs were released by addition of 1 % SDS, phenol-chloroform extracted and precipitated by ammonium acetate/ethanol overnight at -20 °C. RNA levels were determined in Celf1 and control IP fractions as well as 10 % of the input by quantitative RT-PCR (see Chapter 2.7.7). Sequences of oligonucleotides used for qPCR amplifications are listed in Table 2.9. The enrichment of localizing RNAs in Celf1-containing RNPs was calculated as described in Arthur et al. (2009).

2.7.9. RNA stability analysis

wild-type and mutant *dnd1*-LE 5'del1 fragments were cloned into pBK-CMV vector containing the firefly luciferase ORF. RNA was transcribed using mMessage mMachine T3 transcription kit (Ambion) from linearized vectors. Reporter RNA constructs of *firefly luciferase* harboring

wild-type or mutant *dnd1*-LE 5'del1 were co-injected with *renilla luciferase* RNA into stage III-IV oocytes and cultured for 24 or 48 h. Injected amounts were 0.05 fmol per oocyte of *firefly* constructs and 0.01 fmol per oocyte of *renilla* RNA. Total RNA was isolated from a pool of five oocytes at each time point. RNA levels of *firefly* reporter constructs and *renilla* were analyzed by qPCR. Sequences of oligonucleotides used for qPCR amplifications are listed in Table 2.9. ΔC_T values were calculated by subtracting C_T values of *renilla* from *firefly* reporter RNAs. $\Delta\Delta C_T$ values were obtained by subtracting the ΔC_T values of *firefly* wild-type *dnd1*-LE from that of *firefly* mutant *dnd1*-LE. Relative fold changes of RNA levels were calculated as $2^{-\Delta\Delta CT}$.

2.7.10. Whole mount *in situ* hybridization (WMISH)

In situ hybridization was performed as described previously (Harland, 1991; Hollemann et al., 1999). Localization of *lacZ*-tagged *dnd1*-LE in oocytes was detected using a digoxygenin-labeled antisense *lacZ* riboprobe. Wild-type or mutant 5'del1 *dnd1*-LE reporter RNAs were detected in embryos using a digoxygenin-labeled antisense *gfp* riboprobe. Localization of endogenous mRNAs in zebrafish oocytes was detected using digoxygenin- or fluorescein-labeled antisense riboprobes against respective mRNAs. In brief, the WMISH procedure was as follows: Embryos or oocytes were rehydrated in PBT and permeabilized with 10 µg/ml Proteinase K in PBT for 2 min (*Xenopus* oocytes), 16 min (*Xenopus* embryos) or 10 min (zebrafish oocytes). Samples were re-fixed in MEMFA for 30 min, washed in PBT and pre-hybridized in hybridization mix for 5-6 h at 65 °C. Hybridization was performed at 65 °C overnight in hybridization mix containing the probe. After one wash step in hybridization mix and three wash steps in 2x SSC at 65 °C, single stranded RNAs were digested by RNase A (1 µl/mL) and RNase T1 (0.033 µl/mL) treatment for 60 min at 37 °C in 2x SSC. After one wash in 2x SSC at RT and a 1 h incubation at 65 °C in 0.2x SSC, samples were transferred to MABT and subsequently blocked in blocking solution for 4-5 h at RT. Binding to alkaline phosphatase coupled anti-digoxygenin antibodies was performed overnight at 4 °C in 1/5000 dilutions in blocking solution. After 6-8 wash steps in MABT at RT, samples were transferred to APB and color development was performed in color reaction solution. For double *in situ* hybridization, the primary antibody was inactivated by two washes in 0.1 M glycine pH 2.2 for 10 min followed by one wash in 2 % blocking solution for 30 min and rotation over night in alkaline phosphatase coupled anti-fluorescein antibody in a 1/5000 dilution in blocking solution at 4 °C. Subsequent wash steps as described above were carried out and the color was developed in color substrate without NBT. Color reactions were stopped by wash steps in water and subsequent methanol series (100 %, 70 %, 50 %, 30 %). Samples were re-fixed

in MEMFA for 30 min and kept at 4 °C.
Following WMISH procedure, *Xenopus* embryos were bleached to remove pigments. After wash steps in 5x SSC, embryos were incubated in bleaching solution for 1 to 2 h. After additional wash steps in 5x SSC, embryos were refixed for 1 h in MEMFA.

2.7.11. Quantitative NanoString nCounter multiplex analysis

RNA samples were analyzed using the nCounter® Gene Expression assay (NanoString Technologies) according to manufacturer's instructions. 500 ng of each RNA sample were incubated for 16 h at 65 °C in hybridization buffer containing the CodeSet, which consists of a reporter and a capture probe. Each reporter probe has a 5' color code signal that is unique for each target RNA analyzed within the CodeSet. After hybridization, the complex was bound by its biotin-labeled capture probe on a streptavidin-coated glass slide and stretched within an electric field. Data acquisition was done by imaging on a digital analyzer. Raw counts were normalized using internal positive controls, and target genes were normalized to the internal housekeeping genes *odc, gapdh, laminB1* and *h4*. For background correction, the mean of 8 negative control counts was added to two times the standard deviation and this sum was substracted from each target gene count. For data processing, the nSolver software v1.1 (NanoString Technologies) was used. The raw and processed data of all analyzed RNAs are shown in Tables S1-S4.

2.8. Protein methods

2.8.1. Protein expression in bacteria

His-tagged recombinant Celf1 and Tia1 were expressed in *E. coli* strain BL21 (DE3), cells were disrupted using a fluidizer and proteins were purified using Ni-NTA columns (Qiagen) essentially as described in Git and Standart (2002). After wash steps with HNTA and MNTA containing 10 mM Imidazol, proteins were eluted in MNTA containing 400 or 1000 mM Imidazol and dialyzed against storage buffer M (Git and Standart, 2002). Proteins were frozen in liquid nitrogen and stored at -80 °C. Quantification of proteins was done using the Bradford assay (Bradford, 1976) and by comparison of coomassie stained protein bands to BSA bands of known quantity.
Recombinant Hnrnpab and Ptbp1 proteins were kindly provided by M. Claußen/H. Wessels and recombinant Elavl1, Elavl2 and Igf2bp3 were kindly provided by M. Claußen.

2.8.2. *In vitro* translation

Proteins were *in vitro* translated in reticulocyte lysate using the TnT® Quick Coupled Transcription/Translation System (Promega) according to manufacturer's instructions. TNT reactions were carried out in a 12.5 µl reaction volume.

2.8.3. Co-immunoprecipitations

For co-immunoprecipitations of proteins from oocyte lysate, oocytes were injected with capped RNA encoding Flag-tagged proteins. After a 24 h incubation at 18 °C in MBSH, 200 oocytes were homogenized in IPP145 buffer. The yolk was removed by a 10 min centrifugation at 4 °C and protein complexes were immuniprecipitated from clear lysate by incubation with Anti-FLAG M2 affinity gel (A2220, Sigma-Aldrich) at 4 °C for 1 h. Precipitated proteins were separated using a 12 % SDS gel and visualized by Western blot.

2.8.4. Phosphatase treatment of oocyte extracts

20 oocytes were homogenized in 50 µl Lambda Phosphatase buffer (NEB) and centrifuged for 10 min at 4 °C. The clear supernatant was supplemented with 5 µl Lambda Phosphatase (NEB) and incubated at 30 °C for 1 h. After the addition of 50 µl 2x SDS loading buffer, extracts were analyzed by SDS-PAGE.

2.8.5. Protein electrophoresis

Proteins were size-separated using SDS-PAGE according to Laemmli (1970) in SDS running buffer on 12 % SDS-gels prepared according to standard methods (Sambrook et al., 2001).

2.8.6. Western blotting

Size separated protein samples were blotted onto nitrocellulose membranes using the Western blot method according to Towbin et al. (1979); (1991). The transfer process was carried out using the BioRad wet blot system according to manufacturer's instructions. Nitrocellulose membranes were blocked in blotting solution at RT for 1 h and primary

antibodies were diluted in 5 % non-fat milk in TBST as follows: rabbit anti-FLAG (F7425; Sigma) 1/500, anti-Celf1 (anti-CUBBP1, sc-20003, Santa-Cruz Biotechnology, Inc.) 1/1000, anti-TIA-1 (sc-1751, Santa-Cruz Biotechnology, Inc.) 1/1000, anti-HuR (Elavl1/2) (sc-5261; Santa Cruz Biotechnology, Inc.) 1/4000, anti-Vg1RBP (Igf2bp3) (Zhang et al., 1999) 1/10000, anti-XStaufen 1 (Allison et al., 2004) 1/10000, and anti-40LoVe (Hnrnpab) (Czaplinski et al., 2005) 1/5000 and incubated at 4 °C overnight. Protein detection was performed using the Enhanced Chemiluminescence (ECL) system (GE Healthcare) or the Odyssey Infrared imaging system (LiCor) according to manufacturer's instructions. For the protein detection using the Odyssey Infrared-system, secondary donkey anti-mouse or anti-rabbit IRDye 680 or 800 (LiCor) were used at 1/20000 dilutions in TBST and they were incubated at RT for 1 h. For the protein detection using the ECL-system, secondary horseradish peroxidase-coupled anti-mouse (Santa Cruz) and anti-rabbit (Cell Signaling) antibodies were used at 1/10000 and 1/3000 dilutions respectively and they were incubated as described above.

2.8.7. Immunofluorescence staining of *Xenopus* and zebrafish oocytes

Immunostaining was done as described in Gagnon and Mowry (2011a). Primary antibodies were anti-Celf1 (anti-CUGBP1, sc-20003, Santa Cruz), anti-TIA-1 (sc-1751 Santa-Cruz Biotechnology, Inc.) and anti-Vg1RBP (Igf3bp2) (Zhang et al., 1999), rabbit anti-Syntabulin (Nojima et al., 2010) (kindly provided by Masahiko Hibi, Bioscience and Biotechnology Center, Nagoya University, Japan). Secondary antibodies were anti-mouse-Alexa633 (A21052, Invitrogen), anti-goat-Alexa633 (A21082, Invitrogen) and anti-rabbit-Oregon-Green488 (O-11038, Invitrogen). All antibodies were diluted 1/500 in PBT + 2 % horse serum + 2 % BSA, except for anti-Celf1 which was diluted 1/250.

2.9. Oocyte and embryo manipulations

2.9.1. Preparation of *Xenopus laevis* oocytes and extracts

Oocytes were obtained from pigmented or albino *X. laevis*. The ovaries were treated with collagenase at RT for up to 1.5 h in 0.1 mg/ml Liberase (Roche) in collagenase buffer. Isolated oocytes were washed in MBSH, staged according to Dumont (1972) and kept at 18 °C. Oocytes were homogenized in IPP145 buffer, centrifuged 10 min at 4 °C and the clear lysate was transferred to 2x SDS loading buffer or it was used for immunoprecipitations. Nuclei and cytoplasms were dissected manually in IPP145 buffer and homogenized in a 200

µl volume. 1 ml acetone was added and proteins were precipitated at -20 °C for 1 h. After centrifugation for 30 min at 4 °C, protein pellets were dried and resuspended in 2x SDS loading buffer. For Western blot analysis two oocytes or nuclei/cytoplasm were used per lane.

2.9.2. *Xenopus* oocyte injection and localization assay

Oocyte injection was done essentially as described in Claussen and Pieler (2004). For injection of RNA encoding Flag-tagged proteins, 1-1.5 ng capped RNA, if not indicated differently, were injected into the cytoplasm of stage III oocytes in a 3 nl volume. Modified antisense DNA oligos (Table 2.4) were dissolved in water and 10 ng per oocyte were injected in a 3 nl volume. The peptides corresponding to the Celf1 oligomerization domain (amino acids 183-210) or scrambled are described in Cosson et al. (2006) and they were synthesized by JPT Peptide Technologies GmbH (Berlin, Germany). Peptides were dissolved in water at 20 µg/µl and 4 or 40 ng were injected per oocyte in a 2 nl volume.
Pre-injected oocytes were incubated at 18 °C for 24 h in MBSH and then either homogenized or injected with reporter RNA. 75 pg Cy3-labeled *dnd1*-LE or 100 pg *lacZ*-tagged *dnd1*-LE were injected in a 1 nl volume into the oocyte nuclei and oocytes were incubated at 18 °C in vitellogenin-enriched L-15 culture medium. Oocytes for immunofluorescent staining and *in situ* hybridization were fixed after 48 h and oocytes for the RNA localization time-course were fixed after indicated time periods.

2.9.3. *Xenopus* embryo injections and culture

Eggs were obtained from female frogs, injected approximately 16 h before egg-laying with 800-1000 U hCG. Eggs were *in vitro* fertilized with minced testis in 0.1x MBSH, de-jellied with 2 % cysteine-HCl pH 7.5 and cultured in 0.1x MBSH at 12.5 °C. For injections, embryos are transferred into injection buffer and after approximately one hour, embryos were re-transferred into 0.1x MBSH. For WMISH, 2-cell stage embryos were injected vegetally in both blastomeres with indicated amounts of capped RNA and 500 pg *dnd1*-LE reporter RNA in a volume of 4 nl. Embryos were cultivated at 12.5 °C for 6 days and fixed at stages 32-34. For nanostring analyses, embryos were injected in both blastomeres with indicated amounts of capped RNA in a volume of 4 nl, grown until stages 8, 11 or 14 and subjected to total RNA extraction.

2.9.4. Preparation of zebrafish oocytes

Ovaries were dissected from female zebrafish and treated with collagenase for 1 h in 0.1 mg/ml Liberase (Roche) in collagenase buffer. Then, oocytes were fixed in 4 % formaldehyde in PBS at 4 °C overnight and dehydrated in methanol. Oocytes were stored at -20 °C and rehydrated before subjection to *in situ* hybridization or immunofluorescence.

2.9.5. Zebrafish embryo injections

1-cell zebrafish wild-type embryos (ABxTLF) were co-injected with 600 pg RNA encoding Cas9 and 25 pg of respective sgRNA. After 24 h, 30 % of embryos were used for the evaluation of mutation efficiency by T7E1 assay. Remaining embryos were raised to adulthood and mutation efficiencies were analyzed by T7E1 assays with DNA isolated from fin clips.

2.9.6. Luciferase assays

The MS2-tethering assay was done essentially as described in Minshall and Standart (2004). In brief, 2.5 fmol RNA encoding MS2-fusion proteins were injected per oocyte. After 24 h of incubation in MBSH at 18 °C, 0.05 fmol RNA encoding firefly luciferase fused to MS2 binding-sites were co-injected together with 0.01 fmol *renilla luciferase* RNA. After additional 24 h of incubation, the luciferase activities were measured in a luminometer (Berthold) using the Dual-GloTM Luciferase Assay System (Promega) according to manufacturer's instructions. Renilla luciferase activities were used as internal standards.
For analyses of the translational effects of mutated versions of *dnd1*-LE, 0.05 fmol RNA encoding firefly luciferase fused to wild-type or mutant *dnd1*-LE versions or the *gdf1* translational control element (VTE) (Colegrove-Otero et al., 2005) were co-injected together with 0.01 fmol *renilla luciferase* RNA per oocyte. Luciferase activities were measured as described above.

3. Results

3.1. Celf1 and Tia1 are novel components of vegetal localization complexes in *Xenopus* oocytes

3.1.1. Celf1 and Tia1 form one complex with known vegetal localization factors

Celf1 and Tia1 were identified to interact with a vegetally localizing RNA in *Xenopus* oocytes. In order to verify the association of Celf1 and Tia1 with vegetal localization RNPs, Flag-tagged Celf1 and Tia1 proteins were expressed in transport competent stage III/IV oocytes and immuno-precipitated from corresponding oocyte extracts. Like the previously characterized vegetal localization factor Ptbp1 (Cote et al., 1999), Celf1 and Tia1 co-precipitate the known localization factors Stau1, Igf2bp3, Elavl1/2 and Hnrnpab (Figure 3.1). Thus, Celf1 and Tia1 are indeed components of vegetal localization RNPs in *Xenopus* oocytes. RNAse treatment of corresponding oocyte extracts abolished co-precipitation of known localization factors (Figure 3.1), indicating that Celf1 and Tia1 interact with these known localization factors via an RNA scaffold.

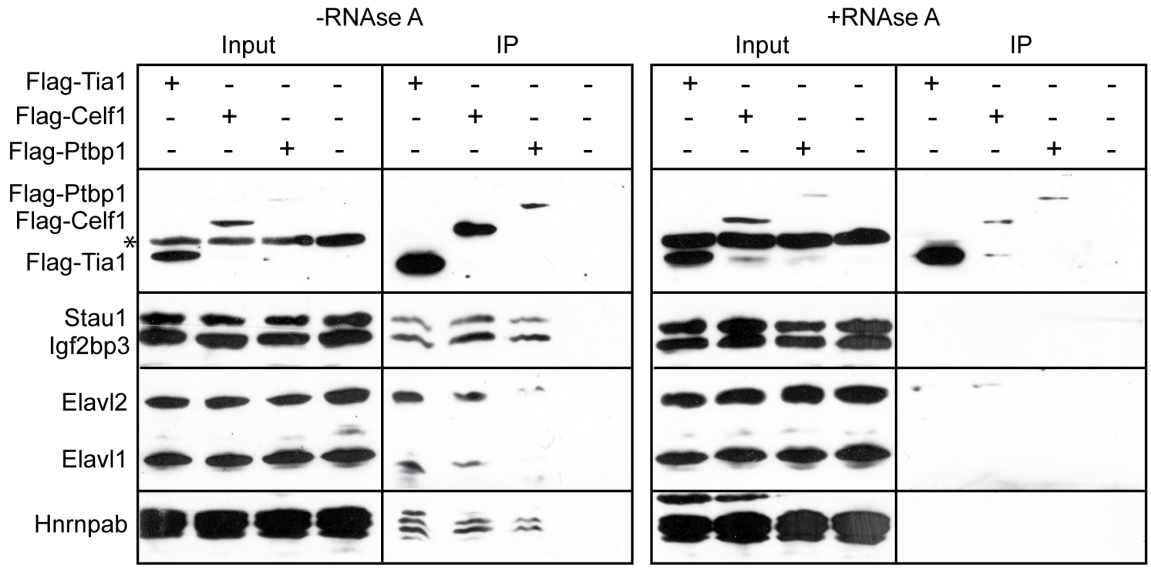

Figure 3.1. Celf1 and Tia1 co-precipitate known localization RNP complex components in *Xenopus* oocytes. Western blot analysis for co-precipitation of known localization complex components with Flag-tagged Tia1, Celf1 and Ptbp1 in the absence or presence of RNase. Extracts of uninjected oocytes served as negative controls. The asterisk indicates an unspecific protein band caused by cross reactions of the anti-Flag antibody

3.1.2. Celf1 and Tia1 are predominantly located in the cytoplasm and co-localize with *dnd1*-LE at the vegetal cortex

In order to analyze endogenous protein levels of Celf1 and Tia1 during oogenesis, extracts of staged oocytes were analyzed by Western blot using Celf1- or Tia1-antibodies. Endogenous Celf1 is detected throughout oogenesis and embryogenesis (Figure 3.2A). The reduced electrophoretic mobility of Celf1 after oocyte maturation has been reported to be caused by Celf1 phosphorylation (Detivaud et al., 2003). However, Celf1 protein bands appear as doublets throughout oogenesis and embryogenesis (Figure 3.2A). Phosphatase treatment of stage III and VI oocyte extracts abolished the slower migrating band (Figure S5), indicating that a fraction of Celf1 might be partially phosphorylated throughout oogenesis and embryogenesis. Two isoforms of Tia1 are generated by alternative splicing, Tia1a and Tia1b of 43 and 40 kDa, respectively (Beck et al., 1996; Figure 1.10). Both Tia1a and Tia1b are detected throughout oogenesis and embryonic development with highest protein levels during later stages of oogenesis and embryogenesis (Figure 3.2A).

Celf1 and Tia1 orthologs are detected in nuclei and cytoplasm of different cell types (Kedersha et al., 1999; Ladd and Cooper, 2004; Zhang et al., 2005). To examine the subcellular distributions of Celf1 and Tia1 in *Xenopus* oocytes, endogenous protein levels were analyzed in nuclear and cytoplasmic fractions of staged oocytes by Western blot. Celf1 is detected in the cytoplasm, but not in the nucleus, throughout oogenesis (Figure 3.2B). Tia1 is predominantly detected in cytoplasmic extracts with a minor fraction in the nuclear extracts of late stage oocytes (Figure 3.2B). Igf2bp3 has been shown to be predominantly localized in the cytoplasm (Loeber et al., 2010) and Hnrnpab to be enriched in the nucleus (Czaplinski et al., 2005). Thus, immuno-blots for Igf2bp3 and Hnrnpab served as loading controls for cytoplasmic and nuclear fractions, respectively (Figure 3.2B).

In order to analyze the intracellular distributions of Tia1 and Celf1 in oocytes in more detail, immunostaining of endogenous Celf1 and Tia1 in stage III albino oocytes was performed. To detect a potential co-localization of these proteins with vegetally localizing RNAs, oocytes were injected with Cy3-labeled *dnd1*-LE RNA prior to immunostaining and protein and RNA signals were analyzed by confocal microscopy. Cy3-*dnd1*-LE RNA is detected in granular structures in the vegetal cytoplasm and at the vegetal cortex (Figure 3.2C, D). Both Celf1 and Tia1 co-localize with Cy3-*dnd1*-LE-RNA at the vegetal cortex and in the more vegetally located granular structures (Figure 3.2C). Tia1 protein signals are additionally detected as small particles, which appear to be attached to the RNA granules (Figure 3.2C). Co-staining of Celf1 together with the localization factor Igf2bp3 revealed co-localization with Cy3-*dnd1*-

LE in the vegetal granules and at the vegetal cortex (Figure 3.2D). In summary, these results show that Celf1 and Tia1 are predominantly located in the cytoplasm and they co-localize with vegetally localizing RNA in *Xenopus* oocytes.

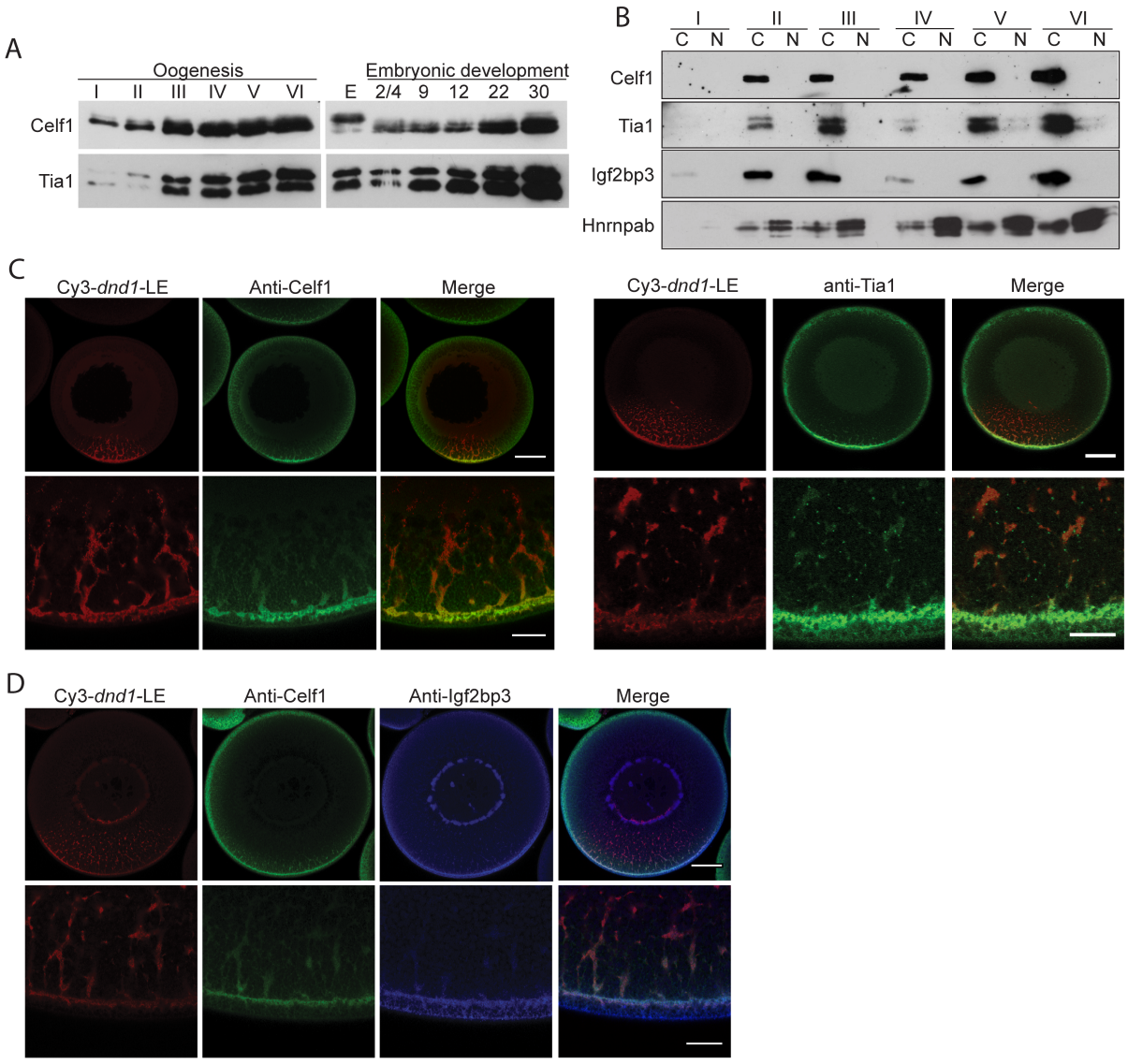

Figure 3.2. Celf1 and Tia1 are predominantly cytoplasmic and co-localize with *dnd1*-LE at the vegetal cortex of *Xenopus* oocytes. A) Temporal analysis of endogenous Celf1 and Tia1 protein expression during *Xenopus* oogenesis and embryogenesis. Celf1 and Tia1 were detected by Western blot using equivalent amounts of oocyte, egg (E) and embryonic extracts of indicated stages. B) Analysis of nuclear/cytoplasmic distributions of Celf1 and Tia1 in *Xenopus* oocytes. Endogenous Tia1 and Celf1 were detected by Western blot using equivalent amounts of nuclear (N) and cytoplasmic (C) extracts of staged oocytes. Igf2bp3 and Hnrnpab served as controls for a predominantly cytoplasmic or nuclear protein, respectively. C) Analysis of intracellular protein distribution and co-localization of Celf1 and Tia1 with vegetal RNA. Immunostainings of Celf1 and Tia1 were performed with stage III oocytes that were pre-injected with Cy3-*dnd1*-LE RNA. D) Analysis of Celf1 co-localization with the known localization factor Igf2bp3. Co-immunostaining of Celf1 and Igf2bp3 was performed with stage III oocytes that were pre-injected with Cy3-*dnd1*-LE RNA. Scale bars indicate 100 µm for whole oocytes and 20 µm for the magnified vegetal cortex.

3.2. Celf1 participates in vegetal localization of *dnd1*-LE

3.2.1. Celf1 and Tia1 bind to the 5' region of *dnd1*-LE

The identification of Celf1 and Tia1 by an RNA affinity purification using the *dnd1*-LE RNA suggests a direct or indirect interaction with this RNA. In order to analyze if Celf1 and Tia1 directly bind to the *dnd1*-LE and to determine the regions within the *dnd1*-LE that are critical for Celf1 and Tia1 binding, *in vitro* binding studies with *in vitro* translated Flag-tagged proteins (Figure 3.3B) and Cy3-labeled full length and truncated fragments of *dnd1*-LE were performed (Figure 3.3A). These experiments revealed that 5' deletions of *dnd1*-LE beyond nucleotide 40 (5'del2) results in loss of Tia1 binding, while 3' deletions up to nucleotide 106 (3'del5) maintained Tia1 binding (Figure 3.3A). Thus, the region critical for Tia1 binding is located between nucleotides 40-106 (Figure 3.3A). Celf1 binding to *dnd1*-LE is lost with 5' deletions of nucleotides 86-116 (5'del3) and 3' deletions beyond nucleotide 145 (3'del5), delineating the region critical for Celf1 binding to nucleotides 86 to 145 (Figure 3.3A). Thus, Tia1 and Celf1 binding requires adjacent and overlapping regions in the 5' part of the *dnd1*-LE.

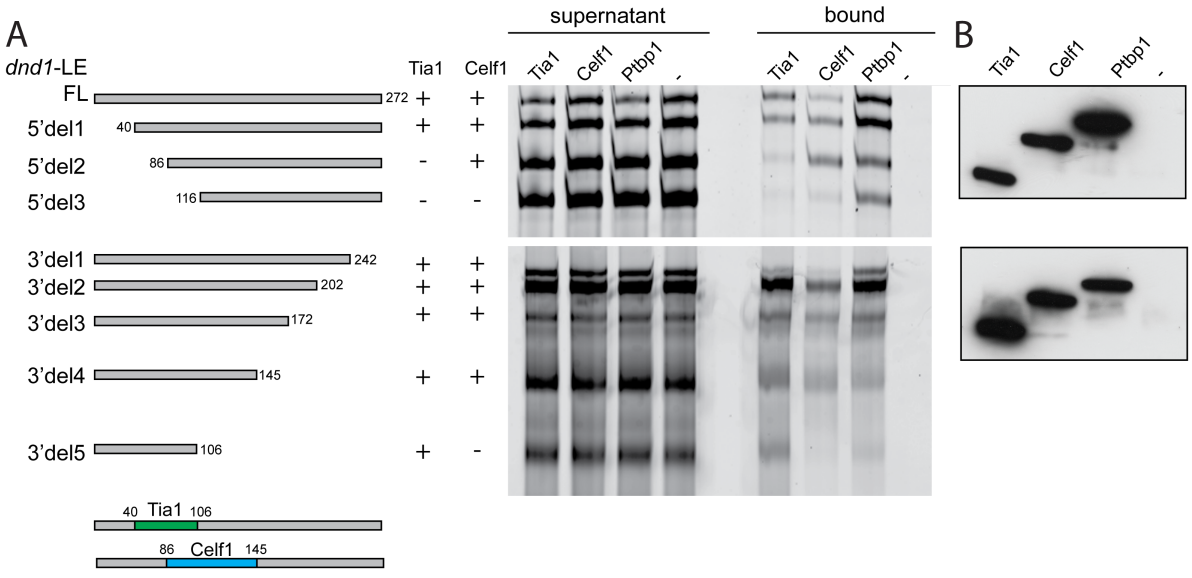

Figure 3.3. Celf1 and Tia1 binding requires the 5' region of the *dnd1*-LE. *In vitro* interaction analysis of Tia1 and Celf1 with full length (FL) and 5'- and 3'- deleted fragments of *dnd1*-LE. Cy3-labeled LE RNAs were co-immunoprecipitated with *in vitro* translated Flag-tagged Tia1, Celf1 and Ptbp1. Unprogrammed reticulocyte lysate served as negative control (-). The region critical for Tia1 binding is located between nucleotides 40 and 106 (green box) and the region critical for Celf1 binding is located between nucleotides 86 and 145 (blue box). B) Expression control for *in vitro* translated Flag-tagged proteins used in A). Proteins were detected by anti-Flag Western blotting.

3.2.2. *dnd1*-LE mutagenesis interferes with binding of Celf1 and Tia1

The region within the *dnd1*-LE that is critical for Celf1 binding contains several "UGU" motifs embedded in uracil-rich regions (Figure 3.4A). Indeed, Celf1 was reported to bind "UG"-rich sequences (Marquis et al., 2006; Edwards et al., 2011). In order to create a mutant version of the *dnd1*-LE that is deficient in Celf1 binding, several uracil/cytosine bases in the region of *dnd1*-LE that is critical for Celf1 binding were substituted for adenines (Figure 3.4A). Since the 5'del1 truncated *dnd1*-LE fragment shows full localization activity (data not shown), the effect of point mutations was analyzed using this 232 nucleotide 5'del1 *dnd1*-LE fragment (Figure 3.4A, B). Celf1 affinity for this mutant *dnd1*-LE version (mut_{Celf1}) in comparison to the wild-type *dnd1*-LE was analyzed by electrophoretic mobility shift assays (EMSA) using bacterially expressed proteins and Cy3-labeled RNAs (Figure S2A-C). Binding of Celf1 to mut_{Celf1} *dnd1*-LE is significantly reduced, with a dissociation constant (K_D) approximately three fold increased as compared to the wild-type version (Figure 3.4B). Other localization factors bind to mut_{Celf1} *dnd1*-LE with approximate the same affinity as to wild-type *dnd1*-LE (Figure 3.4B). Thus, the mutation of multiple "UGU" motifs within the Celf1 binding site creates a mutant version of the *dnd1*-LE that is specifically reduced in binding Celf1 but maintains high affinity binding to other localization factors.

The region in the *dnd1*-LE that is critical for Tia1 binding exhibits several adenines within uracil-rich stretches (Figure 3.4A). Such motifs are described as AU-rich elements (ARE) and they serve as binding sites for multiple proteins involved in gene regulation including Tia1 proteins (Dember et al., 1996; Piecyk et al., 2000; Barreau et. al., 2005; López de Silanes et al., 2005). In order to create a mutant version of the *dnd1*-LE that is deficient in Tia1 binding, several uracil to adenine point mutations were introduced into the critical region for Tia1 binding (Figure 3.4A). The effect of these mutations on Tia1 binding was analyzed in the context of the 232 nucleotide 5'del1 *dnd1*-LE (Figure 3.3A, 3.4C) as described above. The *dnd1*-LE that is mutated in the critical region for Tia1 binding (mut_{Tia1}) has reduced affinity for Tia1 with a K_D approximately 5 fold increased as compared to the wild-type *dnd1*-LE (Figure 3.4C). As the localization factor Elavl2 binds to same AU-rich region in the *dnd1*-LE as Tia1 (Arthur et al., 2009), binding affinities of Elavl2 to mut_{Tia1} *dnd1*-LE were analyzed. The mut_{Tia1} *dnd1*-LE also shows reduced affinity for Elavl2 (Figure 3.4C). However, although *dnd1*-LE mut_{Tia1} has reduced affinity for Tia1 and Elavl2, this RNA shows full localization capacity, when injected in oocytes (data not shown). This observation indicates that efficient binding of Tia1 could to be dispensable or that low affinity binding of Tia1 is sufficient for the vegetal localization of *dnd1*-LE RNA. In summary, mutagenesis of the Celf1 binding site in the *dnd1*-LE reduces binding of Celf1, but retains binding of other localization factors. Mutagenesis of

the Tia1 binding site reduces binding of Tia1 as well as Elavl2. However, mut_{Tia1} *dnd1*-LE shows full localization capacity, when injected in oocytes. The localization activity of the *dnd1*-LE with reduced affinity for Celf1 binding (mut_{Celf1}) is analyzed in further detail in Chapter 3.2.3.

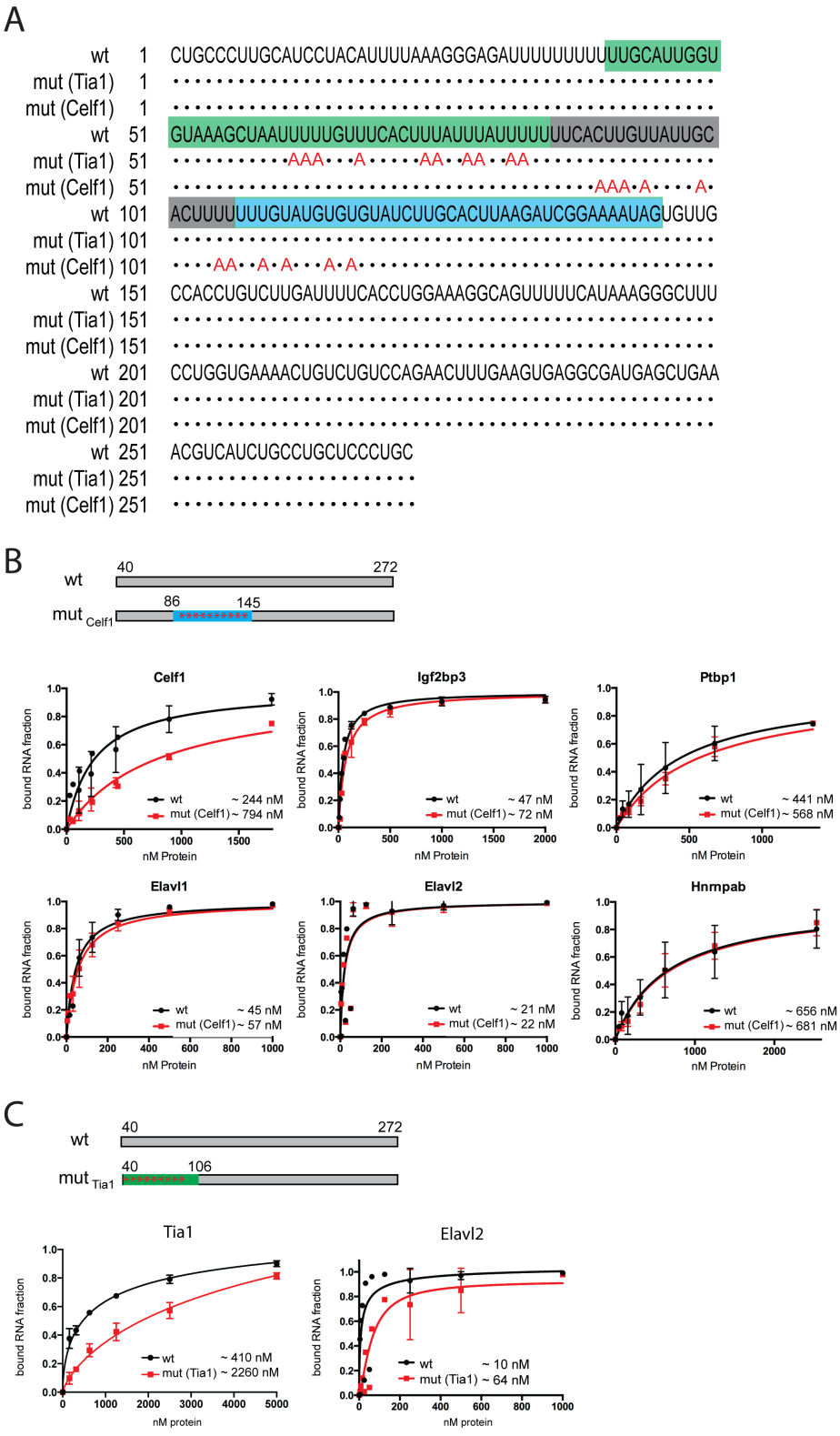

Figure 3.4. *dnd1*-LE mutagenesis of the Celf1 binding-site reduces Celf1 binding, but mutagenesis of the Tia1 binding-site also affects Elavl2 binding. A) Sequence of full length wild-type (wt) and two mutant versions of *dnd1*-LE created by replacing single uracil or cytosin bases by adenins (red letters) in the Celf1 binding site (blue box) or in the Tia1 binding site (green box). The overlapping binding sites of Celf1 and Tia1 are boxed in grey. B)-C) Binding affinities of bacterially expressed proteins to the versions of *dnd1*-LE mutated in the Celf1 binding site (mut_{Celf1}) or mutated in the Tia1 binding site (mut_{Tia1}) were compared to wild-type (wt) *dnd1*-LE by electrophoretic mobility shift assays.

3.2.3. Efficient binding of Celf1 to *dnd1*-LE RNA is required for vegetal RNA localization

In order to analyze if efficient binding of Celf1 is required for RNA localization, the mutant *dnd1*-LE that has reduced affinity for Celf1 (mut_{Celf1}) was tested for the ability to localize in oocytes. Cy3-labeled wild-type and mut_{Celf1} *dnd1*-LE RNAs were injected into stage III oocytes and their localization was visualized after different time periods in fixed oocytes by confocal microscopy. Both wild-type and mut_{Celf1} *dnd1*-LE are exported from the nucleus after 2-5 hours (Figure 3.5A). Approximately five hours after injection, wild-type *dnd1*-LE starts to localize to the wedge-shaped region in the vegetal hemisphere and it is highly enriched in vegetal granules after 48 hours (Figure 3.5A). In contrast, mut_{Celf1} *dnd1*-LE RNA becomes more slowly enriched in the wedge-shaped region and after 48 hours a high proportion of this RNA is still distributed in the cytoplasm (Figure 3.5A). Quantification of RNA enrichment at the vegetal cortex shows that, after 48 hours, wild-type *dnd1*-LE is highly enriched, while mut_{Celf1} *dnd1*-LE is only slightly enriched at the vegetal cortex (Figure 3.5B). In order to compare the RNA stability of both *dnd1*-LE versions, reporter RNAs that contain wild-type or mut_{Celf1} *dnd1*-LE were analyzed by qPCR at 0-48 hours after injection. Similar RNA levels of wild-type and mut_{Celf1} *dnd1*-LE show that *dnd1*-LE mutagenesis does not affect RNA stability (Figure 3.5C). In order to control for variations in the localization capacity of oocytes, localization efficiencies of differently labeled wild-type and mut_{Celf1} *dnd1*-LE RNAs were analyzed by co-injection into the same oocyte. Cy3- and Atto633-labeled wild-type *dnd1*-LE RNAs localize with high efficiency (Figure 3.5D, E). However, Atto633-labeled RNAs are slightly reduced in localization activity as compared to Cy3-labeled RNAs (Figure 3.5D, E). Still, mut_{Celf1} *dnd1*-LE RNA shows impaired localization efficiency as compared to wild-type *dnd1*-LE (Figure 3.5D, E). In summary, mutations in *dnd1*-LE RNA that reduce Celf1 binding, significantly interfere with RNA localization activity in *Xenopus* oocytes. This result argues for a critical role of Celf1 during vegetal transport of the *dnd1*-LE.

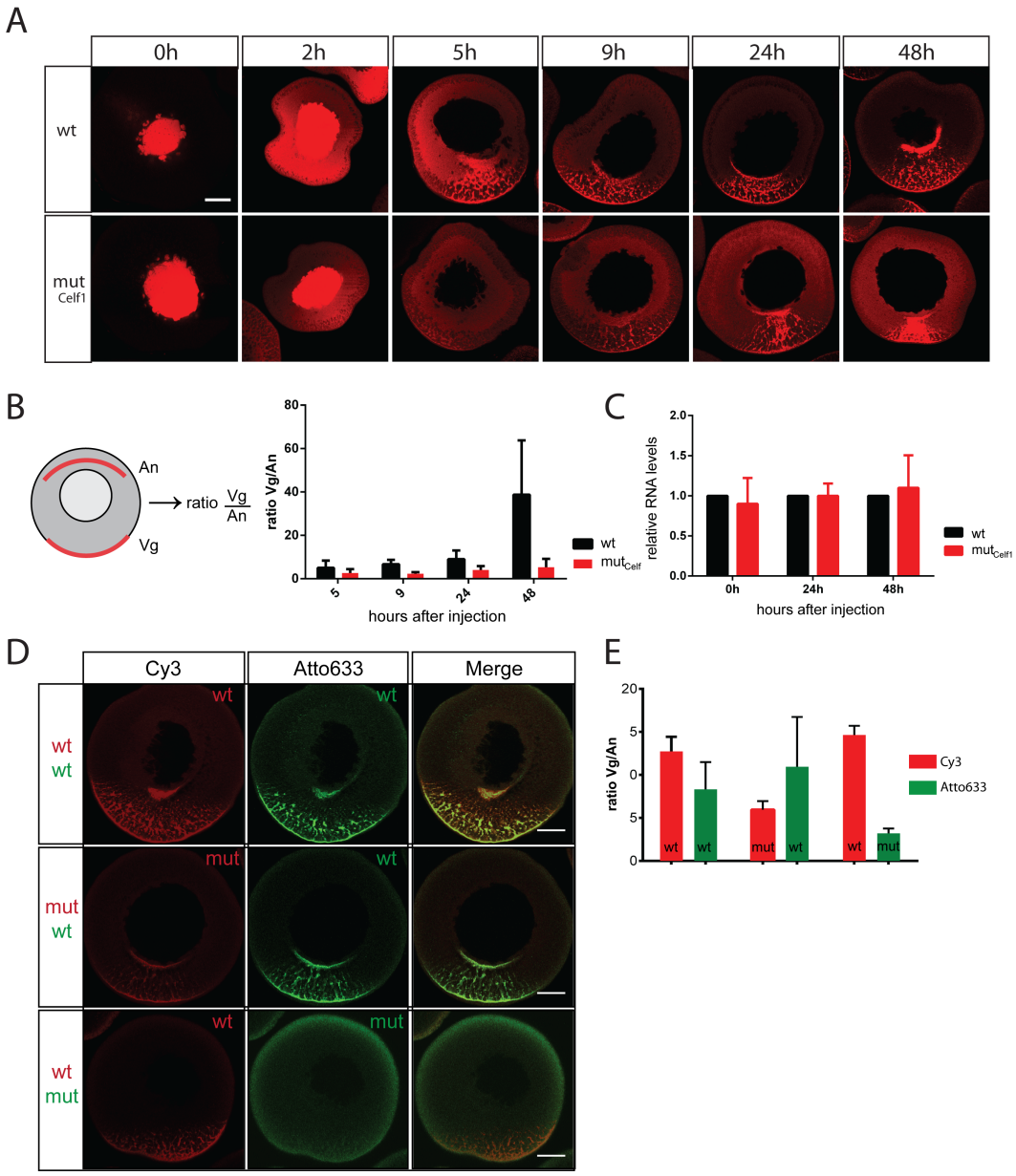

Figure 3.5. Efficient binding of Celf1 is required for vegetal localization of *dnd1*-LE in *Xenopus* oocytes. A) A Cy3-labeled wild-type (wt) and mutant version of the *dnd1*-LE with reduced affinity for Celf1 (mut_{Celf1}) were injected into the nucleus of stage III oocytes, they were fixed after 0-48 hours, and analyzed by confocal microscopy. B) Vegetal RNA enrichments of wild-type and mutant *dnd1*-LEs in oocytes that were fixed after 5-48 hours were estimated by measuring the ratio of the mean fluorescence along a line at the vegetal cortex (Vg) versus a line in the animal cytoplasm (An). Error bars indicate standard deviation of approx. 10 oocytes. C) RNA stability analysis of wild-type and mutant *dnd1*-LE RNAs. Wild-type (wt) and mutant (mut_{Celf1}) *dnd1*-LE reporter RNAs fused to the *firefly luciferase* ORF were co-injected with *renilla luciferase* RNA into stage III oocytes and incubated for 0-48 hours. *firefly luciferase* reporter RNA levels were analyzed by qPCR and normalized to *renilla luciferase* RNA levels; wild-type *dnd1*-LE reporter RNA levels were set to 1. Mean values from three independent experiments are shown, the error bars indicate standard error of the mean. D) Wild-type (wt) and mutant (mut) Cy3- (shown in red) and Atto633-labeled (shown in green) *dnd1*-LE RNAs were co-injected into stage III oocytes. Oocytes were fixed after 48 hours. Scale bars indicate 100 µm. E) Localization efficiency of wild-type (wt) and mutant (mut) *dnd1*-LE was quantified as shown in B). Mean values from three independent experiments are shown, the error bars indicate standard error of the mean.

3.2.4. Low protein turn over rates prevent depletion of maternal Celf1

In order to further support a function of Celf1 in RNA localization, the depletion of endogenous Celf1 protein was attempted by knock-down of the *celf1* mRNA. Micro-injection of antisense DNA oligonucleotides into stage III/IV oocytes successfully depleted endogenous *celf1* mRNA (Figure 3.6A). However, Celf1 protein is detected up to 72 hours after injection, indicating a low protein turnover (Figure 3.6B). Although a slight reduction of Celf1 protein levels is observed in oocytes that were *i*njected with the *celf1* antisense oligo, this protein reduction is also observed in oocytes that were injected with a control oligo (Figure 3.6B). This slight reduction in Celf1 protein levels does not affect vegetal localization of *dnd1*-LE (Figure S3). Thus, a low protein turnover prevents effective depletion of maternal Celf1 in *Xenopus* oocytes.

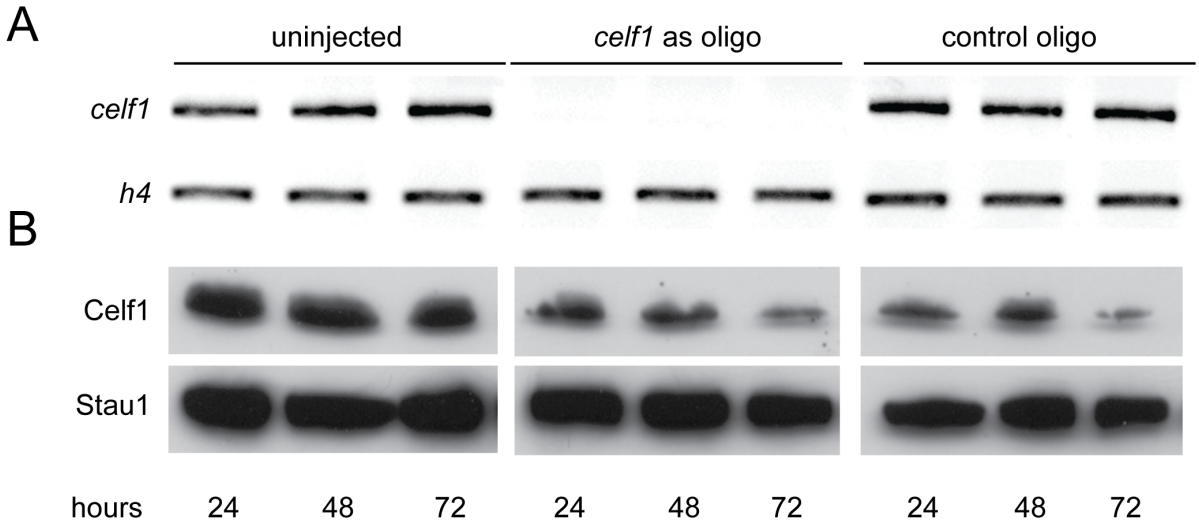

Figure 3.6. Maternal Celf1 has low protein turnover rates. A) A modified *celf1* antisense DNA oligo or a control oligo were injected into *Xenopus* oocytes. After 24, 48 and 72 hours, *celf1* mRNA levels were detected in uninjected, antisense (as) or control oligo injected oocytes by RT-PCR. *h4* mRNA levels served as expression control. B) Celf1 protein levels were detected after 24, 48 and 72 hours by Western blot. Stau1 immuno-blots served as loading control.

3.2.5. Overexpression of Celf1 inhibits vegetal localization of *dnd1*-LE RNA in a dose dependent manner

In an alternative approach to interfere with Celf1 protein function, several mutant versions of Celf1 with deficiencies in oligomerization, nuclear export, RNA binding, or mutants that mimic phosphorylation, were overexpressed in oocytes in order to achieve a dominant negative effect on RNA localization.

Celf1 was reported to be able to oligomerize via a domain in its central region (Cosson et al., 2006). Furthermore, Cosson et al. showed that a peptide corresponding to the oligomerization domain of Celf1 competitively inhibits oligomerization of full length Celf1 (Cosson et al., 2006). The interference with Celf1 oligomerization might affect the assembly of vegetal localization RNPs in oocytes. Thus, we overexpressed a mutant version of Celf1 lacking the oligomerization domain (Figure S4A) and injected the peptide corresponding to this domain in oocytes and analyzed vegetal RNA localization (Figure S4B-F). However, none of these approaches significantly affected vegetal RNA localization (Figure S4D, F).

As mentioned above, Celf1 is phosphorylated after egg maturation (Detivaud et al., 2003) (Figure 3.2A, S5A). Strikingly, phosphorylation of the localization complex component Igf2bp3 upon oocyte maturation correlates with a release of localized *gdf1* mRNA from the vegetal cortex (Git et al., 2009). Thus, the expression of a version of Celf1 that mimics phosphorylation might cause a release of localized RNAs from oocyte cortex. Potential serine, threonine and tyrosine phosphorylation sites within Celf1, as predicted by the Scansite motif scan program (Obenauer et al., 2003) and the NetPhos 2.0 Server (Blom et al., 1999), were mutated to aspartic acid (Figure S5B) that mimic the negative charges of phosphate residues. However, overexpression of this phosphomimetic Celf1 mutant in oocytes did not affected vegetal RNA localization (Figure S5C-E).

Although Celf1 shows predominantly cytoplasmic steady state distribution, Celf1 orthologs have been reported to shuttle between the nucleus and the cytoplasm (Ladd and Cooper, 2004). Assuming a potential role of Celf1 in initiating RNA localization in the nucleus, a mutant version with deficient nuclear export activity might affect vegetal RNA localization by trapping localization RNPs in the nucleus. In order to map regions within the Celf1 protein sequence that contain potential nuclear export activity, different Flag-tagged Celf1 deletion fragments (Figure 3.7A) were expressed in stage III oocytes and their intracellular distribution was detected by anti-Flag immuno-staining (Figure 3.7B). A nuclear localization signal has been detected in the C-terminal region of Celf proteins (Ladd and Cooper, 2004). Indeed, Celf1 lacking the C-terminal region is locates in the cytoplasm, while the C-terminus locates in the nucleus (Figure 3.7B). The deletion of amino acids 119-236 led to a fraction of this protein retained in the nucleus, while further deletions within this region decreased nuclear enrichment (Figure 3.7A, B). Thus, Celf1 contains nuclear export activity in amino acids 119-236. In order to create a mutant version of Celf1 that is trapped in the nucleus, the Celf1 version lacking amino acids 119-236 was fused to a nuclear localization signal (NLS) (Figure S6A). However, it must be pointed out, that this version shows reduced RNA binding ability (data not shown), due to deletion of RRM2. This Celf1 mutant version highly enriches

in the nucleus of stage III oocytes (Figure S6B). However, Cy3-*dnd1*-LE is exported from the cytoplasm and localizes to the vegetal cortex in oocytes that overexpress Celf1 del119-236-NLS (Figure S6B-E).

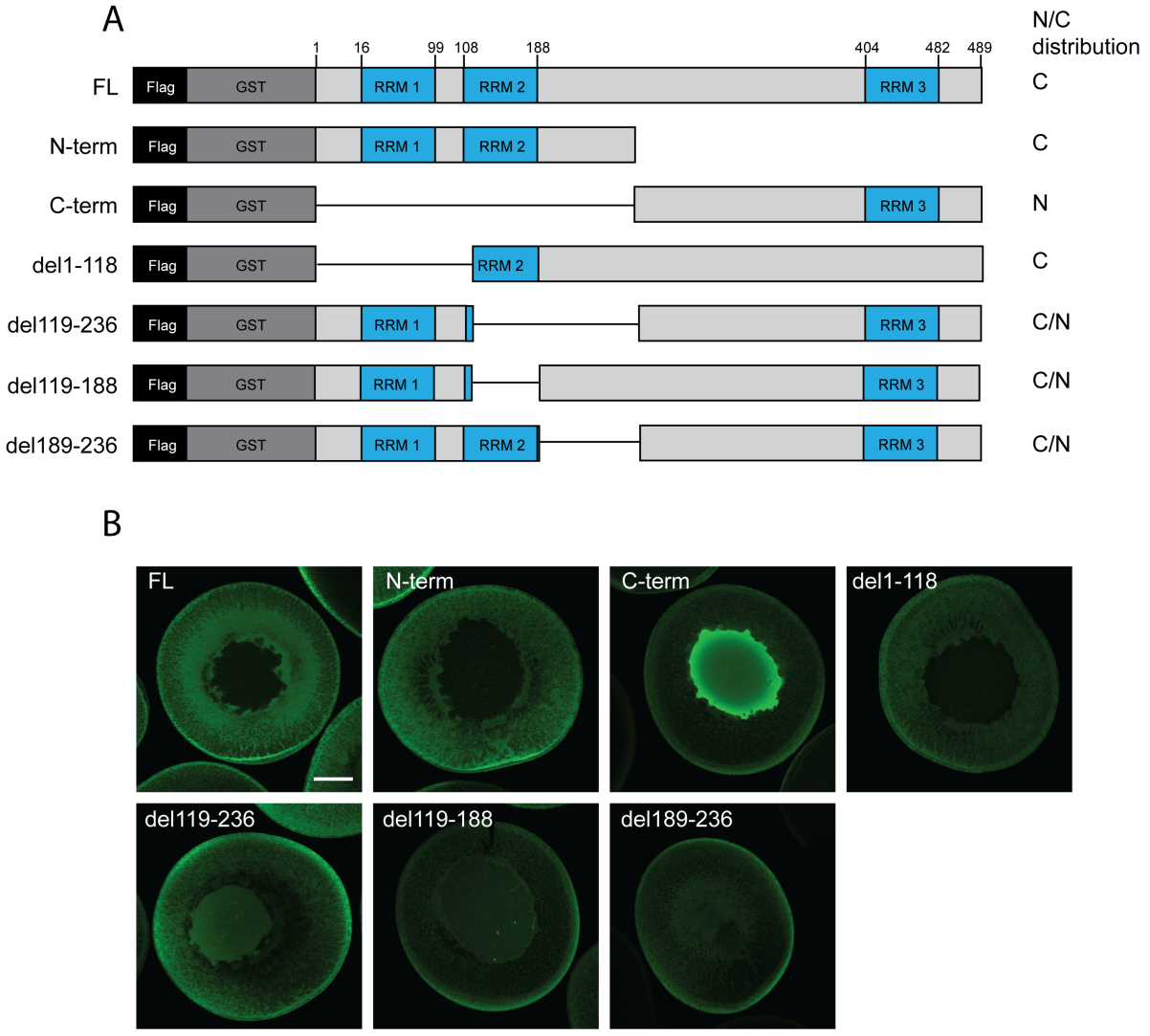

Figure 3.7. Celf1 contains nuclear export activity in the N-terminal region. A) Flag- and GST-tagged Celf1 deletion fragments were expressed in *Xenopus* stage III oocytes. B) Oocytes were stained by anti-Flag immuno-fluorescence and proteins were detected by confocal imaging. The nuclear (N) or cytoplasmic (C) distribution of corresponding Celf1 fragments is indicated in A) to the right.

In a next attempt to achieve a dominant negative effect on RNA localization, versions of Celf1 that are deficient in RNA binding were created. Such mutants might sequester other localization factors and prevent interactions with localizing RNAs. *Xenopus* Celf1 has been reported to require both N-terminal RRMs for RNA binding (Bonnet-Corven et al., 2002). In order to interfere with Celf1 RNA binding capacities, phenylalanines that have been reported to be critical for RNA binding (reviewed in Maris et al., 2005) in RRM1 (F63), RRM2 (F152) or

both were substituted for alanines (Figure S7A).

The RNA binding capacities of these mutants were analyzed by RNA co-immunoprecipitation of Cy3-labeled *dnd1*-LE with *in vitro* translated proteins (Figure S7B). While the mutation in RRM1 does not affect *dnd1*-LE binding, the mutation in RRM2 and both RRM1 and 2, slightly reduce RNA binding (Figure S7B). Overexpression of two of these mutant Celf1 in oocytes affects RNA localization (Figure S7C-E). However, the effect of these Celf1 RNA binding mutants on RNA localization is similar to the wild-type Celf1 (Figure S7C-E).

Although none of the mutants described above led to a strong dominant negative effect on vegetal RNA localization, overexpression of Flag-tagged wild-type Celf1 interfered with *dnd1*-LE localization in comparison to oocytes that were injected with a control protein (Figure S4-S7). In order to further investigate this effect, wild-type Celf1 was overexpressed in different doses followed by *dnd1*-LE injection (Figure 3.8A-C). Analysis of *dnd1*-LE localization revealed that over expression of wild-type Celf1 impairs RNA localization in oocytes in a dose dependent manner as compared to a control protein (Figure 3.8A-C). This result could indicate that excess wild-type Celf1 sequesters other localization factors into non-functional protein-protein complexes. Besides, the excess of Celf1 proteins might bind to low affinity binding sites of the RNA and thus block binding of other localization factors. Both options would interfere with localization RNP complex formation and vegetal RNA localization.

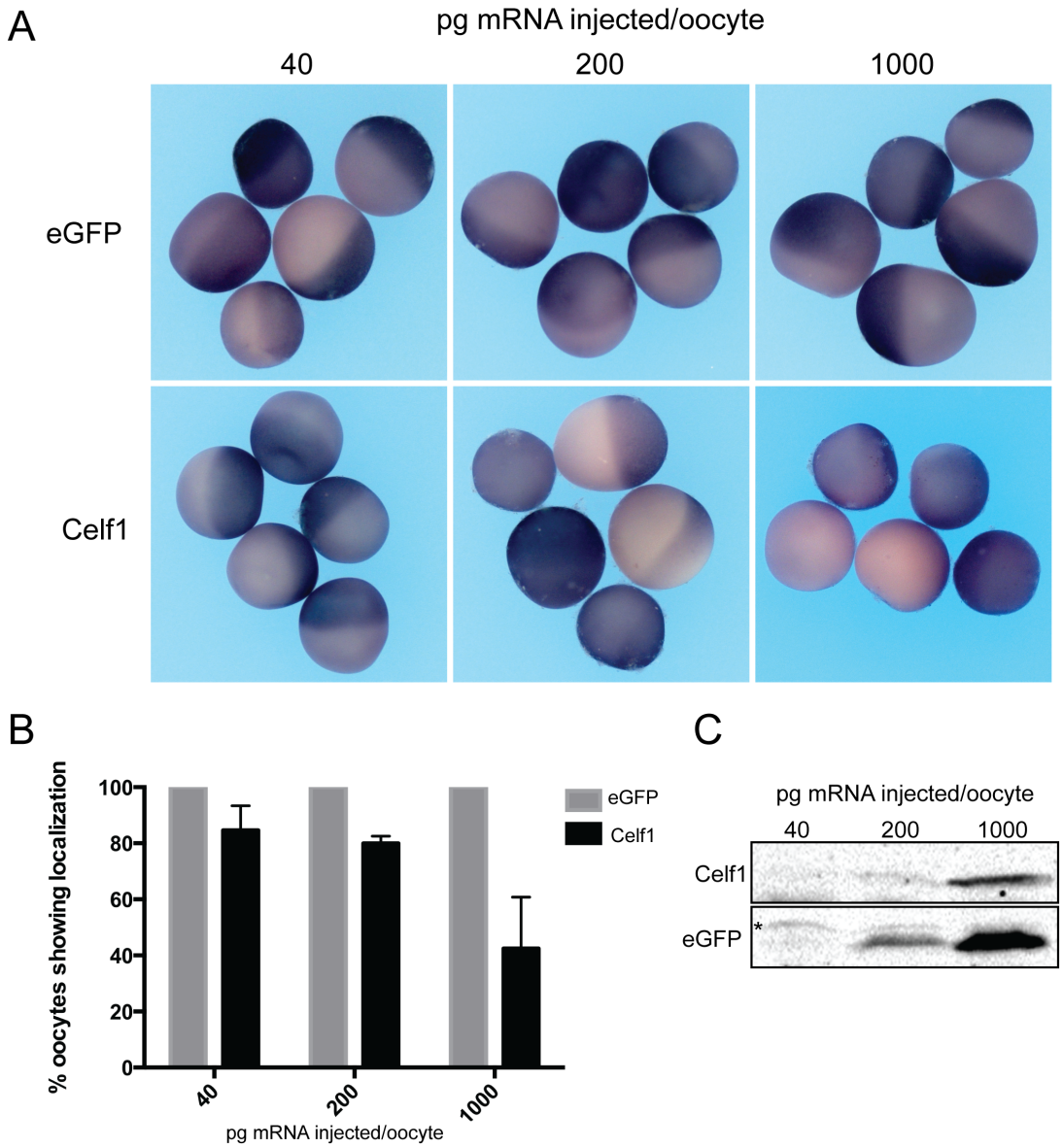

Figure 3.8. Overexpression of Celf1 reduces vegetal localization of *dnd1*-LE in *Xenopus* oocytes. A) Stage III oocytes pre-injected with RNA encoding Flag-tagged Celf1 or eGFP were injected with *lacZ-dnd1*-LE RNA and localization was detected by whole mount *in situ* hybridization against *lacZ*. B) Quantification of *lacZ-dnd1*-LE localization efficiency. Variations in oocyte localization activity were normalized to the localization activity in eGFP injected oocytes, which was set to 100 %. Average values of three independent experiments are shown; error bars indicate standard error of the mean. C) Expression control of Flag-tagged proteins. Equivalent amounts of extracts from oocytes that were injected with different amounts of RNA encoding Flag-tagged Celf1 or eGFP were analyzed by anti-Flag Western blotting. The asterisk indicates a non-specific band due to a cross-reaction of the GFP-antibody.

3.2.6. Celf1 interacts with different vegetally localizing RNAs

Celf1 recruitment is critical for vegetal localization of the *dnd1*-LE (Figure 3.3-3.5). In order to analyze if Celf1 interacts with LEs of other vegetally localizing RNAs, *in vitro* interaction assays were performed using *in vitro* translated Flag-tagged proteins and different Cy3-labeled LE RNAs (Figure 3.9A, B). Celf1 binds in addition to the *dnd1*-LE, to the *grip*2-LE, whereas no interactions were observed with the *gdf1*-LE, the *velo1*-LE and the non-localizing control RNA *ß-globin*-3'UTR (Figure 3.9A). Ptbp1 served as control as it has been shown to interact with the *dnd1*-LE, the *grip2*-LE and the *gdf1*-LE (Claussen et al., 2011) (Figure 3.9A).

Specific RNA-protein interactions might require post-translational modifications or protein-protein interactions with different other proteins in the oocyte. In order to analyze the association of Celf1 with different endogenous localizing RNAs in oocytes, Celf1 was precipitated from stage III/IV oocyte extracts and co-precipitated RNAs were detected by qPCR. The relative enrichment of RNAs in Celf1-RNPs, as compared to the input and to control IP-fractions, showed an enrichment of *dnd1*, *vegt*, *spire1* and *trim36* mRNAs (Figure 3.9B). Although Celf1 shows interactions with *grip2*-LE *in vitro* (Figure 3.9A), *grip2* mRNA was not detected in Celf1-IP fractions (Figure 3.9B). Thus, post-translational modifications or interacting proteins might lead to a higher specificity of Celf1 binding to RNAs in oocyte extracts. In summary, Celf1 interacts with the *dnd1* mRNA and with different other late and early localizing RNAs *in vitro* and in oocyte extracts, suggesting that it might be involved in their vegetal localization.

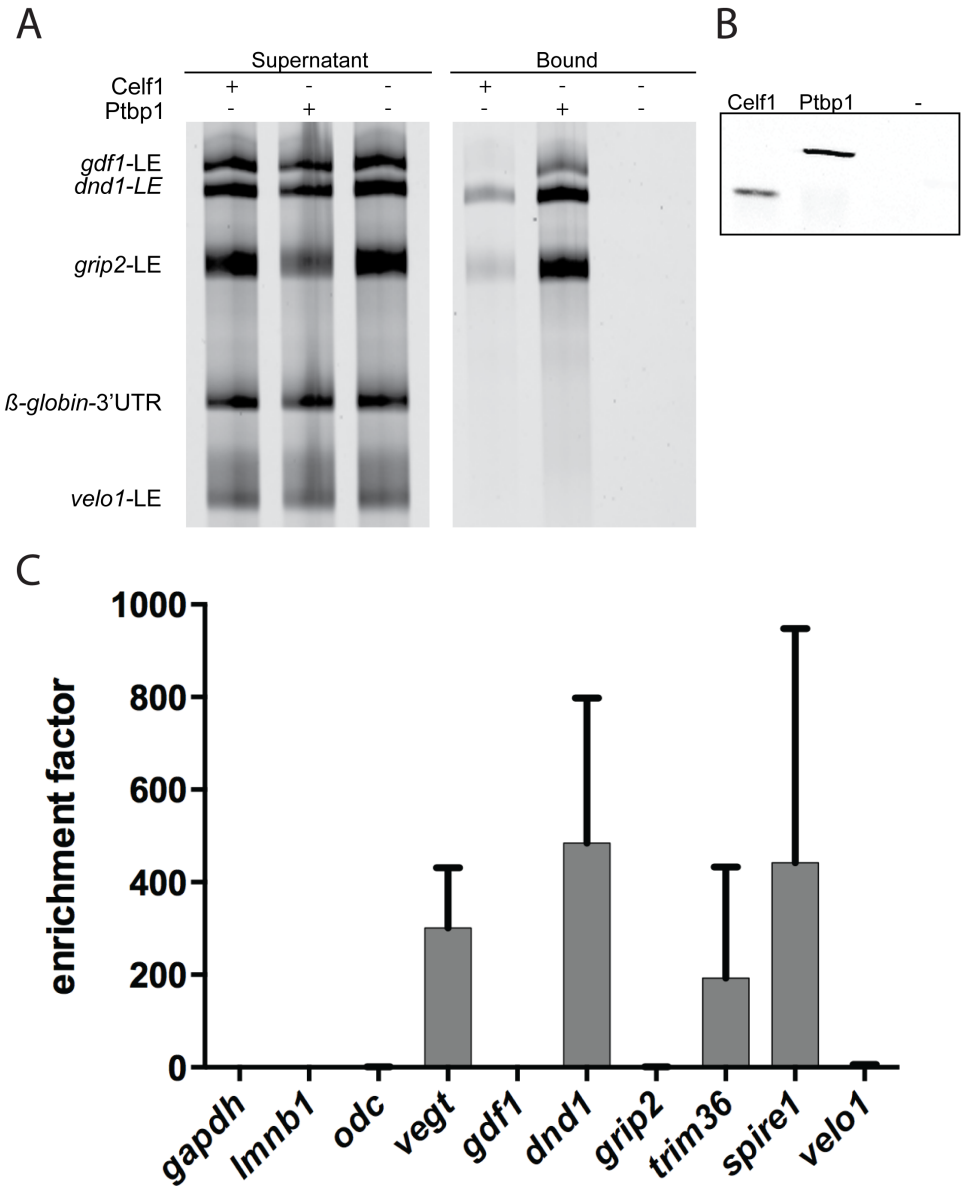

Figure 3.9. Celf1 interacts with different vegetally localizing RNAs from *Xenopus* oocytes. A) *In vitro* interaction analysis of Celf1 with different LE RNAs. Cy3-labeled LE RNAs or *ß-globin* 3'UTR (control) were co-immunoprecipitated with *in vitro* translated Flag-tagged Celf1 and Ptbp1. Unprogrammed reticulocyte lysate served as negative control (-). RNAs were separated by urea-PAGE and detected by fluorescence imaging. B) Expression control for *in vitro* translated Flag-tagged proteins used in A). Proteins were detected by anti-Flag Western blotting. C) Enrichment of endogenous localizing mRNAs in Celf1 containing RNPs. Immunoprecipitations were performed from stage III/IV oocyte extracts using anti-Celf1 or anti-Myc (control) antibodies; co-precipitated RNAs were detected by qPCR. The relative enrichment of mRNAs in the anti-Celf1 fraction versus the control IP fraction is depicted. Average values of three independent experiments are shown. Error bars indicate standard error of the mean.

3.3. Celf1 and Tia1 counteract degradation of localizing RNAs in *Xenopus* embryos

3.3.1. Ectopic expression of Celf1 and Tia1 antagonizes somatic microRNA-mediated decay of *dnd1*-LE reporter RNA in *Xenopus* embryos

Previous studies showed that the *dnd1*-LE mediates, in addition to vegetal localization, the restriction of *dnd1* transcripts to germ cells in *Xenopus* embryos (Koebernick et al., 2010). This restriction is based on the miR-mediated somatic degradation and germ cell specific protection of the *dnd1*-LE. Strikingly, proteins that are components of vegetal localization complexes in oocytes are involved in the protection of *dnd1* mRNA from somatic degradation in embryos (Arthur et al., 2009; Koebernick et al., 2010). In order to analyze if Celf1 and Tia1 are involved in the stabilization of *dnd1* RNA in embryos, a wild-type *dnd1*-LE reporter RNA was either injected alone or together with RNA encoding Celf1 or Tia1 into 2-cell stage *Xenopus* embryos (Figure 3.10A,). Reporter RNA levels were analyzed after the maternal to zygotic transition (MZT) at stage 32 by whole mount *in situ* hybridization (Figure 3.10B, E). While the *dnd1*-LE reporter RNA alone is degraded during MZT and only detectable in primordial germ cells (PGCs), ectopic expression of Celf1 or Tia1 leads to a somatic stabilization of the *dnd1*-LE reporter RNA (Figure 3.10B-E). This result indicates that Celf1 and Tia1 may function in the germ cell specific *dnd1* RNA protection in embryos. The mut_{Celf1} *dnd1*-LE reporter RNA contains mutations in the miR-430/18 binding site (Figure 3.4A) (Koebernick et al., 2010) that probably interfere with miR-mediated decay. Thus, overexpression of Celf1 in embryos that were injected with mut_{Celf1} *dnd1*-LE reporter RNA, was not considered. The miR-430/18 binding site is not affected in mut_{Tia1} *dnd1*-LE (Koebernick et al., 2010; Figure 3.4A). In order to control for the specificity of Tia1 mediated RNA stabilization, a reporter RNA that contains the mut_{Tia1} *dnd1*-LE with reduced affinity for Tia1 was injected alone or together with RNA encoding Tia1 (Figure 3.10D). Although mut_{Tia1} *dnd1*-LE reporter RNA is degraded in the soma (Figure 3.10E, F), it is stable in PGCs. However, the signal of the mut_{Tia1} *dnd1*-LE is slightly weaker as compared to the wild-type *dnd1*-LE reporter RNA (Figure 3.10E). This PGC specific stabilization might be caused by low affinity binding of Tia1 and Elavl2 (Figure 3.4C). Still, the mut_{Tia1} *dnd1*-LE-reporter RNA is not stabilized in the soma by Tia1 overexpression (Figure 3.10E, F), indicating that overexpression of Tia1 specifically protects target RNAs from somatic degradation. In summary, these experiments suggest that Celf1 and Tia1 counteract *dnd1*-LE-reporter RNA degradation in PGCs.

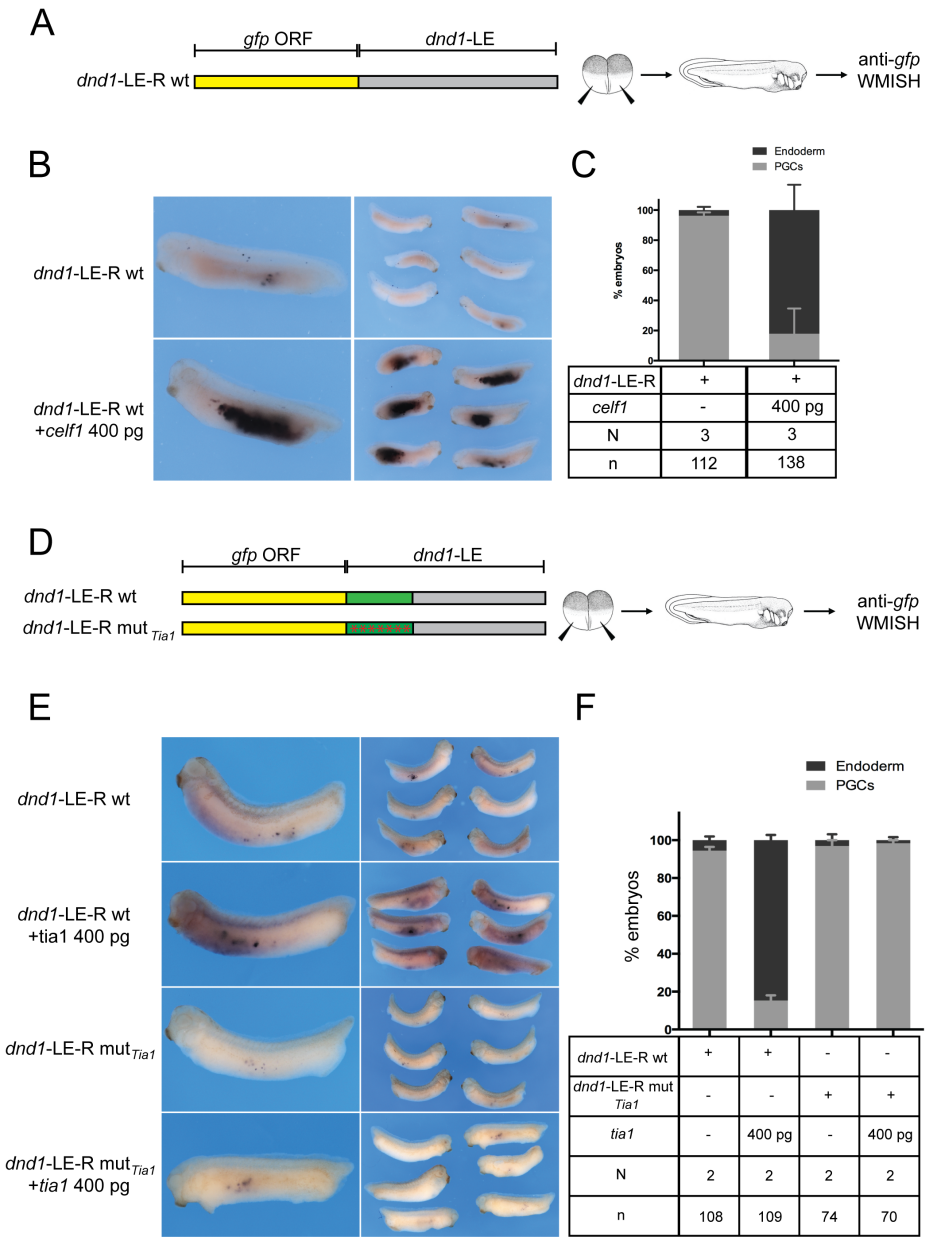

Figure 3.10. Ectopic expression of Celf1 and Tia1 stabilizes *dnd1*-LE reporter RNA in *Xenopus* embryos. A) A reporter RNA that comprises the *gfp* open reading frame (ORF) and the wild-type (wt) *dnd1*-LE (*dnd1*-LE-R) was injected into both vegetal blastomeres of two-cell stage *Xenopus* embryos. At stage 32, embryos were analyzed by WMISH against *gfp*. B) Embryos injected with only the *dnd1*-LE reporter RNA (*dnd1*-LE-R) or co-injected with RNA encoding Celf1. *dnd1*-LE reporter RNA alone is degraded in the soma and stable in germ cells. Co-expression of Celf1 leads to somatic stabilization of *dnd1*-LE reporter RNA. C) Quantification of *dnd1*-LE reporter RNA levels scored in the injected embryos. Mean values of three independent experiments are shown. Error bars indicate standard error of the mean. D) Wild-type (wt) and mutant (mut_{Tia1}) *dnd1*-LE reporter RNAs were injected as described above. E) Embryos injected with wild-type (wt) or mutant (mut_{Tia1}) *dnd1*-LE reporter RNAs alone or co-injected with RNA encoding Tia1. Wild-type and mutant *dnd1*-LE reporter RNAs are degraded in the soma and stable in PGCs. Co-expression of Tia1 leads to somatic stabilization of wild-type *dnd1*-LE, but not of mutant *dnd1*-LE reporter RNA. F) Quantification of *dnd1*-LE reporter RNA levels (only in PGCs or stabilized in the endoderm) scored in the injected embryos. Mean values of two independent experiments are shown, error bars indicate standard error of the mean.

3.3.2. Tia1 synergizes with Dnd1 in the stabilization of *dnd1*-LE reporter RNA in *Xenopus* embryos

tia1 mRNA is mainly expressed outside of germ cells, e.g. in neuronal structures (Rothé et al., 2006). Thus, it is unclear how Tia1 is able to specifically protect *dnd1*-LE in PGCs. However, *tia1* transcripts were detected in *Xenopus* PGCs by RNA sequencing (Aliaksandr Dzementsei, unpublished), suggesting the presence of Tia1 proteins in PGCs. Thus, germ cell specific protection of RNAs by Tia1 might involve interactions with germ cell specific proteins. Elavl2 has been shown to synergize with the germ cell specific protein Dnd1 in germline specific RNA stabilization (Koebernick et al., 2010). To test wether Tia1 also synergizes with Dnd1 in *dnd1* RNA stabilization, both proteins were co-expressed in embryos and *dnd1*-LE reporter RNA stability was analyzed by WMISH. Ectopic expression of low doses of either Tia1 or Dnd1 proteins do not or only weakly stabilize co-injected wild-type *dnd1*-LE reporter RNA in the soma (Figure 3.11A, B). But, if low doses of both proteins are co-expressed in embryos, *dnd1*-LE reporter RNA stability is highly increased (Figure 3.11A, B). Thus, Tia1 and Dnd1 proteins synergize in the protection of germline RNAs from miR-mediated decay.

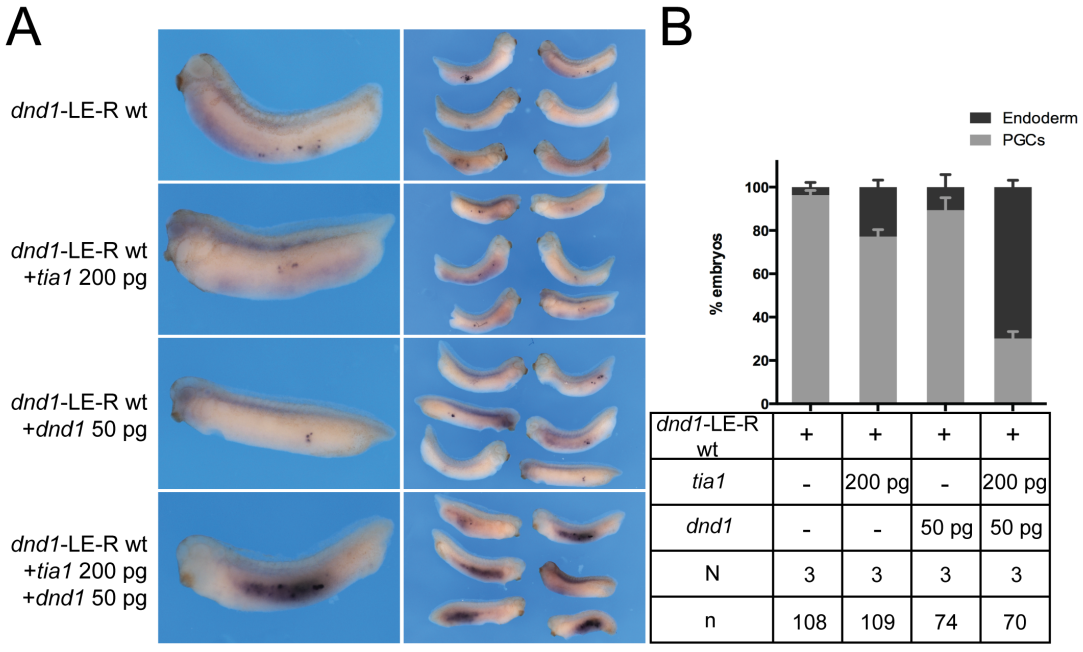

dnd1-LE-R wt	+	+	+	+
tia1	-	200 pg	-	200 pg
dnd1	-	-	50 pg	50 pg
N	3	3	3	3
n	108	109	74	70

Figure 3.11. Tia1 synergizes with Dnd1 in the stabilization of *dnd1*-LE reporter RNA in *Xenopus* embryos. A) Embryos injected with *gfp-dnd1*-LE reporter RNA (*dnd1*-LE-R wt) alone or co-injected with low doses of RNA encoding Tia1, Dnd1, or both. Reporter RNA levels were detected by WMISH at stage 32. Injected wild-type *dnd1*-LE reporter RNA alone is degraded in the soma and stable in PGCs. Co-expression of low doses of Tia1 or Dnd1 does not stabilize *dnd1*-LE reporter RNA in the soma. Co-expression of same doses of Tia1 and Dnd1 leads to somatic stabilization of *dnd1*-LE reporter RNA. B) Quantification of *dnd1*-LE reporter RNA levels scored in the injected embryos. Mean values of three independent experiments are shown, error bars indicate standard error of the mean.

3.3.3. Ectopic expression of Tia1 leads to the stabilization of several vegetally localizing and germ cell specific RNAs in *Xenopus* embryos

Tia1 interacts with the *dnd1*-LE *in vitro* and mediates protection of a *dnd1*-LE reporter RNA from miR-mediated decay in embryos (Figure 3.3, 3.10, 3.11). In order to analyze if Tia1 also interacts with other LE RNAs, an *in vitro* interaction assay was performed using *in vitro* translated Flag-tagged proteins and different Cy3-labeled LE RNAs (Figure 3.12A, B). Tia1 binds to the *dnd1*-LE, the *grip*2-LE and the *gdf1*-LE, while it does not bind to the *velo1*-LE and to the non-localizing control RNA *ß-globin*-3'UTR (Figure 3.12A). This *in vitro* interaction assay suggests that Tia1 might also stabilize the corresponding mRNAs in embryos.

In order to analyze the effect of Tia1 overexpression on different other mRNAs, endogenous RNA levels were assayed after ectopic expression of Tia1 by nanostring multiplex analysis. Whereas Tia1 overexpression did not affected RNA levels before MZT (stage 8) and only slightly during MZT (stage 11), several mRNA levels are highly increased after MZT (stage 14) (Figure 3.12C, Table S1-4), suggesting that Tia1 antagonizes miR-mediated decay during MZT. In concordance with RNA binding *in vitro* (Figure 3.12A), endogenous *dnd1*, *gdf1* and *grip2* mRNAs show increased RNA levels in Tia1 overexpressing oocytes (Figure 3.12C). Other localizing mRNAs including *pgat* and *velo1* and the non-localizing, but miR regulated, RNA *cyclin b2* (Lund et al., 2009) are not affected by Tia1 overexpression (Figure 3.12C). The mRNAs that are stabilized upon Tia1 over-expression include the germ cell specific transcripts *germes*, *dnd1*, *grip2* and *cpeb1a* (Figure 3.12C), suggesting that Tia1 counteracts miR-mediated decay of germline RNAs. However, *gdf1* mRNA levels are also increased up to three fold upon Tia1 overexpression, although this mRNA is not germ cell specific (Figure 3.12C). Thus, Tia1 might also stabilize RNAs which are not germ cell specific by counteracting other decay mechanisms that are not mediated by miRs.

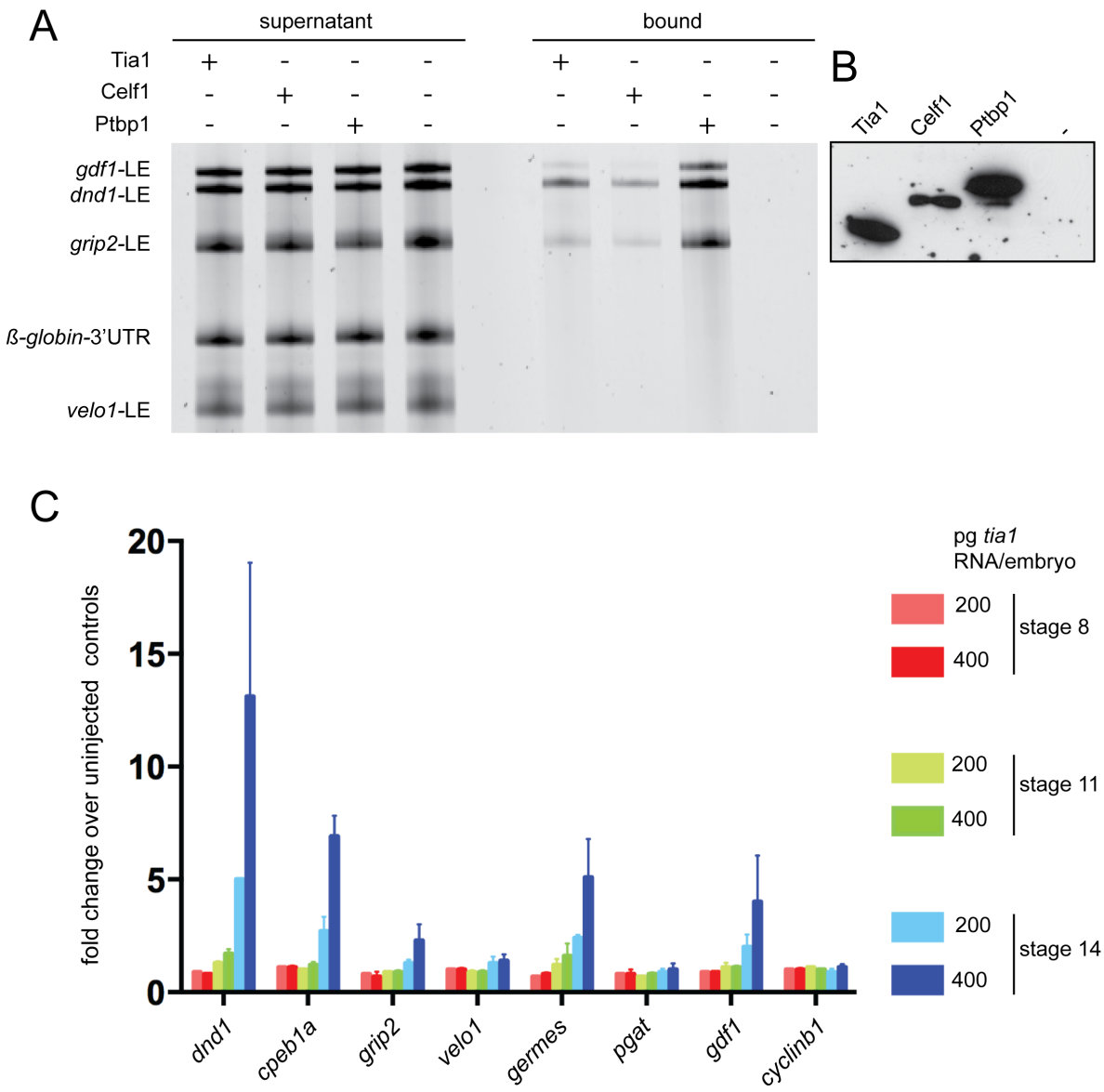

Figure 3.12. Tia1 binds to several LEs *in vitro* and ectopic expression of Tia1 leads to stabilization of vegetally localizing and germ cell specific RNAs in *Xenopus* embryos. A) *In vitro* interaction analysis of Tia1 with different LE RNAs. Cy3-labeled LE RNAs or *ß-globin* 3'UTR (control) were co-immunoprecipitated with *in vitro* translated Flag-tagged Tia1, Celf1 and Ptbp1 proteins. Unprogrammed reticulocyte lysate served as negative control (-). RNAs were separated by urea-PAGE and detected by fluorescence imaging. B) Expression control for *in vitro* translated Flag-tagged proteins used in A). Proteins were detected by anti-Flag Western blotting. C) Fold change RNA levels of different localizing and control mRNAs at indicated developmental stages after overexpression of Tia1 in embryos. *Xenopus* 2-cell stage embryos were injected with 200 or 400 pg *tia1* RNA. Embryos were grown until stages 8, 11 or 14 and subjected to total RNA extraction. RNA samples were analyzed using the nCounter® Gene Expression assay (NanoString Technologies). The averaged fold changes of selected genes over uninjected control embryos of two independent experiments are shown, error bars indicate standard error of the mean.

3.4. Zebrafish *celf1* mutants primarily develop as males

A further approach to deplete maternal Celf1 in oocytes would be a *celf1* gene knockout in females. Due to a partial tetraploid genome and a long generation time, genetic manipulations of *Xenopus laevis* are not applicable. However, efficient genome editing is possible in the zebrafish. The creation of zebrafish *celf1* mutants would allow for the analysis of RNA localization in a genetic *celf1* loss of function system. In contrast to *Xenopus*, zebrafish *dnd1* mRNA does not localize in oocytes (data not shown). However, several RNAs e.g. *dazl* and *syntabulin,* localize to the vegetal pole during zebrafish oogenesis (Howley and Ho, 2000; Kosaka et al., 2007) similar to their orthologs in *Xenopus*. Although it is not much known about the localization mechanism in zebrafish oocytes, the ability of zebrafish *vasa* 3'UTR to localize in *Xenopus* oocytes, suggests a conserved localization machinery between fish and frog (Knaut et al., 2002).

3.4.1. Vegetal localization of Celf1 is conserved between zebrafish and *Xenopus* oocytes

In order to analyze if Celf1 protein is localized at the vegetal cortex of zebrafish oocytes, as shown in *Xenopus* oocytes (Figure 3.2C, D), zebrafish oocytes were immuno-stained for endogenous Celf1. To determine the vegetal pole, oocytes were co-immunostained for Syntabulin, which was reported to be vegetally localized in zebrafish eggs (Nojima et al., 2010). While Celf1 is homogeneously distributed in stage I, it is vegetally enriched in stage II-III zebrafish oocytes (Figure 3.13). Thus, the vegetal localization of Celf1 protein is conserved between fish and frog. This finding could suggest, that zebrafish Celf1 is a component of vegetal localization RNPs in zebrafish oocytes and that it might also be involved in the vegetal RNA transport during zebrafish oogenesis.

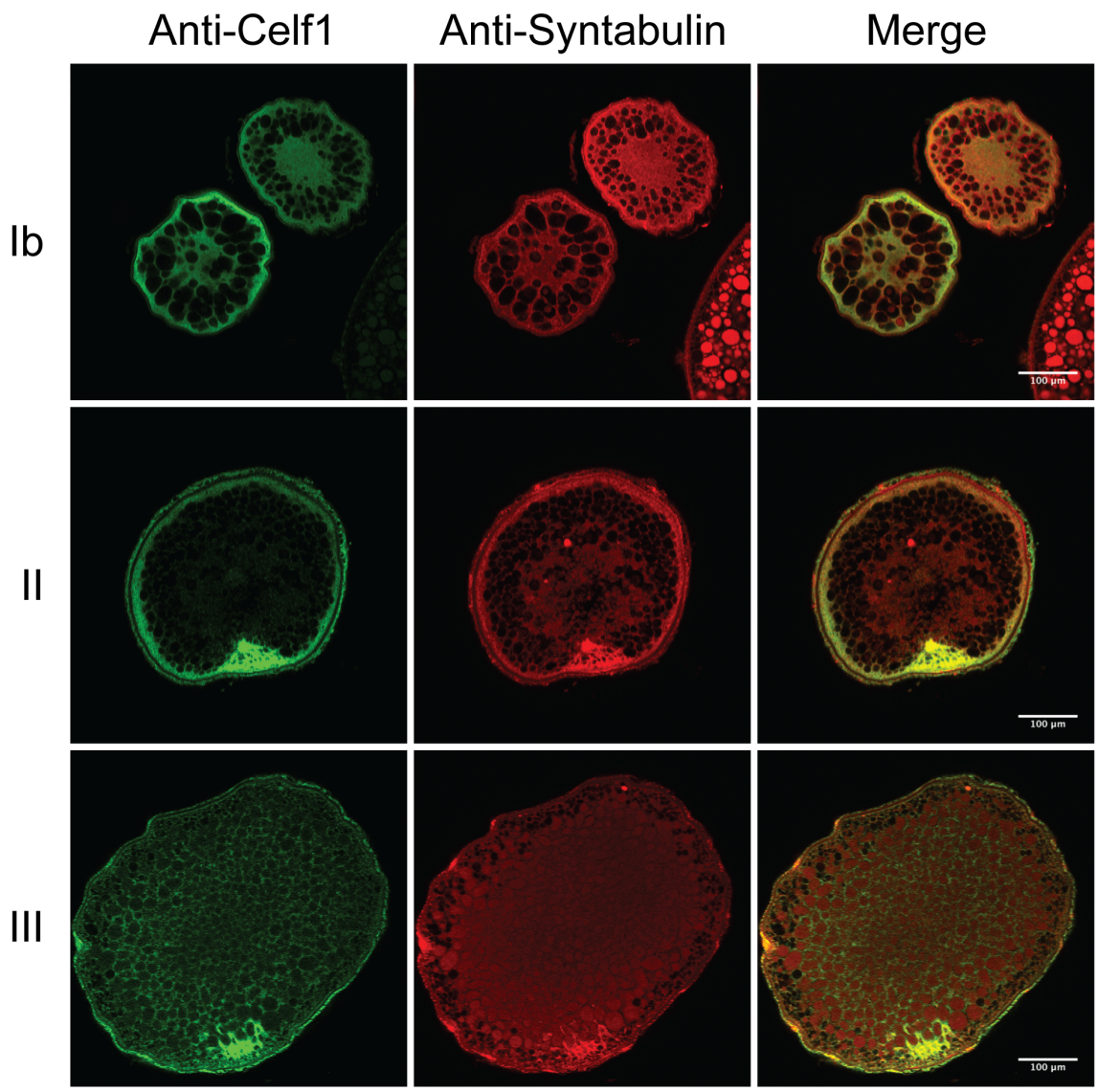

Figure 3.13. Celf1 is localized at the vegetal cortex of stage II-III zebrafish oocytes. Analysis of the intracellular protein distribution of Celf1 in zebrafish oocytes. Different stages (Ib-III) of zebrafish oocytes were co-immunostained using anti-Celf1 and anti-Syntabulin antibodies. Scale bars indicate 100 µm.

3.4.2. The generation of zebrafish *celf1* mutants

As Celf1 localization is conserved between *Xenopus* and zebrafish (Figure 3.13), the analysis of vegetal RNA localization in zebrafish oocytes that lack endogenous Celf1 protein was attempted. In order to create zebrafish *celf1* mutants, the clustered regularly interspaced short palindromic repeats (CRISPR)/CRISPR-associated (Cas) system was applied, which was reported to allow efficient genome editing in zebrafish (Hwang et al., 2013).

In zebrafish, five *celf1* splice variants are described (Figure 3.14B). Three target regions that contain a protospacer adjacent motif (PAM) were selected in the first exon that is shared by all putative alternative transcripts (exon 4) (Figure 3.14B). These regions correspond to the N-terminal region of Celf1 and overlap with RRM1 (Figure 3.14C). Non-sense or miss-sense mutations in this region by the error prone repair of CRISPR/Cas mediated double strand breaks would interrupt the majority of the Celf1 protein sequence. Due to the delayed translation of the Cas nuclease after the first cell divisions, the induced mutations differ per cell. During further cell cleavages, different mutations are inherited that lead to the development of a mosaic mutants.

In order to also analyze a homozygous zebrafish *celf1* mutant line, the zebrafish line sa11143 that contains an allele with a single C to A point mutation in *celf1* exon 10, was obtained from the European Zebrafish Resource Centre (EZRC, Karlsruhe) (Figure 3.14A, B). This point mutation converts amino acid 269 into a premature stop-codon and leads to a truncated version of the Celf1 protein (Figure 3.14C).

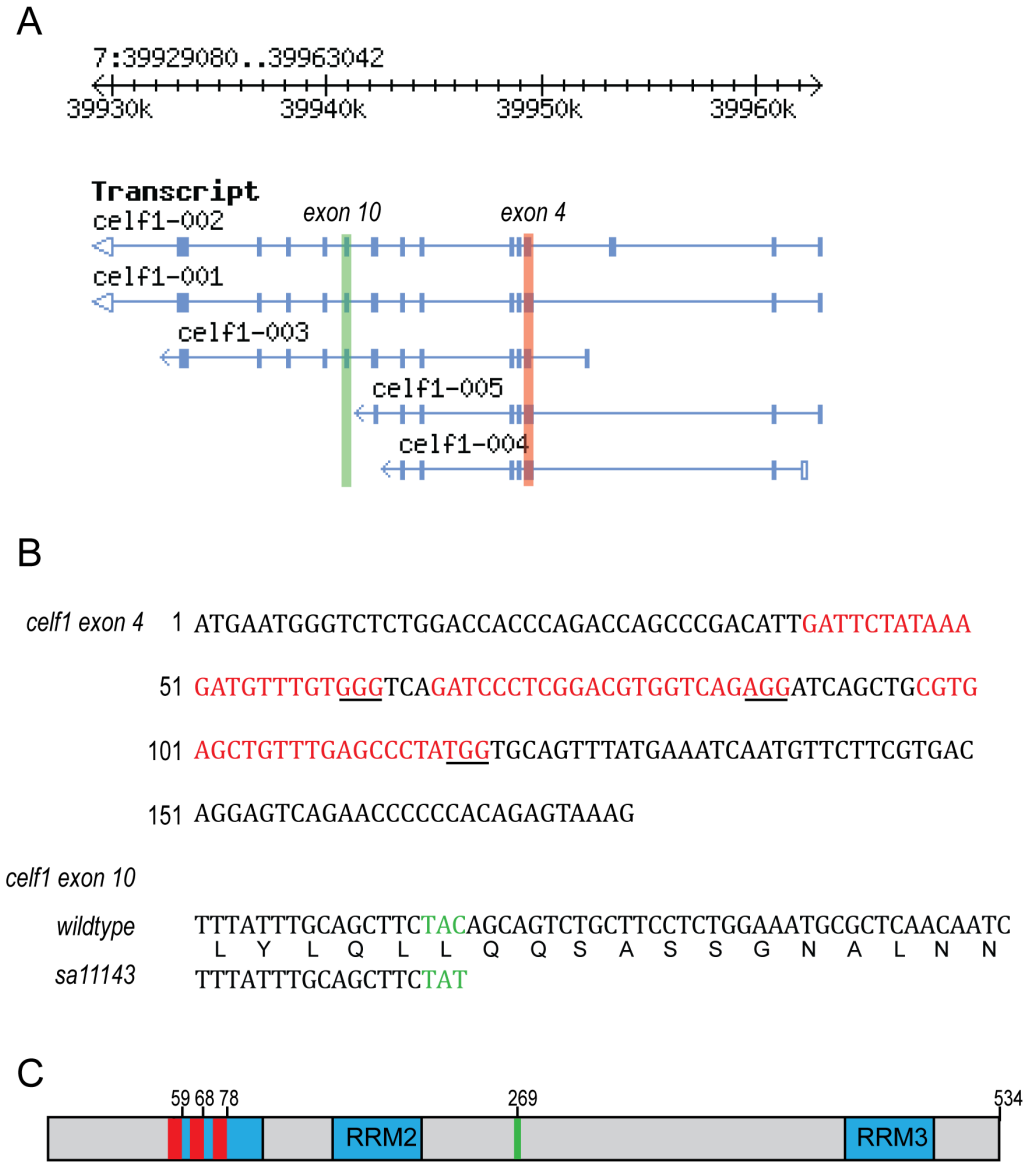

Figure 3.14. Zebrafish *celf1* exon4 is targeted in CRISPR/Cas mutants and exon10 is affected in the *celf1* mutant line sa11143. A) Schematic presentation of the five *celf1* splice variants described in zebrafish (retrieved from the Zebrafish Model Organism Database (ZFIN), University of Oregon, Eugene; URL: http://zfin.org/). Transcripts are oriented from right to left and exons are depicted as blue boxes. The first exon shared by all 5 transcripts (exon 4, boxed in red) was selected for CRISPR/Cas targeting. The *celf1* mutant line sa11143 obtained from the European zebrafish resource centre (EZRC, Karlsruhe) contains a premature stop codon in exon 10 (boxed in green). B) Partial nucleotide sequences of *celf1* exon 4 and exon 10. Red letters mark three target regions for the CRISPR/Cas system in exon 4. PAM sequences are underlined. *celf1* exon 10 is shown, encoded amino acids are below the central nucleotide of each codon. Green letters mark the codon that is affected by the C to T point mutation leading to the conversion of leucine (L) into a stop codon. C) Schematic presentation of the longest Celf1 protein isoform in zebrafish (adapted from Hashimoto et al., 2006). The CRISPR/Cas target regions (red lines) in *celf1* exon 4 correspond to the N-terminal region of Celf1 protein and overlap with RRM1. The point mutation of the zebrafish line sa11143 leads to a premature stop codon at amino acid 269 (green line) of the longest Celf1 isoform. Amino acid positions are indicated on top.

3.4.3. Zebrafish *celf1* mutants primarily develop as males with some females showing moderate germline mutation rates

In order to create zebrafish *celf1* mutants using the CRISPR/Cas system, 1-cell stage wild-type embryos were injected with RNA encoding Cas9 and single guide RNAs (sgRNAs) that target three regions in exon 4 (Figure 3.14B, 3.15A). After the injected fish reached the juvenile stage, their somatic mutation rates were analyzed by T7 endonuclease 1 (T7E1) assay and fish were divided into groups of individuals with high, intermediate, low, or no detectable somatic mutation rates (Figure 3.15A, S8-9). Sequencing of the *celf1* target region of two fish out of each category confirmed these somatic mutation rates (Figure S10). Thus, the fish that show high somatic mutation rates were chosen for further analyses. Out of 49 fish that were classified into a high somatic mutation rate, only nine developed as females (Figure 3.15B). In order to analyze the *celf1* mutations in the germline of these female fish, the *celf1* exon 4 region was amplified from their unfertilized eggs and sequenced. The females showed non-sense or miss-sense mutation rates up to 60 %, while two females showed no germline mutations (Figure 3.15C, S11A, B). Thus, the CRISPR/Cas approach produced mosaic *celf1* mutant zebrafish females with moderate *celf1* germline mutation rates. However, CRISPR/Cas treated *celf1* mutant zebrafish appear to develop primarily as males (Figure 3.15B). Strikingly, the loss of oocytes leads to the development of zebrafish males (Uchida et al., 2002; Rodríguez-Marí et al., 2010). Thus, a loss of Celf1 might affect oocyte survival and lead to the development of males. The development of the nine females might have been enabled by their low germline mutation rates and thus oocyte survival.

In order to analyze if Celf1 is required for vegetal RNA localization in zebrafish, oocytes of mosaic zebrafish females were analyzed for their localization capacity. s*yntabulin* and *dazl* mRNAs were chosen as vegetal markers, as they are vegetally localized in zebrafish stage II-III oocytes (Abrams and Mullins, 2009; Nojima et al., 2010), as observed for Celf1 protein (Figure 3.13). However, the moderate *celf1* mutation rates do not affect vegetal localization of s*yntabulin* and *dazl* mRNAs (Figure S13). Nevertheless, the oocytes analyzed might have been heterozygous and thus could still express maternal Celf1 protein. In order to exclude the presence of maternal Celf1 protein in oocytes, the creation of homozygous *celf1* mutants was aimed by crossing CRISPR/Cas treated siblings. However, only wild-type or heterozygous offspring were obtained, suggesting that biallelic *celf1* mutants are not viable.

The *celf1* mutant line sa11143 obtained from the European Zebrafish Resource Centre (EZRC, Karlsruhe) produces a truncated Celf1 protein that lacks the C-terminal half (Figure 3.14). In order to obtain homozygous mutants that express truncated Celf1 proteins,

heterozygous zebrafish of the line sa11143 were crossed (Figure 3.15D). Genotyping of the offsprings revealed five homozygous *celf1* mutants out of 112 fish (Figure 3.15D, E). Although the homozygous fish show a wild-type phenotype, their low proportion indicates a reduced viability. Still, all of the five homozygous fish show a male phenotype (Figure 3.15E), supporting the assumption that *celf1* mutants develop as males. However, further experiments using higher embryo numbers are required to support this assumption.

In summary, the creation of zebrafish *celf1* mutants using the CRISPR/Cas system or a *celf1* mutant line revealed a bias towards male development, while mosaic *celf1* mutant females show only moderate germline mutation rates indicating they might produce heterozygous oocytes. Thus, the analysis of RNA localization in homozygous *celf1* mutants was not possible. However, the results indicate that Celf1 might have an important function in oocyte viability and thus female development in zebrafish.

A

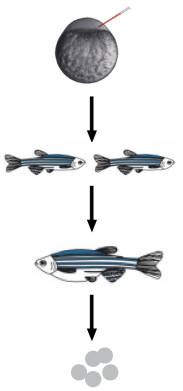

Injection of Cas9 + guide RNAs targeting *celf1* in 1-cell wildtype embryos

Identification of fish with high somatic mutation rates by T7E1 assay using fin DNA

Verification of germline mutations in females by sequencing target region in DNA from unfertilized eggs

Analysis of RNA localization in oocytes of females with high germline mutation rates by WMISH

B

CRISPR/Cas

Somatic mutation rate	Batch 1		Batch 2	
	Fish (n)	Female (n)	Fish (n)	Female (n)
High	26	9	23	0
Intermediate	16	5	12	3
Low	4	n.d.	9	n.d.
no	24	n.d.	32	n.d.

C

CRISPR/Cas

Female #	clones with frame shift inducing mutations/ clones sequenced (n)	Germline mutation rate (%)
1	4/10	36
2	5/10	63
3	0/9	20
4	2/19	16
5	6/10	16
6	4/10	40
7	0/7	0
8	5/10	50
9	0/9	0

D

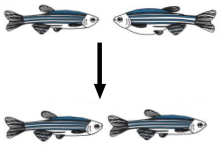

Marting of *celf1* +/- (sa11143) siblings

Genotyping of offspring

E

sa11143

celf1 genotype	Fish (n)	Females (n)	Males (n)
-/-	5	-	5
+/-	54	21	33
+/+	42	18	24

Figure 3.15. Zebrafish *celf1* mutants develop primarily as males with few females showing moderate mutation rates in their germline. A) Workflow for creation of *celf1* germline mutations in zebrafish. Cas9 and customized sgRNAs targeting *celf1* exon 4 were injected into 1-cell stage wild-type zebrafish embryos. Somatic mutation rates of the *celf1* target region were estimated in fins of juvenile fish using T7 endonuclease 1 (T7E1) assay. Females that show high somatic mutation rates were analyzed for germline mutations by sequencing the *celf1* target region, which was amplified from their unfertilized eggs. B) Female proportions of fish groups that show high, intermediate, low or no somatic mutation rates. C) Germline mutation rates of the 9 females that show high somatic mutation rates. The *celf1* target region was amplified from DNA of 20 unfertilized eggs per fish, cloned and approx. 10 clones were sequenced. D) Homozygous *celf1* mutants were obtained by inbreeding heterozygous *celf1* (+/-) mutants of the line sa11143. Offspring was genotyped by amplification and sequencing of exon 10 and mutations were identified by single base substitutions in the chromatogram. E) Female/male distribution in wild-type (+/+), homozygous (-/-) and heterozygous (+/-) *celf1* mutants of the line sa11143.

4. Discussion

This study identifies the RRM-type RNA binding proteins Celf1 and Tia1 as novel components of vegetal RNA localization complexes in *Xenopus* oocytes. Both proteins co-precipitate with known localization RNP components from oocyte extracts and they directly interact and co-localize with vegetal LE RNAs. Interference with Celf1 binding by LE mutagenesis indicates that Celf1 is involved in vegetal RNA localization in *Xenopus* oocytes. Celf1 overexpression also interferes with *dnd1*-LE localization, supporting the idea of an active role of Celf1 in RNA localization. Celf1 interactions with other endogenous localizing mRNAs indicates a function in vegetal localization of multiple different mRNAs. Somatic expression of Celf1 and Tia1 in *Xenopus* embryos leads to somatic stabilization of *dnd1*-LE RNA, indicating that both proteins might remain associated with localizing RNAs after fertilization and function in their stabilization during embryonic development. Co-expression of Tia1 together with Dnd1 highly increases *dnd1*-LE RNA stabilization, indicating that Tia1 and Dnd1 synergize in counteracting RNA degradation. Tia1 overexpression specifically stabilizes several endogenous localizing mRNAs, suggesting a general role for Tia1 in the stabilization of localizing and germ cell specific transcripts in *Xenopus* embryos. Furthermore, Celf1 protein is enriched at the vegetal cortex of zebrafish oocytes, suggesting that its function in RNA localization is conserved between different animal classes. However, *celf1* mutant zebrafish develop primarily as males, indicating that Celf1 acts in zebrafish sex determination or female viability.

4.1. Celf1 is required for vegetal RNA localization in *Xenopus* oocytes

This study shows that Celf1 is a novel component of vegetal localization RNPs and that it actively participates in RNA transport. Thus, it is of interest to elucidate the particular function of Celf1 during the different steps of RNA localization. Implications for Celf1 function during the vegetal RNA localization process are discussed in the following sections.

4.1.1. Nuclear initiation of RNA localization

Although Celf1 was described to act in the nucleus and cytoplasm of different cell types (reviewed in Dasgupta and Ladd, 2011), Celf1 steady state distribution is predominantly cytoplasmic in *Xenopus* oocytes. However, Morgan detected Celf1 on lampbrush chromosomes of *Xenopus* oocytes, suggesting that Celf1 binds to nascent transcripts in the

nucleus (Morgan, 2007). Thus, Celf1 might transiently enter and bind localizing RNAs already in the nucleus. Indeed, we revealed nuclear localization activity in the C-terminal and nuclear export activity in the N-terminal part of Celf1. Similar regions responsible for nucleo-cytoplasmic shuttling were defined in chicken CELF2 (ETR-3) (Ladd and Cooper, 2004), a CELF family member with high functional as well as sequence similarity to Celf1 (Ladd et al., 2001). Thus, Celf1 might bind localizing RNAs already in the nucleus and could be involved in their nuclear export. However, efforts to trap vegetally localizing RNA in the nucleus by overexpression of a mutant Celf1 version, that lacks nuclear export activity, were not successful. Concordantly, a mutant version of the *dnd1*-LE with reduced affinity for Celf1 shows proper nuclear export. Thus, although Celf1 shows shuttling abilities, it may be dispensable for nuclear export of localizing RNAs. However, further investigation of localization RNPs in respect to their dynamic composition before and after nuclear export are required to elucidate if Celf1 assembles localization RNPs in the nucleus or in the cytoplasm, and how this impacts RNA localization.

4.1.2. Cytoplasmic RNP composition and remodeling

Cytoplasmic remodeling

Although Celf1 shows indications for transient nuclear localization, cytoplasmic steady state protein levels indicate a recruitment of Celf1 to localization RNPs in the cytoplasm. Localization RNPs were proposed to change their composition after nuclear export (reviewed in Lewis and Mowry, 2007; Lewis et al., 2008). Celf1 might be involved in the recruitment of other factors leading to complex remodeling. Indeed, Stau1 and Prrp assemble into localization RNPs in the cytoplasm, possibly by protein-protein interactions with Igf2bp3 and Ptbp1 (Kress et al., 2004). However, the association of Celf1 with known localization factors is abolished by RNAse treatment of oocyte extracts. Thus, Celf1 may not directly interact with other known localization factors, or their protein-protein interactions are unstable. Localization RNP remodeling is also suggested to involve post-translational modifications, as Ptbp1 is unphosphorylated in the nucleus and phosphorylated in the cytoplasm (Xie et al., 2003). A fraction of Celf1 proteins appears to be phosphorylated throughout oogenesis. Thus, Celf1 phosphorylation might control a transition between nuclear and cytoplasmic functions. Still, it is unclear if Celf1 is phosphorylated in the nucleus or the cytoplasm. Overexpression of a mutant version of Celf1 that mimics phosphorylation did not affected vegetal RNA localization. Thus, further approaches using a mutant version of Celf1 that is non-phosphorylatable might give insight in the relation of Celf1 post-translational modifications and vegetal RNA localization.

Formation of "super-complexes"

It has been hypothesized that single localization RNPs oligomerize into larger "super-complexes" that are co-transported (reviewed in Pratt and Mowry, 2012; Xing and Bassell, 2013). It has been shown that *Xenopus* Celf1 oligomerizes via a domain in its central region (Cosson et al., 2006). Similarly, Igf2bp3 is able to self-dimerize (Git and Standart, 2002; Farina et al., 2003). The ability of localization factors to oligomerize might promote a multimerization of localization RNPs into larger granules. Indications for such a function are given in *Drosophila* oocytes, where Celf1 and Ptbp1 orthologs seem to be involved in the aggregation of localization RNPs (Chekulaeva et al., 2006; Besse et al., 2009). However, expression of a mutant Celf1 that lacks the oligomerization domain or injection of a peptide that corresponds to this domain, did not interfered with RNA localization.

Do different localization factors act redundantly or cooperatively?

Remarkably, most localization factors tested bind in the same relatively short uracil rich region of the *dnd1*-LE. However, it is still unclear, if multiple proteins can bind simultaneously to one and the same RNA molecule. It is possible that localization factors act redundantly in RNA localization. This would mean that several proteins are able to compensate the potential dysfunction of another. In contrast to such redundant functions of localization factors, specific reduction of Celf1 binding to *dnd1*-LE severely reduces its localization. Thus, Celf1 might exert a specific function in the localization of *dnd1* that other proteins are not able to compensate.

On the other hand, this observation also suggests that protein cooperations might still be crucial for RNA localization *in vivo*, although not detectable *in vitro*. In accordance, overexpression of Celf1 inhibits *dnd1*-LE localization in oocytes, suggesting that an excess of Celf1 proteins might sequester other localization factors into non-functional complexes. Otherwise, excess Celf1 proteins might occupy low affinity binding sites and prevent other factors from RNA binding. Both options point towards a complex interplay between different localization factors with each of them being involved in RNA localization. Consistently, interference with functions of Stau1 or Hnrnpab reduce vegetal RNA localization, supporting the importance of individual localization complex components (Yoon and Mowry, 2004b; Czaplinski et al., 2005). However, more sensitive analyses of protein-protein interactions might be required to identify if single localization factors act cooperatively as well as the mechanism of their interplay during the RNA localization process.

4.1.3. Translational Regulation during RNA localization

Celf1 functions in translational regulation of transcripts via mRNA deadenylation in *Xenopus* embryos (Paillard et al., 1998). The *Drosophila* ortholog Bruno has also been shown to regulate translation of localizing RNAs during oogenesis (Filardo and Ephrussi, 2003; Chekulaeva et al., 2006). However, using *Xenopus* oocytes, we could not detect a difference in translational efficiency between wild-type and the mutant *dnd1*-LE, that has reduced affinity for Celf1, in luciferase reporter assays. Furthermore, tethering of Celf1 to a reporter RNA in oocytes led to a slight translational activation. Thus, Celf1 is not considered to function in translational repression of *dnd1*-LE. Nevertheless, it might be possible that the full length *dnd1* mRNA is required for translational regulation, to allow Celf1 interaction with proteins that bind to other regions in the mRNA.

4.1.4. Vegetal anchoring

Celf1 co-localizes with localized RNA at the vegetal cortex, suggesting a function in cortical RNA anchoring. Inefficient anchoring at the cortex might also account for the reduced localization efficiency of the mutant *dnd1*-LE with reduced affinity for Celf1. The localization factors Igf2bp3 and Stau1 are implicated in vegetal anchoring of *gdf1* mRNA (Allison et al., 2004; Git et al., 2009). Both proteins are phosphorylated upon egg maturation and that correlates with a release of *gdf1* mRNA, Igf2bp3 as well as Stau1 from the vegetal cortex (Git et al., 2009). Phosphorylation of Igf2bp3 does not affect RNA binding (Git et al., 2009), suggesting that *gdf1* mRNA and Igf2bp3 are associated upon release from the cortex. Similarly, Celf1 phosphorylation upon egg maturation might lead to a cortical release of this protein and its bound RNAs due to altered interactions with protein components of the localization RNP or the cytoskeleton. Indeed, mouse Celf1 was described to increase RNA affinity upon phosphorylation of a serine in RRM1 (Salisbury et al., 2008), suggesting that Celf1 phosphorylation does not lead to the loss of RNA binding. However, overexpression of a Celf1 version that mimics phosphorylation in oocytes did not affect vegetal anchoring of RNAs. Still, it has to be mentioned that it is unclear if the phospho-mimicking mutations in Celf1 affect RNA binding or protein-protein interactions in the *Xenopus* oocyte. Thus, a possible function of Celf1 in vegetal anchoring of RNAs remains to be demonstrated experimentally. However, it is possible that localized RNAs are anchored by several proteins in order to ensure tight association with the cortex. But so far, none of the known localization factors shows compelling evidence for a role in vegetal anchoring and the identification of such a function might be difficult if all of them are involved.

4.2. Tia1 is a component of vegetal localization RNPs in *Xenopus* oocytes

Tia1 was identified to be a component of vegetal localization complexes, to directly interact with vegetal LEs and to co-localize with RNA at the vegetal cortex of *Xenopus* oocytes. Tia1 has not been described to function in RNA localization processes in any systems before. However, *Xenopus* Tia1 was demonstrated to interact with the FUSE-BP2 (FBP2, also named KSRP) (Rothé et al., 2006) that is associated with several vegetally localizing RNAs in *Xenopus* oocytes and acts in the localization of *ß-actin* mRNA in chicken fibroblasts and neurons (Gu et al., 2002; Kroll et al., 2002). However, a mutant version of the *dnd1*-LE that is reduced for Tia1 binding shows full localization capacity, suggesting that efficient binding of Tia1 is dispensable for vegetal localization of *dnd1*-LE. Nevertheless, *dnd1*-LE mutagenesis also reduces binding of the known localization factor Elavl2. Thus, the low affinity binding of Tia1 and Elavl2 could be sufficient for vegetal localization of *dnd1*-LE and it is still unclear if Tia1 is required for this process. On the other hand, Tia1 might exert other functions on localizing RNAs that are not involved in vegetal transport, but for example in their translational regulation. Possible functions of Tia1 in the context of vegetal RNA localization are discussed in the following sections.

4.2.1. A possible function of Tia1 in translational regulation of localizing RNAs

Tia1 orthologs were reported to act in translational repression (Piecyk et al., 2000; Dixon et al., 2003; Kandasamy et al., 2005). Numerous other localization complex components were shown to act in translational repression of localized transcripts in different systems (Kim-Ha et al., 1995; Colegrove-Otero et al., 2005; Hüttelmaier et al., 2005). However, translational activity of a mutant *dnd1*-LE reporter RNA with reduced affinity for Tia1 was not affected compared to a wild-type *dnd1*-LE reporter RNA. In accordance, tethering of Tia1 to a reporter RNA did not mediate translational repression in oocytes. Consistently, Colegrove-Otero et. al. showed that Tia1 binds to the *gdf1* translational element, but depletion of Tia1 from oocyte extracts did not affected translational activity of a *gdf1* reporter RNA (Colegrove-Otero et al., 2005). However, other regions of the mRNA might be required for Tia1 mediated translational regulation. Furthermore, Tia1 binds to other vegetal LEs *in vitro* and it needs to be analyzed if Tia1 translationally represses these transcripts in oocytes.

4.2.2. Self aggregation of Tia1 - formation of stress granules and multimerization of localization RNPs?

Tia1 is a known component of stress granules in somatic cells and promotes their aggregation by self-assembly via its prion-like C-terminal domain (Tian et al., 1991; Gilks et al., 2004). Other known localization complex components like Stau1 and Elavl proteins are reported to be components of stress granules in other systems (Gallouzi et al., 2000; Thomas et al., 2005). Although the presence of stress granules in *Xenopus* oocytes is unknown, *C. elegans* oocytes form large Tia1 containing RNP granules in response to stress (Jud et al., 2008; Patterson et al., 2011). Thus, localization RNPs and stress granules might contain overlapping components and they could interchange proteins in response to environmental conditions. Immunostaining of oocytes show Tia1 containing particles that appear to contact the localization RNP granules. Thus, the ability of Tia1 to self aggregate might be involved in the formation of localization RNP granules in oocytes. However, the mutant *dnd1*-LE with reduced affinity for Tia1 shows full localization capacity and forms similar granular particles as observed for wild-type *dnd1*-LE. Thus, localization complex components might act redundantly in the multimerization of localization RNPs, or a multimerization of Tia1 is dispensable for vegetal transport. Still, the functional relation between localization RNPs and stress granules is unknown, and it is of future interest to identify the function of RNP components in both aspects.

4.3. Celf1 and Tia1 counteract maternal mRNA degradation in *Xenopus* embryos

We found that Celf1 and Tia1 are novel components of vegetal localization complexes in *Xenopus* oocytes. Ectopic expression of Celf1 or Tia1 in *Xenopus* embryos counteracts degradation of a *dnd1*-LE reporter RNA. Futhermore, Tia1 seems to be involved in the protection of several endogenous localizing and germ cell specific transcripts during MZT. Moreover, Tia1 synergizes with the germ cell specific protein Dnd1 in the protection of the *dnd1* transcript from miR-mediated decay.

4.3.1. Localization RNP components counteract RNA degradation in embryos

During MZT, a large fraction of maternal transcripts is degraded in order to shift the control of embryonic development to zygotically produced RNA and proteins (Tadros and Lipshitz, 2009). Several mRNAs that are involved in germ cell specification are protected from

degradation within PGCs (Koebernick et al., 2010). Celf1 is involved in the vegetal transport of *dnd1*-LE in oocytes and counteracts the somatic degradation of this transcript in embryos. Tia1 also interacts with the localizing *dnd1*-LE in oocytes, but it is still unclear, if Tia1 has a function in vegetal RNA transport. However, Tia1 stabilizes *dnd1*-LE as well as several other maternal localizing and germ cell specific transcripts in embryos. Thus, Tia1 or Celf1 binding to localizing RNAs in oocytes might predetermine those transcripts that are stabilized during embryogenesis. Indeed, Tia1 and Celf1 co-localize with vegetally localized RNA, suggesting that they remain bound to localizing RNAs upon fertilization. Similarly, Elavl2 was shown to bind localizing RNAs in oocytes and stabilize same transcripts in embryos (Koebernick et al., 2010). Such an initial binding in oocytes might ensure immediate stabilization upon the start of transcript degradation during MZT. Strikingly, the miR processing and effector machinery might also be maternally provided, as injection of pre-miRNAs that are known to mediate deadenylation of maternal mRNA during MZT, into 1-cell stage embryos causes a premature deadenylation of target mRNAs (Lund et al., 2009). Thus, the supply of proteins in oocytes that are required only later during embryogenesis might be a general feature to ensure their immediate action when they are required. However, the germ cell specific mRNA *cpeb1a* is stabilized in embryos after ectopic expression of Tia1, although this mRNA does not localize in oocytes (A. Smarandache, M. Claussen, unpublished). Thus, Tia1 also stabilizes germ cell specific RNAs in embryos that are not localizing during oogenesis. However, so far Celf1 and Tia1 proteins were not detected in PGCs of *Xenopus* embryos and thus, their function in the stabilization of germline transcripts *in vivo* is unclear.

4.3.2. Tia1 counteracts miR-mediated decay of localizing and germ cell specific RNAs in *Xenopus* embryos

Tia1 might be involved in the protection of germline transcripts, as ectopic expression of Tia1 leads to somatic stabilization of several germ cell specific mRNAs including *dnd1, germes,* and *grip2*. Other germ cell specific mRNAs are not or only slightly affected by Tia1 overexpression, suggesting that Tia1 does not generally stabilize all germ cell specific transcripts. Indeed, Tia1 also interacts with the LEs of *dnd1* and *grip2 in vitro*. However, *tia1* is mainly expressed in neural tissues of *Xenopus* embryos, whereas *tia1* transcripts have not been not detected in germ cells by WMISH (Rothé et al., 2006). Still, *tia1* transcripts have been detected in germ cells by RNA sequencing (Aliaksandr Dzementsei, unpublished), suggesting that Tia1 proteins are present in PGCs. The stabilization of germ cell specific mRNAs by Tia1 could involve interactions with germ cell specific proteins. Indeed, Tia1 synergizes with Dnd1 in the protection of a *dnd1* reporter RNA from somatic degradation.

Tia1 ectopic expression also leads to stabilization of localizing mRNAs, which are not restricted to the germline, like *gdf1*. Although the LE of *gdf1* does not mediate somatic degradation (Koebernick et al., 2010), *gdf1* transcript levels decrease during MZT (Birsoy et al., 2006). The blockage of miR processing by inhibiting the activity of the Dicer complex does not stabilize *gdf1* transcripts (Juliane Wellner, unpublished), suggesting that maternal *gdf1* mRNA is degraded by other mechanism than miR-mediated decay, and that endogenous Tia1 might counteract these mechanism. Indeed, a fraction of maternal *gdf1* transcripts seems to be essential for early development, as the antisense depletion of *gdf1* mRNA in *Xenopus* embryos leads to gastrulation defects (Birsoy et al., 2006). Thus, Tia1 might protect a small fraction of maternal *gdf1* transcripts during the MZT, that is required for early embryonic development.

4.3.3. How do Celf1 and Tia1 mediate protection of mRNAs from miR-mediated decay?

We found that ectopic expression of Celf1 leads to somatic stabilization of a *dnd1*-LE reporter RNA, suggesting that Celf1 might be involved in the protection of *dnd1* from miR mediated decay during MZT. In contrast to a function of Celf1 in transcript stabilization, Paillard et al. described Celf1 to function in the deadenylation of maternal mRNAs in *Xenopus* embryos (Paillard et al., 1998) that is followed by their degradation at blastula stage (Audic et al., 1997). Celf1 might promote deadenylation via interactions with the poly(A)-specific ribonuclease (PARN) (Moraes et al., 2006). Similarly, the cytoplasmic polyadenylation element binding protein (CPEB) interacts with PARN in the deadenylation of maternal transcripts in *Xenopus* oocytes (Kim and Richter, 2006). However, phosphorylation of CPEB leads to the dissociation of PARN, and CPEB function is inverted to polyadenylation activity (Kim and Richter, 2006). Thus, Celf1 might destabilize certain mRNAs by deadenylation, but stabilize others by polyadenylation. However, the mechanism of Celf1 mediated stabilization of *dnd1* is unclear and it remains to be determined whether post-translational modifications of Celf1 influence the opposing effects on transcript stability.

Several maternal RNAs are degraded during MZT in embryos by miR-mediated decay (Lund et al., 2009; Koebernick et al., 2010). The degradation of *dnd1* mRNA during MZT is mediated by miR-18 (Koebernick et al., 2010). Thus, Tia1 and Celf1 might protect target RNAs by antagonizing miR binding. Similarly, Dnd1 protein is suggested to prevent binding of microRNA 430 to the germline mRNAs *nanos* and *tdrd7* in zebrafish (Kedde et al., 2007). Indeed, both Celf1 and Tia1 bind to the 5' part of the *dnd1*-LE overlapping the miR-18 target site. Thus, both proteins might prevent miR-mediated decay by physically blocking the target

site of miR-18. On the other hand, Celf 1 and Tia1 could also change the RNA structure and thereby inhibit miR binding. However, further approaches are required to identify the mechanism of Tia1 and Celf1 mediated RNA stabilization.

4.4. RNA localization and germ cell formation - Evolutionary considerations

4.4.1. RNA localization and germ cell specific stabilization - two mechanism to determine germ cell fate?

Germ cell specific RNAs are localized to the vegetal cortex during oogenesis, where they associate with the germ plasm (MacArthur et al., 2000; Horvay et al., 2006). During cleavage cycles, cells that inherit the germ plasm are directed to germ cell fate. Thus, RNA localization is an initial mechanism in oocytes to promote germ cell formation. After fertilization, during the MZT, maternal RNAs are degraded in the soma, while germline RNAs are protected by germ plasm components in germ cells (Kedde et al., 2007; Koebernick et al., 2010). One might ask why two mechanism are required to restrict RNAs to the germline. Assuming a partial inheritance of germline RNAs by somatic cells during cleavage cycles, somatic degradation and germ cell specific protection might support the restriction of germline RNAs to germ cells. Indeed, *dnd1* mRNA localizes to a broad region at the vegetal pole via the late pathway (Horvay et al., 2006), what might lead to the presence of *dnd1* outside of the germ plasm in embryos. Thus, the somatic degradation of *dnd1* transcripts could be required in order to avoid somatic malformations. However, other germline RNAs including *pgat* and *dazl* localize to a narrow region at the vegetal cortex via the early pathway leading to their restriction to the germ plasm (Hudson and Woodland, 1998; Houston and King, 2000). Thus, the somatic degradation of these transcripts seems redundant. Still, vegetal localization in oocytes might be inefficient leading to the inheritance of a minor fraction of transcripts by somatic cells and their somatic degradation might be required to ensure their restriction to PGCs.

On the other hand, the somatic degradation mechanism of germline RNAs might be the consequence of a global degradation of maternal RNAs. The germ cell specific protection of germline RNAs by protecting the sequences responsible for somatic degradation might have been evolutionary favourable than alterations in their RNA sequence in order to exclude them from microR-mediated decay.

4.4.2. The convergent evolution of RNA localization as mechanism for germ cell pre-determination

Two major modes of germ cell formation exist in the animal kingdom, the induction of germ cells by signals from surrounding tissues during embryonic development, or the pre-determination of germ cells by the inheritance of germ plasm from the egg (Saffman and Lasko, 1999). A distribution of both mechanism throughout the animal kingdom raises some controversy about the ancestral mode of germ cell formation. For instance, in anuran amphibians (frogs), germ cells are pre-determined, while in its sister lineage of urodeles (salamanders) germ cells are formed by inductive signals. Based on the comparison of morphological processes with germ cell formation between both amphibian lineages, Johnson et. al. suggested inductive germ cell formation to be ancestral and the mechanism of pre-formation to be derived (Johnson et al., 2003). Interestingly, a recent study that compared gene sequences of species using pre-formation with their sister lineages using inductive germ cell formation, revealed that species employing pre-formation evolve faster. Evans et. al. (2014) suggested the initial localization of germ plasm components to liberate constraints on somatic development and thus to accelerate evolution. This might have enforced the repeated invention of localized germ plasm within the animal kingdom (Evans et al., 2014).

4.5. Indications for functions of Celf1 during zebrafish oogenesis

Zebrafish and *Xenopus* oogenesis and their RNA localization patterns share striking similarities. The vegetal localization of Celf1 is conserved between fish and frog, suggesting a conserved role of Celf1 in RNA localization. Indeed, a conservation of the localization machinery has been suggested before, as zebrafish *vasa* 3'UTR localizes in *Xenopus* oocytes after microinjection (Knaut et al., 2002). Furthermore, the zebrafish Igf2bp3 co-localizes with *cyclinb1* mRNA at the animal cortex (Takahashi et al., 2014), suggesting a conserved role of Igf2bp3 in RNA localization during *Xenopus* and zebrafish oogenesis. However, our attempt to analyze the function of Celf1 in RNA localization during zebrafish oogenesis by a loss of function approach was not successful, as the creation of zebrafish *celf1* mutants resulted in the primary development of males. Although the creation of mosaic *celf1* mutants led to the development of few females, only approximately half of their unfertilized eggs contain *celf1* miss-sense or non-sense mutations. Thus, it is likely that their eggs derived from heterozygous oocytes, which contain functional Celf1 proteins.

The major development of males could be either caused by female lethality or by female to male sex reversal. During zebrafish development, all juvenile fish are initially hermaphrodite and have immature oocytes. Whereas oocyte maintenance leads to the development of females, their apoptosis alters the gonadal fate and leads to development of males (Uchida et al., 2002; Rodríguez-Marí et al., 2010). The early ablation of germ cells by expression of toxins or knock-down of proteins involved in germ cell maintenance leads the development of sterile males (Slanchev et al., 2005; Houwing et al., 2008). Indeed, Celf1 was shown to be localized in germ plasm structures of early zebrafish embryos (Hashimoto et al., 2006). Furthermore, male and female *celf1* knock-out mice show impaired fertility (Kress et al., 2007). Male *celf1* knock-out mice have defects in spermatogenesis and show a downregulation of germ cell markers, suggesting a general decrease in germ cells. The reason for the infertility of female *celf1* knockout mice is unknown (Kress et al., 2007). These observations suggest that Celf1 might play a conserved role in vertebrate germ cell development or maintenance. However, homozygous *celf1* mutant zebrafish males are fertile, indicating that the maintenance or viability of oocytes is affected, rather than germ cell development in general. Similarly, zebrafish with a mutation in the *fancl* gene that encodes a member of the Fanconi Anemia DNA repair pathway, develop exclusively as fertile males, because their oocytes do not survive through meiosis (Rodríguez-Marí et al., 2010). Thus, Celf1 might play a conserved role in oocyte maintenance and the loss of Celf1 could affect oocyte viability that leads to male development in zebrafish. However, it is still unclear if female viability is affected and further analyses using higher embryo numbers are required to support the sex conversion of *celf1* mutants towards male development. The analysis of these mutants during the critical step of gonad fate decision might provide insight into a function of Celf1 in this process.

4.6. Conclusions

RNA localization has emerged as a key mechanism for gene regulation that impacts a variety of biological processes including embryonic development. The study of vegetal RNA localization during *Xenopus* oogenesis provides an accessible system to gain insight into this important mechanism and its impact on embryonic patterning and germ cell development. The control of vegetal RNA localization involves a complex interplay between *cis*-acting RNA localization elements, *trans*-acting RNA binding proteins as well as additional factors like motor proteins and cytoskeletal elements. Numerous factors that mediate RNA localization during oogenesis have been identified. However, the full composition of localization RNPs as well as their individual functions are far from a detailed understanding. This study revealed two conserved RNA binding proteins to be involved in the localization of mRNAs during oogenesis and their regulation during embryogenesis. The functional characterization of Celf1 suggests this protein to participate in vegetal RNA localization in *Xenopus* oocytes, and a conserved function is suggested for zebrafish oogenesis. While Tia1 is also a component of vegetal localization RNPs, this protein seems to stabilize multiple localizing and germ cell specific transcripts during the critical phase of the maternal to zygotic transition. Thus, this study provides a further step towards the elucidation of the factors that constitute localization RNPs and gives explanations on how they affect early embryonic processes. However, the further dissection of Celf1 and Tia1 functions during the different steps of RNA localization and germ cell formation is required to understand the underlying molecular processes. Future studies could address open questions including their nuclear or cytoplasmic recruitment, their role in RNP assembly, remodelling and vegetal anchoring and how their functions extend to embryonic development.

5. References

Abrams, E.W., Mullins, M.C., 2009. Early zebrafish development: it's in the maternal genes. Current opinion in genetics & development 19(4), 396-403.

Ainger, K., Avossa, D., Morgan, F., Hill, S.J., Barry, C., Barbarese, E., Carson, J.H., 1993. Transport and localization of exogenous myelin basic protein mRNA microinjected into oligodendrocytes. The Journal of cell biology 123(2), 431-441.

Albright, L.M., Slatko, B.E., 2001. Denaturing polyacrylamide gel electrophoresis. Current Protocols in Nucleic Acid Chemistry 00:3B:A.3B.1-00:3BA.3B.5.

Allison, R., Czaplinski, K., Git, A., Adegbenro, E., Stennard, F., Houliston, E., Standart, N., 2004. Two distinct Staufen isoforms in Xenopus are vegetally localized during oogenesis. RNA 10(11), 1751-1763.

Arthur, P.K., Claussen, M., Koch, S., Tarbashevich, K., Jahn, O., Pieler, T., 2009. Participation of Xenopus Elr-type proteins in vegetal mRNA localization during oogenesis. Journal of Biological Chemistry 284(30), 19982-19992.

Audic, Y., Omilli, F., Osborne, H.B., 1997. Postfertilization deadenylation of mRNAs in Xenopus laevis embryos is sufficient to cause their degradation at the blastula stage. Molecular and cellular biology 17(1), 209-218.

Auweter, S.D., Oberstrass, F.C., Allain, F.H.-T., 2006. Sequence-specific binding of single-stranded RNA: is there a code for recognition? Nucleic Acids Research 34(17), 4943-4959.

Bally-Cuif, L., Schatz, W.J., Ho, R.K., 1998. Characterization of the zebrafish Orb/CPEB-related RNA-binding protein and localization of maternal components in the zebrafish oocyte. Mechanisms of development 77(1), 31-47.

Barkan, A., Rojas, M., Fujii, S., Yap, A., Chong, Y.S., Bond, C.S., Small, I., 2012. A combinatorial amino acid code for RNA recognition by pentatricopeptide repeat proteins. PLoS genetics 8(8), e1002910.

Barreau, C., Paillard, L., Osborne, H.B., 2005. AU-rich elements and associated factors: are there unifying principles? Nucleic acids research 33(22), 7138-7150.

Bartlett, J. M. S., Stirling, D., 2003. "A Short History of the Polymerase Chain Reaction". PCR Protocols 226. pp. 3–6.

Bashirullah, A., Cooperstock, R.L., Lipshitz, H.D., 1998. RNA localization in development. Annual Review Of Biochemistry 67, 335-394.

Bassell, G.J., Zhang, H., Byrd, A.L., Femino, A.M., Singer, R.H., Taneja, K.L., Lifshitz, L.M., Herman, I.M., Kosik, K.S., 1998. Sorting of beta-actin mRNA and protein to neurites and growth cones in culture. Journal of Neuroscience 18(1), 251-265.

Bauermeister, D., Claussen, M., Pieler, T., 2014. Biochemical Aspects of Subcellular RNA Transport and Localization, in: V.A. Erdmann, W.T. Markiewicz, J. Barciszewski (Eds.), Chemical Biology of Nucleic Acids. Springer Berlin Heidelberg, pp. 293-308.

Beck, A.R., Medley, Q.G., O'Brien, S., Anderson, P., Streuli, M., 1996. Structure, tissue distribution and genomic organization of the murine RRM-type RNA binding proteins TIA-1 and TIAR. Nucleic Acids Research 24(19), 3829-3835.

Berleth, T., Burri, M., Thoma, G., Bopp, D., Richstein, S., Frigerio, G., Noll, M., Nüsslein-Volhard, C., 1988. The role of localization of bicoid RNA in organizing the anterior pattern of the Drosophila embryo. The EMBO Journal 7(6), 1749-1756.

Besse, F., López de Quinto, S., Marchand, V., Trucco, A., Ephrussi, A., 2009. Drosophila PTB promotes formation of high-order RNP particles and represses oskar translation. Genes and Development 23(2), 195-207.

Betley, J.N., Frith, M.C., Graber, J.H., Choo, S., Deshler, J.O., 2002. A ubiquitous and conserved signal for RNA localization in chordates. Current Biology 12(20), 1756-1761.

Birsoy, B., Kofron, M., Schaible, K., Wylie, C., Heasman, J., 2006. Vg1 is an essential signaling molecule in Xenopus development. Development 133(1), 15-20.

Blitz, I.L., Biesinger, J., Xie, X., Cho, K.W.Y., 2013. Biallelic genome modification in F0 Xenopus tropicalisembryos using the CRISPR/Cas system. Genesis 51, 827-834.

Blom, N., Gammeltoft, S., Brunak, S., 1999. Sequence and structure-based prediction of eukaryotic protein phosphorylation sites. Journal of molecular biology 294(5), 1351-1362.

Blower, M.D., Feric, E., Weis, K., Heald, R., 2007. Genome-wide analysis demonstrates conserved localization of messenger RNAs to mitotic microtubules. The Journal of cell biology 179(7), 1365-1373.

Böhl, F., Kruse, C., Frank, A., Ferring, D., Jansen, R.P., 2000. She2p, a novel RNA-binding protein tethers ASH1 mRNA to the Myo4p myosin motor via She3p. The EMBO journal 19(20), 5514-5524.

Bonnet-Corven, S., Audic, Y., Omilli, F., Osborne, H.B., 2002. An analysis of the sequence requirements of EDEN-BP for specific RNA binding. Nucleic acids research 30(21), 4667-4674.

Bradford, M.M., 1976. A rapid and sensitive method for the quantitation of microgram quantities of protein utilizing the principle of protein-dye binding. Analytical biochemistry 72(1), 248-254.

Broadus, J., Fuerstenberg, S., Doe, C.Q., 1998. Staufen-dependent localization of prospero mRNA contributes to neuroblast daughter-cell fate. Nature 391, 792-795.

Bubunenko, M., Kress, T.L., Vempati, U.D., Mowry, K.L., King, M.L., 2002. A consensus RNA signal that directs germ layer determinants to the vegetal cortex of Xenopus oocytes. Developmental Biology 248(1), 82-92.

Bullock, S.L., Ish-Horowicz, D., 2001. Conserved signals and machinery for RNA transport in Drosophila oogenesis and embryogenesis. Nature 414(6864), 611-616.

Bullock, S.L., Zicha, D., Ish-Horowicz, D., 2003. The Drosophila hairy RNA localization signal modulates the kinetics of cytoplasmic mRNA transport. The EMBO journal 22(10), 2484-2494.

Bullock, S.L., Ringel, I., Ish-Horowicz, D., Lukavsky, P.J., 2010. A' form RNA helices are required for cytoplasmic mRNA transport in Drosophila. Nature 17(6), 703-709.

Chan, A.P., Kloc, M., Etkin, L.D., 1999. fatvg encodes a new localized RNA that uses a 25-nucleotide element (FVLE1) to localize to the vegetal cortex of Xenopus oocytes. Development 126(22), 4943-4953.

Chang, P., Torres, J., Lewis, R.A., Mowry, K.L., Houliston, E., King, M.L., 2004. Localization of RNAs to the mitochondrial cloud in Xenopus oocytes through entrapment and association with endoplasmic reticulum. Molecular Biology of the Cell 15(10), 4669-4681.

Chao, J.A., Patskovsky, Y., Patel, V., Levy, M., Almo, S.C., Singer, R.H., 2010. ZBP1 recognition of beta-actin zipcode induces RNA looping. Genes and Development 24(2), 148-158.

Chartrand, P., Meng, X.H., Singer, R.H., Long, R.M., 1999. Structural elements required for the localization of ASH1 mRNA and of a green fluorescent protein reporter particle in vivo. Current Biology 9(6), 333-336.

Chekulaeva, M., Hentze, M.W., Ephrussi, A., 2006. Bruno acts as a dual repressor of oskar translation, promoting mRNA oligomerization and formation of silencing particles. Cell 124(3), 521-533.

Claussen, M., Tarbashevich, K., Pieler, T., 2011. Functional dissection of the RNA signal sequence responsible for vegetal localization of XGrip2.1 mRNA in Xenopus oocytes. RNA Biology 8(5), 873-882.

Claussen, M., Pieler, T., 2004. Xvelo1 uses a novel 75-nucleotide signal sequence that drives vegetal localization along the late pathway in Xenopus oocytes. Developmental Biology 266(2), 270-284.

Claussen, M., Horvay, K., Pieler, T., 2004. Evidence for overlapping, but not identical, protein machineries operating in vegetal RNA localization along early and late pathways in Xenopus oocytes. Development 131(17), 4263-4273.

Claussen, M., Pieler, T., 2010. Identification of vegetal RNA-localization elements in Xenopus oocytes. Methods 51(1), 146-151.

Colegrove-Otero, L.J., Devaux, A., Standart, N., 2005. The Xenopus ELAV protein ElrB represses Vg1 mRNA translation during oogenesis. Molecular Cell Biology 25(20), 9028-9039.

Cosson, B., Gautier-Courteille, C., Maniey, D., Aït-Ahmed, O., Lesimple, M., Osborne, H.B., Paillard, L., 2006. Oligomerization of EDEN-BP is required for specific mRNA deadenylation and binding. Biology of the Cell 98(11), 653-665.

Cote, C.A., Gautreau, D., Denegre, J.M., Kress, T.L., Terry, N.A., Mowry, K.L., 1999. A Xenopus protein related to hnRNP I has a role in cytoplasmic RNA localization. Molecular Cell 4(3), 431-437.

Cuykendall, T.N., Houston, D.W., 2010. Identification of germ plasm-associated transcripts by microarray analysis of Xenopus vegetal cortex RNA. Developmental dynamics 239(6), 1838-1848.

Czaplinski, K., Köcher, T., Schelder, M., Segref, A., Wilm, M., Mattaj, I.W., 2005. Identification of 40LoVe, a Xenopus hnRNP D family protein involved in localizing a TGF-beta-related mRNA during oogenesis. Developmental Cell 8(4), 505-515.

Czaplinski, K., Mattaj, I.W., 2006. 40LoVe interacts with Vg1RBP/Vera and hnRNP I in binding the Vg1-localization element. RNA 12(2), 213-222.

Danilchik, M.V., Gerhart, J.C., 1987. Differentiation of the animal vegetal axis in Xenopus-laevis oocytes.1. Polarized intracellular translocation of platelets establishes the yolk gradient. Developmental Biology 122(1), 101-112.

Dasgupta, T., Ladd, A.N., 2011. The importance of CELF control: molecular and biological roles of the CUG-BP, Elav-like family of RNA-binding proteins. Wiley Interdisciplinary Reviews: RNA 3(1), 104-121.

De Castro, E., Sigrist, C.J.A., Gattiker, A., Bulliard, V., Langendijk-Genevaux, P.S., Gasteiger, E., Bairoch, A., Hulo, N., 2006. ScanProsite: detection of PROSITE signature matches and ProRule-associated functional and structural residues in proteins. Nucleic acids research 34(Web Server Issue), W362-W365.

Del Gatto, F., Plet, A., Gesnel, M.-C., Fort, C., Breathnach, R., 1997. Multiple interdependent sequence elements control splicing of a fibroblast growth factor receptor 2 alternative exon. Molecular and cellular biology 17(9), 5106-5116.

Dember, L.M., Kim, N.D., Liu, K.Q., Anderson, P., 1996. Individual RNA recognition motifs of TIA-1 and TIAR have different RNA binding specificities. The Journal of Biological Chemistry 271(5), 2783-2788.

Deshler, J.O., Highett, M.I., Schnapp, B.J., 1997. Localization of Xenopus Vg1 mRNA by Vera protein and the endoplasmic reticulum. Science 276(5315), 1128-1131.

Detivaud, L., Pascreau, G., Karaïskou, A., Osborne, H.B., Kubiak, J.Z., 2003. Regulation of EDEN-dependent deadenylation of Aurora A/Eg2-derived mRNA via phosphorylation and dephosphorylation in Xenopus laevis egg extracts. Journal of Cell Science 116, 2697-2705.

Ding, D., Parkhurst, S.M., Halsell, S.R., Lipshitz, H.D., 1993. Dynamic Hsp83 RNA localization during Drosophila oogenesis and embryogenesis. Molecular Cell Biology 13(6), 3773-3781.

Dixon, D.A., Balch, G.C., Kedersha, N., Anderson, P., Zimmerman, G.A., Beauchamp, R.D., Prescott, S.M., 2003. Regulation of cyclooxygenase-2 expression by the translational silencer TIA-1. J Exp erimental Medicine 198(3), 475-481.

Dumont, J., 1972. Oogenesis in Xenopus laevis (Daudin). I. Stages of oocyte development in laboratory maintained animals. Journal of Morphology 136(2), 153-179.

Edwards, J., Malaurie, E., Kondrashov, A., 2011. Sequence determinants for the tandem recognition of UGU and CUG rich RNA elements by the two N—terminal RRMs of CELF1. Nucleic Acids Research 39(19), 1-13.

Ephrussi, A., Dickinson, L.K., Lehmann, R., 1991. Oskar organizes the germ plasm and directs localization of the posterior determinant nanos. Cell 66(1), 37-50.

Ephrussi, A., Lehmann, R., 1992. Induction of germ cell formation by oskar. Nature 358(6385), 387-392.

Evans, T., Wade, C.M., Chapman, F.A., Johnson, A.D., Loose, M., 2014. Acquisition of Germ Plasm Accelerates Vertebrate Evolution. Science 344(6180), 200-203.

Farina, K.L., Singer, R.H., 2002. The nuclear connection in RNA transport and localization. Trends in cell biology 12(10), 466-472.

Farina, K.L., Hüttelmaier, S., Musunuru, K., Darnell, R., Singer, R.H., 2003. Two ZBP1 KH domains facilitate beta-actin mRNA localization, granule formation, and cytoskeletal attachment. Journal of Cell Biology 160(1), 77-87.

Ferrandon, D., Elphick, L., Nüsslein-Volhard, C., St Johnston, D., 1994. Staufen protein associates with the 3'UTR of bicoid mRNA to form particles that move in a microtubule-dependent manner. Cell 79(7), 1221-1232.

Filardo, P., Ephrussi, A., 2003. Bruno regulates gurken during Drosophila oogenesis. Mechanisms of Development 120(3), 289-297.

Fisher, M.P., Dingman, C.W., 1971. Role of molecular conformation in determining the electrophoretic properties of polynucleotides in agarose-acrylamide composite gels. Biochemistry 10(10), 1895-1899.

Förch, P., Puig, O., Kedersha, N., Martínez, C., Granneman, S., Séraphin, B., Anderson, P., Valcárcel, J., 2000. The apoptosis-promoting factor TIA-1 is a regulator of alternative pre-mRNA splicing. Molecular cell 6(5), 1089-1098.

Forrest, K.M., Gavis, E.R., 2003. Live imaging of endogenous RNA reveals a diffusion and entrapment mechanism for nanos mRNA localization in Drosophila. Current biology 13(14), 1159-1168.

Forristall, C., Pondel, M., Chen, L., King, M.L., 1995. Patterns of localization and cytoskeletal association of two vegetally localized RNAs, Vg1 and Xcat-2. Development 121(1), 201-208.

Gagnon, J.A., Mowry, K.L., 2011a. Visualization of mRNA Localization in Xenopus Oocytes, Methods in Molecular Biology. Humana Press, Totowa, NJ, pp. 71-82.

Gagnon, J.A., Mowry, K.L., 2011b. Molecular motors: directing traffic during RNA localization. Critical Reviews in Biochemistry and Molecular Biology 46(3), 229-239.

Gagnon, J.A., Kreiling, J.A., Powrie, E.A., Wood, T.R., Mowry, K.L., 2013. Directional Transport Is Mediated by a Dynein-Dependent Step in an RNA Localization Pathway. PLoS Biology 11(4), e1001551.

Gallouzi, I.-E., Brennan, C.M., Stenberg, M.G., Swanson, M.S., Eversole, A., Maizels, N., Steitz, J.A., 2000. HuR binding to cytoplasmic mRNA is perturbed by heat shock. Proceedings of the National Academy of Sciences 97(7), 3073-3078.

Ghosh, S., Marchand, V., Gáspár, I., Ephrussi, A., 2012. Control of RNP motility and localization by a splicing-dependent structure in oskar mRNA. Nature Structural and Molecular Biology 19(4), 441-449.

Gilbert, S.F., 2000. Developmental Biology. Sinauer Associates, Inc., Suderland, Massachusetts.

Gilks, N., Kedersha, N., Ayodele, M., Shen, L., Stoecklin, G., Dember, L.M., Anderson, P., 2004. Stress granule assembly is mediated by prion-like aggregation of TIA-1. Molecular Biology of the Cell 15(12), 5383-5398.

Git, A., Standart, N., 2002. The KH domains of Xenopus Vg1RBP mediate RNA binding and self-association. RNA 8(10), 1319-1333.

Git, A., Allison, R., Perdiguero, E., Nebreda, A.R., Houliston, E., Standart, N., 2009. Vg1RBP phosphorylation by Erk2 MAP kinase correlates with the cortical release of Vg1 mRNA during meiotic maturation of Xenopus oocytes. RNA 15(6), 1121-1133.

Gonzalez, I., Buonomo, S.B., Nasmyth, K., von Ahsen, U., 1999. ASH1 mRNA localization in yeast involves multiple secondary structural elements and Ash1 protein translation. Current Biology 9(6), 337-340.

Good, P.J., Chen, Q., Warner, S.J., Herring, D.C., 2000. A family of human RNA-binding proteins related to the Drosophila Bruno translational regulator. Journal of Biological Chemistry 275(37), 28583-28592.

Gu, W., Pan, F., Zhang, H., Bassell, G.J., Singer, R.H., 2002. A predominantly nuclear protein affecting cytoplasmic localization of β-actin mRNA in fibroblasts and neurons. The Journal of cell biology 156(1), 41-52.

Harland, R.M., 1991. In situ hybridization: an improved whole-mount method for Xenopus embryos. Methods in cell biology 36, 685-695.

Hashimoto, Y., Maegawa, S., Nagai, T., Yamaha, E., Suzuki, H., Yasuda, K., Inoue, K., 2004. Localized maternal factors are required for zebrafish germ cell formation. Developmental biology 268(1), 152-161.

Hashimoto, Y., Suzuki, H., Kageyama, Y., Yasuda, K., Inoue, K., 2006. Bruno-like protein is localized to zebrafish germ plasm during the early cleavage stages. Gene expression patterns 6(2), 201-205.

Hausen, P., Riebesell, M., 1991. The Early Development of Xenopus laevis: An Atlas of the Histology.

Havin, L., Git, A., Elisha, Z., Oberman, F., Yaniv, K., Schwartz, S.P., Standart, N., Yisraeli, J.K., 1998. RNA-binding protein conserved in both microtubule- and microfilament-based RNA localization. Genes and Development 12(11), 1593-1598.

Heasman, J., Quarmby, J., Wylie, C.C., 1984. The mitochondrial cloud of Xenopus oocytes: the source of germinal granule material. Developmental Biology 105(2), 458-469.

Heasman, J., Wessely, O., Langland, R., Craig, E.J., Kessler, D.S., 2001. Vegetal localization of maternal mRNAs is disrupted by VegT depletion. Developmental Biology 240(2), 377-386.

Heinrich, B., Deshler, J.O., 2009. RNA localization to the Balbiani body in Xenopus oocytes is regulated by the energy state of the cell and is facilitated by kinesin II. RNA 15(4), 524-536.

Helling, R.B., Goodman, H.M., Boyer, H.W., 1974. Analysis of endonuclease R· EcoRI fragments of DNA from lambdoid bacteriophages and other viruses by agarose-gel electrophoresis. Journal of virology 14(5), 1235-1244.

Ho, R.K., 1992. Cell movements and cell fate during zebrafish gastrulation. Development 116 (Suppl), 65-73.

Hoek, K.S., Kidd, G.J., Carson, J.H., Smith, R., 1998. hnRNP A2 selectively binds the cytoplasmic transport sequence of myelin basic protein mRNA. Biochemistry 37(19), 7021-7029.

Hogg, J.R., Collins, K., 2007. RNA-based affinity purification reveals 7SK RNPs with distinct composition and regulation. RNA 13(6), 868-880.

Hollemann, T., Panitz, F., Pieler, T., 1999. In situ hybridization techniques with Xenopus embryos, A comparative methods approach to the study of oocytes and embryos. Oxford University Press, pp. 279-290.

Horb, L.D., Horb, M.E., 2010. BrunoL1 regulates endoderm proliferation through translational enhancement of cyclin A2 mRNA. Developmental biology 345(2), 156-169.

Horvay, K., 2005. Identifizierung neuer vegetal lokalisierter RNAs in der Xenopus laevis Oozyte und deren funktionelle Charakterisierung. Developmental Biochemistry PhD thesis,

Horvay, K., Claussen, M., Katzer, M., Landgrebe, J., Pieler, T., 2006. Xenopus Dead end mRNA is a localized maternal determinant that serves a conserved function in germ cell development. Developmental Biology 291(1), 1-11.

Houston, D.W., King, M.L., 2000. A critical role for Xdazl, a germ plasm-localized RNA, in the differentiation of primordial germ cells in Xenopus. Development 127(3), 447-456.

Houwing, S., Berezikov, E., Ketting, R.F., 2008. Zili is required for germ cell differentiation and meiosis in zebrafish. The EMBO journal 27(20), 2702-2711.

Howley, C., Ho, R.K., 2000. mRNA localization patterns in zebrafish oocytes. Mechanisms of development 92(2), 305-309.

Hudson, C., Woodland, H.R., 1998. Xpat, a gene expressed specifically in germ plasm and primordial germ cells of Xenopus laevis. Mechanisms of Development 73(2), 159-168.

Hüttelmaier, S., Zenklusen, D., Lederer, M., Dictenberg, J., Lorenz, M., Meng, X., Bassell, G.J., Condeelis, J., Singer, R.H., 2005. Spatial regulation of β-actin translation by Src-dependent phosphorylation of ZBP1. Nature Cell Biology 438(7067), 512-515.

Hwang, W.Y., Fu, Y., Reyon, D., Maeder, M.L., Tsai, S.Q., Sander, J.D., Peterson, R.T., Yeh, J.-R.J., Joung, J.K., 2013. Efficient genome editing in zebrafish using a CRISPR-Cas system. Nature biotechnology 31(3), 227-229.

Jambhekar, A., DeRisi, J.L., 2007. Cis-acting determinants of asymmetric, cytoplasmic RNA transport. RNA 13(5), 625-642.

Jambor, H., Brunel, C., Ephrussi, A., 2011. Dimerization of oskar 3'UTRs promotes hitchhiking for RNA localization in the Drosophila oocyte. RNA 17(12), 2049-2057.

Jambor, H., Mueller, S., Bullock, S.L., Ephrussi, A., 2014. A stem–loop structure directs oskar mRNA to microtubule minus ends. RNA 20(4), 429-439.

Jankovics, F., Sinka, R., Lukácsovich, T., Erdélyi, M., 2002. MOESIN crosslinks actin and cell membrane in Drosophila oocytes and is required for OSKAR anchoring. Current Biology 12(23), 2060-2065.

Jedrusik, A., Parfitt, D.-E., Guo, G., Skamagki, M., Grabarek, J.B., Johnson, M.H., Robson, P., Zernicka-Goetz, M., 2008. Role of Cdx2 and cell polarity in cell allocation and specification of trophectoderm and inner cell mass in the mouse embryo. Genes and Development 22(19), 2692-2706.

Johnson, A.D., Drum, M., Bachvarova, R.F., Masi, T., White, M.E., Crother, B.I., 2003. Evolution of predetermined germ cells in vertebrate embryos: implications for macroevolution. Evolution and development 5(4), 414-431.

Joseph, E.M., Melton, D.A., 1998. Mutant Vg1 ligands disrupt endoderm and mesoderm formation in Xenopus embryos. Development 125(14), 2677-2685.

Jud, M.C., Czerwinski, M.J., Wood, M.P., Young, R.A., Gallo, C.M., Bickel, J.S., Petty, E.L., Mason, J.M., Little, B.A., Padilla, P.A., Schisa, J.A., 2008. Large P body-like RNPs form in C. elegans oocytes in response to arrested ovulation, heat shock, osmotic stress, and anoxia and are regulated by the major sperm protein pathway. Developmental Biology 318(1), 38-51.

Kandasamy, K., Joseph, K., Subramaniam, K., Raymond, J.R., Tholanikunnel, B.G., 2005. Translational control of β2-adrenergic receptor mRNA by T-cell-restricted intracellular antigen-related protein. Journal of Biological Chemistry 280(3), 1931-1943.

Kang, H., Schuman, E.M., 1996. A requirement for local protein synthesis in neurotrophin-induced hippocampal synaptic plasticity. Science 273(5280), 1402-1406.

Katz, Z.B., Wells, A.L., Park, H.Y., Wu, B., Shenoy, S.M., Singer, R.H., 2012. β-Actin mRNA compartmentalization enhances focal adhesion stability and directs cell migration. Genes and development 26(17), 1885-1890.

Kedde, M., Strasser, M.J., Boldajipour, B., Vrielink, J.A.F., Slanchev, K., le Sage, C., Nagel, R., Voorhoeve, P.M., van Duijse, J., Ørom, U.A., Lund, A.H., Perrakis, A., Raz, E., Agami, R., 2007. RNA-binding protein Dnd1 inhibits microRNA access to target mRNA. Cell 131(7), 1273-1286.

Kedersha, N.L., Gupta, M., Li, W., Miller, I., Anderson, P., 1999. RNA-binding proteins TIA-1 and TIAR link the phosphorylation of eIF-2α to the assembly of mammalian stress granules. The Journal of cell biology 147(7), 1431-1442.

Kim-Ha, J., Kerr, K., Macdonald, P.M., 1995. Translational regulation of oskar mRNA by bruno, an ovarian RNA-binding protein, is essential. Cell 81(3), 403-412.

Kim-Ha, J., Smith, J.L., Macdonald, P.M., 1991. oskar mRNA is localized to the posterior pole of the Drosophila oocyte. Cell 66(1), 23-35.

Kim, J.H., Richter, J.D., 2006. Opposing polymerase-deadenylase activities regulate cytoplasmic polyadenylation. Molecular cell 24(2), 173-183.

Kimmel, C.B., Ballard, W.W., Kimmel, S.R., Ullmann, B., Schilling, T.F., 1995. Stages of embryonic development of the zebrafish. Developmental dynamics 203(3), 253-310.

King, M., Zhou, Y., 1999. Polarizing genetic information in the egg: RNA localization in the frog oocyte. BioEssays 21(7), 546-557.

King, M., Messitt, T., Mowry, K.L., 2005. Putting RNAs in the right place at the right time: RNA localization in the frog oocyte. Biology of the Cell 97, 19-33.

Kloc, M., Etkin, L.D., 1994. Delocalization of Vg1 mRNA from the vegetal cortex in Xenopus oocytes after destruction of Xlsirt RNA. Science 265(5175), 1101-1103.

Kloc, M., Larabell, C., Etkin, L.D., 1996. Elaboration of the messenger transport organizer pathway for localization of RNA to the vegetal cortex of Xenopus oocytes. Developmental Biology 180(1), 119-130.

Kloc, M., Etkin, L.D., 1995. 2 distinct pathways for the localization of RNAs at the vegetal cortex in Xenopus oocytes. Development 121(2), 287-297.

Kloc, M., Bilinski, S., Dougherty, M.T., Brey, E.M., Etkin, L.D., 2004. Formation, architecture and polarity of female germline cyst in Xenopus. Developmental Biology 266(1), 43-61.

Knaut, H., Steinbeisser, H., Schwarz, H., Nüsslein-Volhard, C., 2002. An Evolutionary Conserved Region in the vasa 3′ UTR Targets RNA Translation to the Germ Cells in the Zebrafish. Current biology 12(6), 454-466.

Koebernick, K., Loeber, J., Arthur, P.K., Tarbashevich, K., Pieler, T., 2010. Elr-type proteins protect Xenopus Dead end mRNA from miR-18-mediated clearance in the soma. Proceedings of the National Acadamy of Sciences 107(37), 16148-16153.

Kolev, N.G., Huber, P.W., 2003. VgRBP71 Stimulates Cleavage at a Polyadenylation Signal in Vg1 mRNA, Resulting in the Removal of a cis-Acting Element that Represses Translation. Molecular cell 11(3), 745-755.

Kosaka, K., Kawakami, K., Sakamoto, H., Inoue, K., 2007. Spatiotemporal localization of germ plasm RNAs during zebrafish oogenesis. Mechanisms of development 124(4), 279-289.

Kress, C., Gautier-Courteille, C., Osborne, H.B., Babinet, C., Paillard, L., 2007. Inactivation of CUG-BP1/CELF1 causes growth, viability, and spermatogenesis defects in mice. Molecular and cellular biology 27(3), 1146-1157.

Kress, T.L., Yoon, Y.J., Mowry, K.L., 2004. Nuclear RNP complex assembly initiates cytoplasmic RNA localization. Journal of Cell Biology 165(2), 203-211.

Kroll, T.T., Zhao, W.-, Jiang, C., Huber, P.W., 2002. A homolog of FBP2/KSRP binds to localized mRNAs in Xenopus oocytes. Development 129(24), 5609-5619.

Kwon, S., Abramson, T., Munro, T.P., John, C.M., Köhrmann, M., Schnapp, B.J., 2002. UUCAC- and vera-dependent localization of VegT RNA in Xenopus oocytes. Current Biology 12(7), 558-564.

Ladd, A.N., Cooper, T.A., 2004. Multiple domains control the subcellular localization and activity of ETR-3, a regulator of nuclear and cytoplasmic RNA processing events. Journal of Cell Science 117(16), 3519-3529.

Ladd, A., Charlet-B, N., Cooper, T., 2001. The CELF family of RNA binding proteins is implicated in cell-specific and developmentally regulated alternative splicing. Molecular and cellular biology 21(4), 1285-1296.

Laemmli, U.K., 1970. Cleavage of structural proteins during the assembly of the head of bacteriophage T4. Nature 227(5259), 680-685.

Lasko, P., 1999. RNA sorting in Drosophila oocytes and embryos. The FASEB journal 13(3), 421-433.

Lawrence, J.B., Singer, R.H., 1986. Intracellular localization of messenger RNAs for cytoskeletal proteins. Cell 45(3), 407-415.

Lécuyer, E., Yoshida, H., Parthasarathy, N., Alm, C., Babak, T., Cerovina, T., Hughes, T.R., Tomancak, P., Krause, H.M., 2007. Global analysis of mRNA localization reveals a prominent role in organizing cellular architecture and function. Cell 131(1), 174-187.

Lee, M.S., Henry, M., Silver, P.A., 1996. A protein that shuttles between the nucleus and the cytoplasm is an important mediator of RNA export. Genes and Development 10(10), 1233-1246.

Lewis, R.A., Mowry, K.L., 2007. Ribonucleoprotein remodeling during RNA localization. Differentiation 75(6), 507-518.

Lewis, R.A., Gagnon, J.A., Mowry, K.L., 2008. PTB/hnRNP I is required for RNP remodeling during RNA localization in Xenopus oocytes. Molecular and cellular biology 28(2), 678-686.

Li, P., Yang, X., Wasser, M., Cai, Y., Chia, W., 1997. Inscuteable and Staufen mediate asymmetric localization and segregation of prospero RNA during Drosophila neuroblast cell divisions. Cell 90(3), 437-447.

Loeber, J., Claußen, M., Jahn, O., Pieler, T., 2010. Interaction of 42Sp50 with the vegetal RNA localization machinery in Xenopus laevis oocytes. FEBS Journal 277(22), 4722-4731.

Long, R.M., Singer, R.H., Meng, X., Gonzalez, I., Nasmyth, K., Jansen, R.P., 1997. Mating type switching in yeast controlled by asymmetric localization of ASH1 mRNA. Science 277(5324), 383-387.

López de Silanes, I., Galbán, S., Martindale, J.L., Yang, X., Mazan-Mamczarz, K., Indig, F.E., Falco, G., Zhan, M., Gorospe, M., 2005. Identification and functional outcome of mRNAs associated with RNA-binding protein TIA-1. Molecular and Cellular Biology 25(21), 9520-9531.

Lund, E., Liu, M., Hartley, R.S., Sheets, M.D., Dahlberg, J.E., 2009. Deadenylation of maternal mRNAs mediated by miR-427 in Xenopus laevis embryos. RNA 15(12), 2351-2363.

Lunde, B.M., Moore, C., Varani, G., 2007. RNA-binding proteins: modular design for efficient function. Nature Reviews in Molecular and Cell Biology 8(6), 479-490.

MacArthur, H., Houston, D.W., Bubunenko, M., Mosquera, L., King, M.L., 2000. DEADSouth is a germ plasm specific DEAD-box RNA helicase in Xenopus related to eIF4A. Mechanisms of Development 95(1-2), 291-295.

Macdonald, P.M., Kerr, K., 1998. Mutational analysis of an RNA recognition element that mediates localization of bicoid mRNA. Molecular and cellular biology 18(7), 3788-3795.

Mandel, M., Higa, A., 1970. Calcium-dependent bacteriophage DNA infection. Journal of molecular biology 53(1), 159-162.

Maris, C., Dominguez, C., Allain, F.H., 2005. The RNA recognition motif, a plastic RNA-binding platform to regulate post-transcriptional gene expression. FEBS Journal 272(9), 2118-2131.

Marquis, J., Paillard, L., Audic, Y., Cosson, B., Danos, O., Le Bec, C., Osborne, H.B., 2006. CUG-BP1/ CELF1 requires UGU-rich sequences for high-affinity binding. Biochemical Journal 400, 291-301.

Martin, K.C., Ephrussi, A., 2009. mRNA localization: gene expression in the spatial dimension. Cell 136(4), 719-730.

Martin, K.C., Zukin, R.S., 2006. RNA trafficking and local protein synthesis in dendrites: an overview. The Journal of neuroscience 26(27), 7131-7134.

Mei, W., Jin, Z., Lai, F., Schwend, T., Houston, D.W., King, M.L., Yang, J., 2013. Maternal Dead-End1 is required for vegetal cortical microtubule assembly during Xenopus axis specification. Development 140, 2334-2344.

Messitt, T.J., Gagnon, J.A., Kreiling, J.A., Pratt, C.A., Yoon, Y.J., Mowry, K.L., 2008. Multiple kinesin motors coordinate cytoplasmic RNA transport on a subpopulation of microtubules in Xenopus oocytes. Developmental Cell 15(3), 426-436.

Mhlanga, M.M., Bratu, D.P., Genovesio, A., Rybarska, A., Chenouard, N., Nehrbass, U., Olivo-Marin, J.-C., 2009. In vivo colocalisation of oskar mRNA and trans-acting proteins revealed by quantitative imaging of the Drosophila oocyte. PloS One 4(7), e6241.

Mili, S., Moissoglu, K., Macara, I.G., 2008. Genome-wide screen reveals APC-associated RNAs enriched in cell protrusions. Nature 453(7191), 115-119.

Minshall, N., Standart, N., 2004. The active form of Xp54 RNA helicase in translational repression is an RNA-mediated oligomer. Nucleic acids research 32(4), 1325-1334.

Moraes, K., Wilusz, C.J., Wilusz, J., 2006. CUG-BP binds to RNA substrates and recruits PARN deadenylase. RNA 12(6), 1084-1091.

Morgan, G.T., 2007. Localized co-transcriptional recruitment of the multifunctional RNA-binding protein CELF1 by lampbrush chromosome transcription units. Chromosome research 15(8), 985-1000.

Mowry, K.L., Melton, D.A., 1992. Vegetal messenger RNA localization directed by a 340-nt RNA sequence element in Xenopus oocytes. Science 255(5047), 991-994.

Müller, M., Heym, R.G., Mayer, A., Kramer, K., Schmid, M., Cramer, P., Urlaub, H., Jansen, R.-P., Niessing, D., 2011. A cytoplasmic complex mediates specific mRNA recognition and localization in yeast. PLoS Biology 9(4), e1000611.

Nevo-Dinur, K., Govindarajan, S., Amster-Choder, O., 2012. Subcellular localization of RNA and proteins in prokaryotes. Trends in genetics 28(7), 314-322.

Niessing, D., Hüttelmaier, S., Zenklusen, D., Singer, R.H., Burley, S.K., 2004. She2p is a novel RNA binding protein with a basic helical hairpin motif. Cell 119(4), 491-502.

Nieuwkoop, P.D., Faber, J., 1967. Normal Table of Xenopus laevis (Daudin). 2nd ed. North Holland Publishing, Amsterdam.

Nojima, H., Rothhämel, S., Shimizu, T., Kim, C.-H., Yonemura, S., Marlow, F.L., Hibi, M., 2010. Syntabulin, a motor protein linker, controls dorsal determination. Development 137(6), 923-933.

Norvell, A., Kelley, R.L., Wehr, K., Schupbach, T., 1999. Specific isoforms of squid, a Drosophila hnRNP, perform distinct roles in Gurken localization during oogenesis. Genes and Development 13(7), 864-876.

Obenauer, J.C., Cantley, L.C., Yaffe, M.B., 2003. Scansite 2.0: Proteome-wide prediction of cell signaling interactions using short sequence motifs. Nucleic acids research 31(13), 3635-3641.

Okita, T.W., Choi, S.B., 2002. mRNA localization in plants: targeting to the cell's cortical region and beyond. Current opinion in plant biology 5(6), 553-559.

Otero, L.J., Devaux, A., Standart, N., 2001. A 250-nucleotide UA-rich element in the 3' untranslated region of Xenopus laevis Vg1 mRNA represses translation both in vivo and in vitro. RNA 7(12), 1753-1767.

Paillard, L., Omilli, F., Legagneux, V., Bassez, T., Maniey, D., Osborne, H., 1998. EDEN and EDEN-BP, a cis element and an associated factor that mediate sequence-specific mRNA deadenylation in Xenopus embryos. The EMBO Journal 17(1), 278-287.

Pannese, M., Cagliani, R., Pardini, C.L., Boncinelli, E., 2000. Xotx1 maternal transcripts are vegetally localized in Xenopus laevis oocytes. Mechanisms of Development 90(1), 111-114.

Patel, V.L., Mitra, S., Harris, R., 2012. Spatial arrangement of an RNA zipcode identifies mRNAs under post-transcriptional control. Genes and Development 26(1), 43-53.

Patterson, J.R., Wood, M.P., Schisa, J.A., 2011. Assembly of RNP granules in stressed and aging oocytes requires nucleoporins and is coordinated with nuclear membrane blebbing. Developmental biology 353(2), 173-185.

Pelegri, F., 2003. Maternal factors in zebrafish development. Developmental Dynamics 228(3), 535-554.

Piecyk, M., Wax, S., Beck, A.R., Kedersha, N., Gupta, M., Maritim, B., Chen, S., Gueydan, C., Kruys, V., Streuli, M., Anderson, P., 2000. TIA-1 is a translational silencer that selectively regulates the expression of TNF-alpha. The EMBO Journal 19(15), 4154-4163.

Piñol-Roma, S., Dreyfuss, G., 1992. Shuttling of pre-mRNA binding proteins between nucleus and cytoplasm. Nature 355(6362), 730-732.

Poon, M.M., Choi, S.-H., Jamieson, C.A.M., Geschwind, D.H., Martin, K.C., 2006. Identification of process-localized mRNAs from cultured rodent hippocampal neurons. The Journal of neuroscience 26(51), 13390-13399.

Pratt, C.A., Mowry, K.L., 2012. Taking a cellular road-trip: mRNA transport and anchoring. Current opinion in cell biology 1-8.

Reyon, D., Tsai, S.Q., Khayter, C., Foden, J.A., Sander, J.D., Joung, J.K., 2012. FLASH assembly of TALENs for high-throughput genome editing. Nature biotechnology 30(5), 460-465.

Rodríguez-Marí, A., Cañestro, C., BreMiller, R.A., Nguyen-Johnson, A., Asakawa, K., Kawakami, K., Postlethwait, J.H., 2010. Sex reversal in zebrafish fancl mutants is caused by Tp53-mediated germ cell apoptosis. PLoS genetics 6(7), e1001034.

Rothé, F., Gueydan, C., Bellefroid, E., Huez, G., Kruys, V., 2006. Identification of FUSE-binding proteins as interacting partners of TIA proteins. Biochemical and biophysical research communications 343(1), 57-68.

Saffman, E.E., Lasko, P., 1999. Germline development in vertebrates and invertebrates. Cellular and Molecular Life Sciences 55(8-9), 1141-1163.

Salisbury, E., Sakai, K., Schoser, B., Huichalaf, C., Schneider-Gold, C., Nguyen, H., Wang, G.-L., Albrecht, J.H., Timchenko, L.T., 2008. Ectopic expression of cyclin D3 corrects differentiation of DM1 myoblasts through activation of RNA CUG-binding protein, CUGBP1. Experimental cell research 314(11-12), 2266-2278.

Sambrook, J., Russell, D.W., Russell, D.W., 2001. Molecular cloning: a laboratory manual (3-volume set). Cold spring harbor laboratory press, Cold Spring Harbor, New York, New York.

Sanger, F., Nicklen, S., Coulson, A.R., 1977. DNA sequencing with chain-terminating inhibitors. Proceedings of the National Academy of Sciences 74(12), 5463-5467.

Schier, A.F., 2007. The maternal-zygotic transition: death and birth of RNAs. Science 316(5823), 406-407.

Schupbach, T., Wieschaus, E., 1986. Germline autonomy of maternal-effect mutations altering the embryonic body pattern of Drosophila. Developmental Biology 113(2), 443-448.

Serano, T.L., Cohen, R.S., 1995. A small predicted stem-loop structure mediates oocyte localization of Drosophila K10 mRNA. Development 121(11), 3809-3818.

Sharp, J.A., Plant, J.J., Ohsumi, T.K., Borowsky, M., Blower, M.D., 2011. Functional analysis of the microtubule-interacting transcriptome. Molecular biology of the cell 22(22), 4312-4323.

Sharp, P.A., Sugden, B., Sambrook, J., 1973. Detection of two restriction endonuclease activities in Haemophilus parainfluenzae using analytical agarose-ethidium bromide electrophoresis. Biochemistry 12(16), 3055-3063.

Shen, Z., St-Denis, A., Chartrand, P., 2010. Cotranscriptional recruitment of She2p by RNA pol II elongation factor Spt4-Spt5/DSIF promotes mRNA localization to the yeast bud. Genes and Development 24(17), 1914-1926.

Slanchev, K., Stebler, J., de La Cueva-Méndez, G., Raz, E., 2005. Development without germ cells: the role of the germ line in zebrafish sex differentiation. Proceedings of the National Academy of Sciences of the United States of America 102(11), 4074-4079.

Smith, R., 2004. Moving molecules: mRNA trafficking in Mammalian oligodendrocytes and neurons. Neuroscientist 10(6), 495-500.

Snedden, D.D., Bertke, M.M., Vernon, D., Huber, P.W., 2013. RNA localization in Xenopus oocytes uses a core group of trans-acting factors irrespective of destination. RNA 19, 889-895.

Snee, M.J., Arn, E.A., Bullock, S.L., Macdonald, P.M., 2005. Recognition of the bcd mRNA localization signal in Drosophila embryos and ovaries. Molecular and cellular biology 25(4), 1501-1510.

Souopgui, J., Rust, B., Vanhomwegen, J., Heasman, J., Henningfeld, K.A., Bellefroid, E., Pieler, T., 2008. The RNA-binding protein XSeb4R: a positive regulator of VegT mRNA stability and translation that is required for germ layer formation in Xenopus. Genes and Development 22(17), 2347-2352.

St Johnston, D., Driever, W., Berleth, T., Richstein, S., Nüsslein-Volhard, C., 1989. Multiple steps in the localization of bicoid RNA to the anterior pole of the Drosophila oocyte. Development 107, 13-19.

St Johnston, D., Beuchle, D., Nüsslein-Volhard, C., 1991. Staufen, a gene required to localize maternal RNAs in the Drosophila egg. Cell 66(1), 51-63.

St Johnston, D., Brown, N.H., Gall, J.G., Jantsch, M., 1992. A conserved double-stranded RNA-binding domain. Proceedings of the National Academy of Sciences of the United States of America 89, 10979-10983.

St Johnston, D., Nüsslein-Volhard, C., 1992. The origin of pattern and polarity in the Drosophila embryo. Cell 68(2), 201-219.

Suzuki, H., Maegawa, S., Nishibu, T., Sugiyama, T., Yasuda, K., Inoue, K., 2000. Vegetal localization of the maternal mRNA encoding an EDEN-BP/Bruno-like protein in zebrafish. Mechanisms of Development 93(1-2), 205-209.

Tadros, W., Lipshitz, H.D., 2009. The maternal-to-zygotic transition: a play in two acts. Development 136(18), 3033-3042.

Takahashi, K., Kotani, T., Katsu, Y., Yamashita, M., 2014. Possible involvement of insulin-like growth factor 2 mRNA-binding protein 3 in zebrafish oocyte maturation as a novel cyclin B1 mRNA-binding protein that represses the translation in immature oocytes. Biochemical and biophysical research communications 448(1), 22-27.

Tannahill, D., Melton, D.A., 1989. Localized synthesis of the Vg1 protein during early Xenopus development. Development 106(4), 775-785.

Thomas, M.G., Tosar, L.J.M., Loschi, M., Pasquini, J.M., Correale, J., Kindler, S., Boccaccio, G.L., 2005. Staufen recruitment into stress granules does not affect early mRNA transport in oligodendrocytes. Molecular biology of the cell 16(1), 405-420.

Tian, Q., Streuli, M., Saito, H., Schlossman, S.F., Anderson, P., 1991. A polyadenylate binding protein localized to the granules of cytolytic lymphocytes induces DNA fragmentation in target cells. Cell 67(3), 629-639.

Towbin, H., Staehelin, T., Gordon, J., 1991. Electrophoretic transfer of proteins from polyacrylamide gels to nitrocellulose sheets: procedure and some applications. Biotechnology (Reading, Mass.) 24, 145-149.

Towbin, H., Staehelin, T., Gordon, J., 1979. Electrophoretic transfer of proteins from polyacrylamide gels to nitrocellulose sheets: procedure and some applications. Proceedings of the National Academy of Sciences of the United States of America 76(9), 4350-4354.

Uchida, D., Yamashita, M., Kitano, T., Iguchi, T., 2002. Oocyte apoptosis during the transition from ovary-like tissue to testes during sex differentiation of juvenile zebrafish. Journal of Experimental Biology 205(6), 711-718.

Van De Bor, V., Hartswood, E., Jones, C., Finnegan, D., Davis, I., 2005. Gurken and the I factor retrotransposon RNAs share common localization signals and machinery. Developmental Cell 9(1), 51-62.

Vanzo, N.F., Ephrussi, A., 2002. Oskar anchoring restricts pole plasm formation to the posterior of the Drosophila oocyte. Development 129(15), 3705-3714.

Wang, C., Lehmann, R., 1991. Nanos is the localized posterior determinant in Drosophila. Cell 66(4), 637-647.

Wang, H.-, Fang, J.-, Kuang, X., Miao, L.-, Wang, C., Xia, G.-, King, M.L., Zhang, J., 2012. Activity of long-chain acyl-CoA synthetase is required for maintaining meiotic arrest in Xenopus laevis. Biology of reproduction 87(3), 74.

Weeks, D.L., Melton, D.A., 1987. A maternal mRNA localized to the vegetal hemisphere in Xenopus eggs codes for a growth factor related to TGF-beta. Cell 51(5), 861-867.

Wilhelm, J.E., Vale, R.D., Hegde, R.S., 2000. Coordinate control of translation and localization of Vg1 mRNA in Xenopus oocytes. Proceedings of the National Academy of Sciences of the United States of America 97(24), 13132-13137.

Xie, J., Lee, J.-A., Kress, T.L., Mowry, K.L., Black, D.L., 2003. Protein kinase A phosphorylation modulates transport of the polypyrimidine tract-binding protein. Proceedings of the National Academy of Sciences of the United States of America 100(15), 8776-8781.

Xing, L., Bassell, G.J., 2013. mRNA localization: an orchestration of assembly, traffic and synthesis. Traffic 14(1), 2-14.

Yamaguchi, T., Taguchi, A., Watanabe, K., Orii, H., 2012. DEADSouth protein localizes to germ plasm and is required for the development of primordial germ cells in Xenopus laevis. Biology Open 2(2), 191-199.

Yisraeli, J.K., Sokol, S., Melton, D.A., 1990. A two-step model for the localization of maternal mRNA in Xenopus oocytes: involvement of microtubules and microfilaments in the translocation and anchoring of Vg1 mRNA. Development 108(2), 289-298.

Yisraeli, J.K., 2005. VICKZ proteins: a multi-talented family of regulatory RNA-binding proteins. Biol ogy of the Cell 97(1), 87-96.

Yoon, Y.J., Mowry, K.L., 2004a. Xenopus Staufen is a component of a ribonucleoprotein complex containing Vg1 RNA and kinesin. Development 131(13), 3035-3045.

Yoon, Y.J., Mowry, K.L., 2004b. Xenopus Staufen is a component of a ribonucleoprotein complex containing Vg1 RNA and kinesin. Development 131(13), 3035-3045.

Zarnack, K., Feldbrügge, M., 2010. Microtubule-dependent mRNA transport in fungi. Eukaryotic cell 9(7), 982-990.

Zearfoss, N.R., Chan, A.P., Wu, C.F., Kloc, M., Etkin, L.D., 2004. Hermes is a localized factor regulating cleavage of vegetal blastomeres in Xenopus laevis. Developmental Biology 267(1), 60-71.

Zhang, J., Houston, D.W., King, M.L., Payne, C., Wylie, C., Heasman, J., 1998. The Role of Maternal VegT in Establishing the Primary Germ Layers in Xenopus Embryos. Cell 94(4), 515-524.

Zhang, Q., Yaniv, K., Oberman, F., Wolke, U., Git, A., Fromer, M., Taylor, W.L., Meyer, D., Standart, N., Raz, E., Yisraeli, J.K., 1999. Vg1 RBP intracellular distribution and evolutionarily conserved expression at multiple stages during development. Mechanisms of Development 88(1), 101-106.

Zhang, T., Delestienne, N., Huez, G., Kruys, V., Gueydan, C., 2005. Identification of the sequence determinants mediating the nucleo-cytoplasmic shuttling of TIAR and TIA-1 RNA-binding proteins. Journal of cell science 118(23), 5453-5463.

Zhao, W.M., Jiang, C., Kroll, T.T., Huber, P.W., 2001. A proline-rich protein binds to the localization element of Xenopus Vg1 mRNA and to ligands involved in actin polymerization. The EMBO Journal 20(9), 2315-2325.

Zhou, Y., King, M.L., 1996. RNA transport to the vegetal cortex of Xenopus oocytes. Developmental Biology 179(1), 173-183.

Zhu, H., Hasman, R.A., Young, K.M., Kedersha, N.L., Lou, H., 2003. U1 snRNP-dependent function of TIAR in the regulation of alternative RNA processing of the human calcitonin/CGRP pre-mRNA. Molecular and cellular biology 23(17), 5959-5971.

Appendix

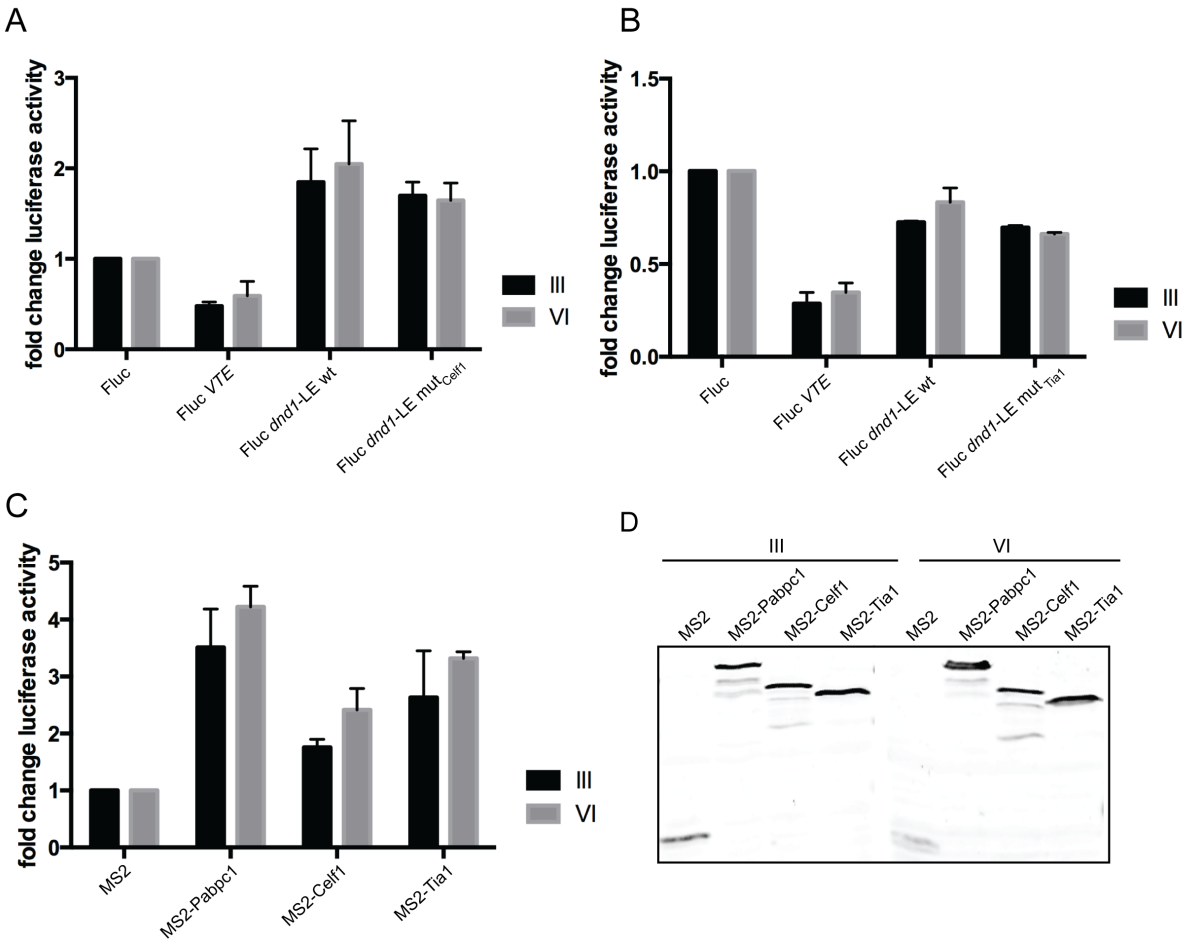

Figure S1. **Reduced binding of Tia1 and Celf1 does not significantly alter translation of *dnd1*-LE reporter RNAs, but both proteins slightly upregulate translation when tethered to a reporter RNA.** A) Translational efficiency of *firefly luciferase* (Fluc) reporter RNAs fused to the wild-type *dnd1*-LE (wt), the version with reduced affinity for Celf1 (mut_{Celf1}) or the *gdf1* translational control element (VTE) (Otero et al., 2001). Reporter RNAs were co-injected into stage III/IV oocytes with *renilla luciferase* RNA. Translational activities of the Firefly luciferase were normalized to the Renilla luciferase activities and the activity of Firefly luciferase was set to 1. B) Translational efficiency of *firefly luciferase* (Fluc) reporter RNAs fused to the *dnd1*-LE version with reduced affinity for Tia1 (mut_{Tia1}) and constructs described in A). Translational efficiencies of the Firefly luciferase were calculated as described in A). C) MS2 tethering assay using Myc-tagged MS2 fusion proteins of Celf1, Tia1 and PABP (control). The fusion proteins were expressed in stage III/IV oocytes followed by co-injection of reporter RNAs containing the *firefly luciferase* ORF fused to MS2 binding sites together with *renilla luciferase* RNA. Firefly luciferase activities were normalized to the Renilla luciferase activities and the activity of Firefly luciferase in the presence of MS2 alone was set to 1. D) Expression control of MS2-fusion proteins in oocytes used for the tethering assay (C). Proteins were detected by Western blot using anti-Myc antibodies.

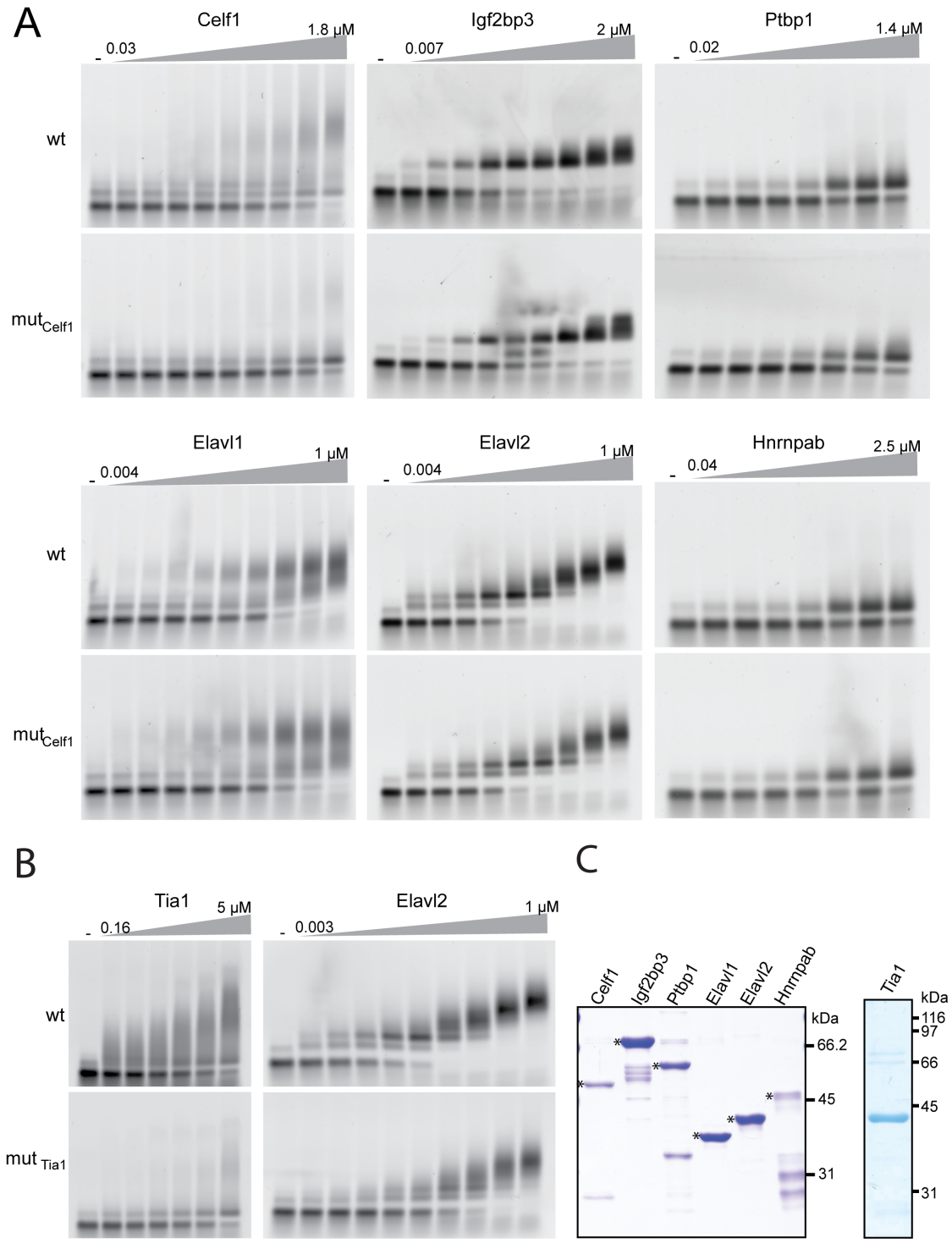

Figure S2. ***dnd1*-LE mutagenesis of the Celf1 binding-site reduces Celf1 binding, but mutagenesis of the Tia1 binding-site also affects Elavl2 binding.** A) Mobility shift analyses of bacterially expressed proteins and Cy3-labeled wild-type *dnd1*-LE (wt) and *dnd1*-LE mutated in the Celf1 binding site (mut_{Celf1}). B) Mobility shift analyses of bacterially expressed Tia1 and Elavl2 and Cy3-labeled wild-type (wt) and *dnd1*-LE mutated in the Tia1 binding site (mut_{Tia1}). C) Bacterially expressed proteins used for affinity analyses of mut_{Celf1} and mut_{Tia1} *dnd1*-LEs. Asteriks mark the relevant protein bands. Proteins were separated by SDS-PAGE and coomassie-blue stained.

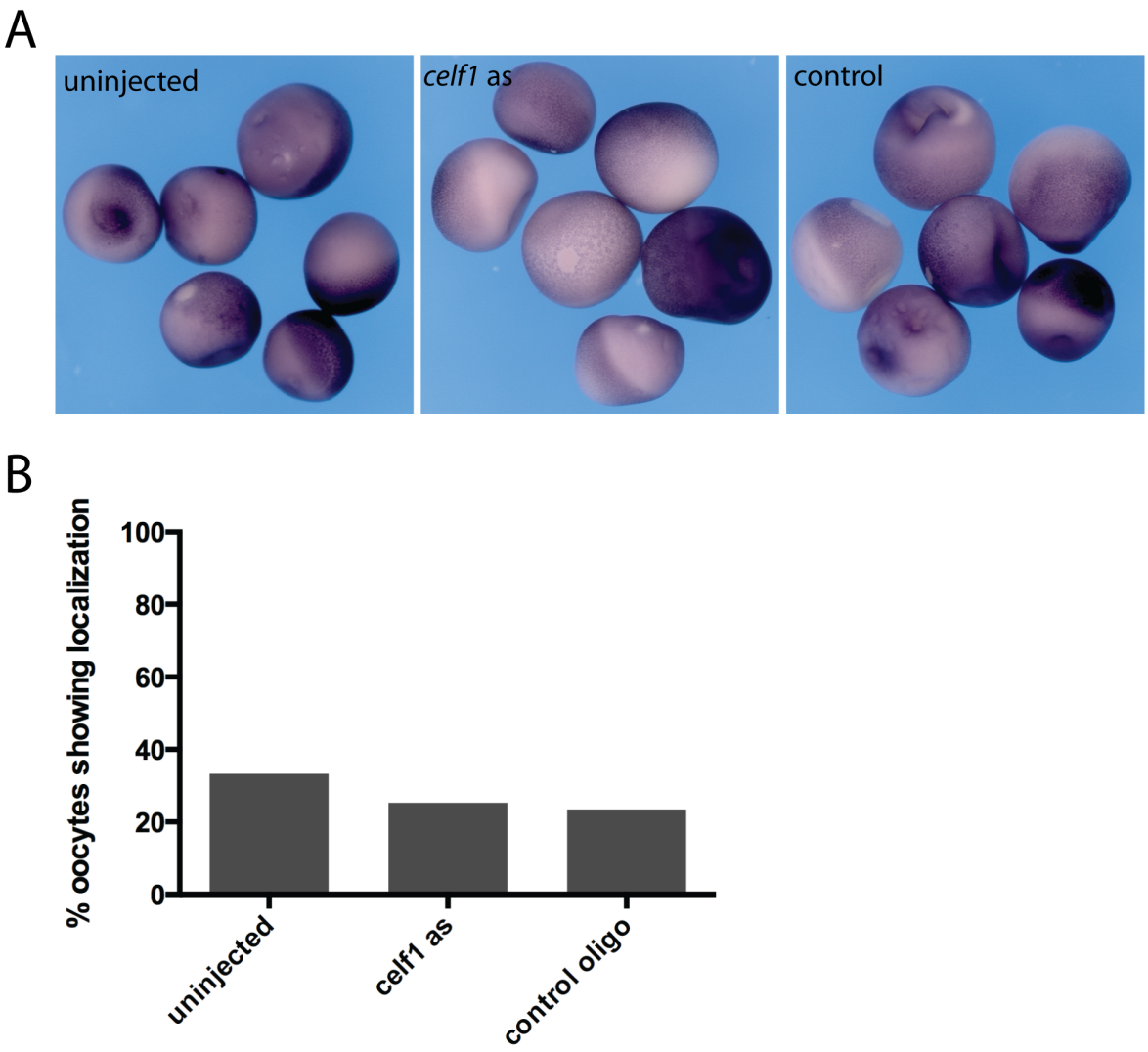

Figure S3. **Depletion of endogenous *celf1* mRNA does not affect vegetal localization of *dnd1*-LE.** A) Stage IV oocytes pre-injected with modified *celf1* antisense DNA oligos or a control oligo were injected with *lacZ-dnd1*-LE RNA. Localization was detected by whole mount *in situ* hybridization against *lacZ*. B) Quantification of *lacZ-dnd1*-LE localization efficiency of one experiment; 80-90 oocytes were analyzed per sample.

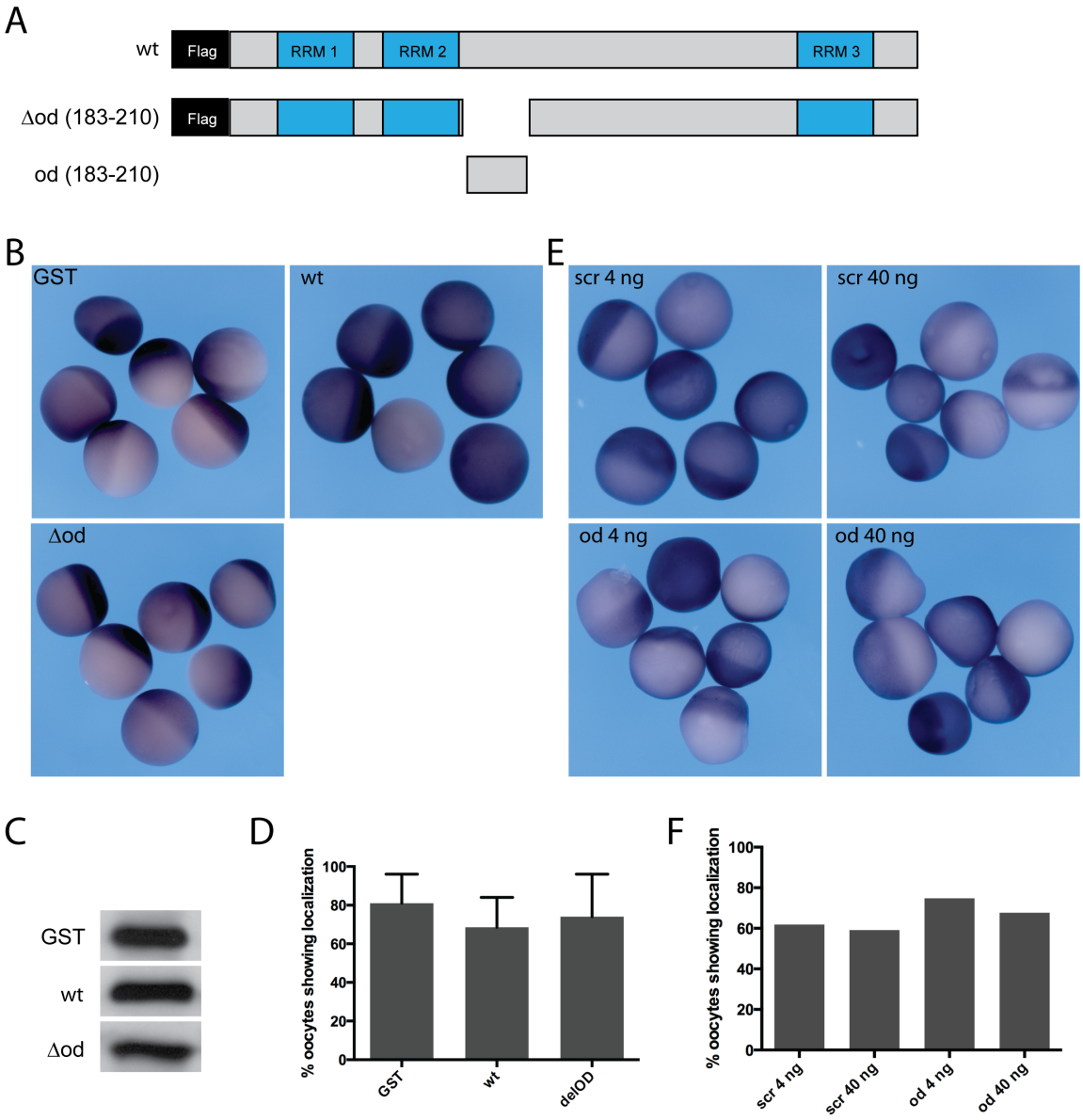

Figure S4. **A mutant version of Celf1 lacking the oligomerization domain and a peptide corresponding to the oligomerization domain do not affect vegetal localization of *dnd1*-LE.** A) Schematic presentation of wild-type (wt) Celf1, a mutant version lacking the oligomerization domain (Δod) and a peptide corresponding to the oligomerization domain (od) (Cosson et al., 2006). B) Stage III oocytes pre-injected with mRNA encoding Flag-tagged Celf1 wt, the mutant version lacking the oligomerization domain (Δod) or GST were injected with *lacZ-dnd1*-LE RNA and localization was detected by whole mount *in situ* hybridization against *lacZ*. C) Expression control of Flag-tagged proteins. Equivalent amounts of respective oocyte extracts were analyzed by anti-Flag Western blotting. D) Quantification of *lacZ-dnd1*-LE localization efficiency of oocytes injected with wt and mutant version of Celf1. Average values of two independent experiments are shown. Error bars indicate standard error of the mean. E) Stage III oocytes pre-injected with 4 or 40 ng of the peptide corresponding to the Celf1 oligomerization domain (od), or a scrambled control peptide (scr) were injected with *lacZ-dnd1*-LE RNA and localization was detected by whole mount *in situ* hybridization against *lacZ*. F) Quantification of *lacZ-dnd1*-LE localization efficiency of one experiment; approximately 100 oocytes were analyzed per sample.

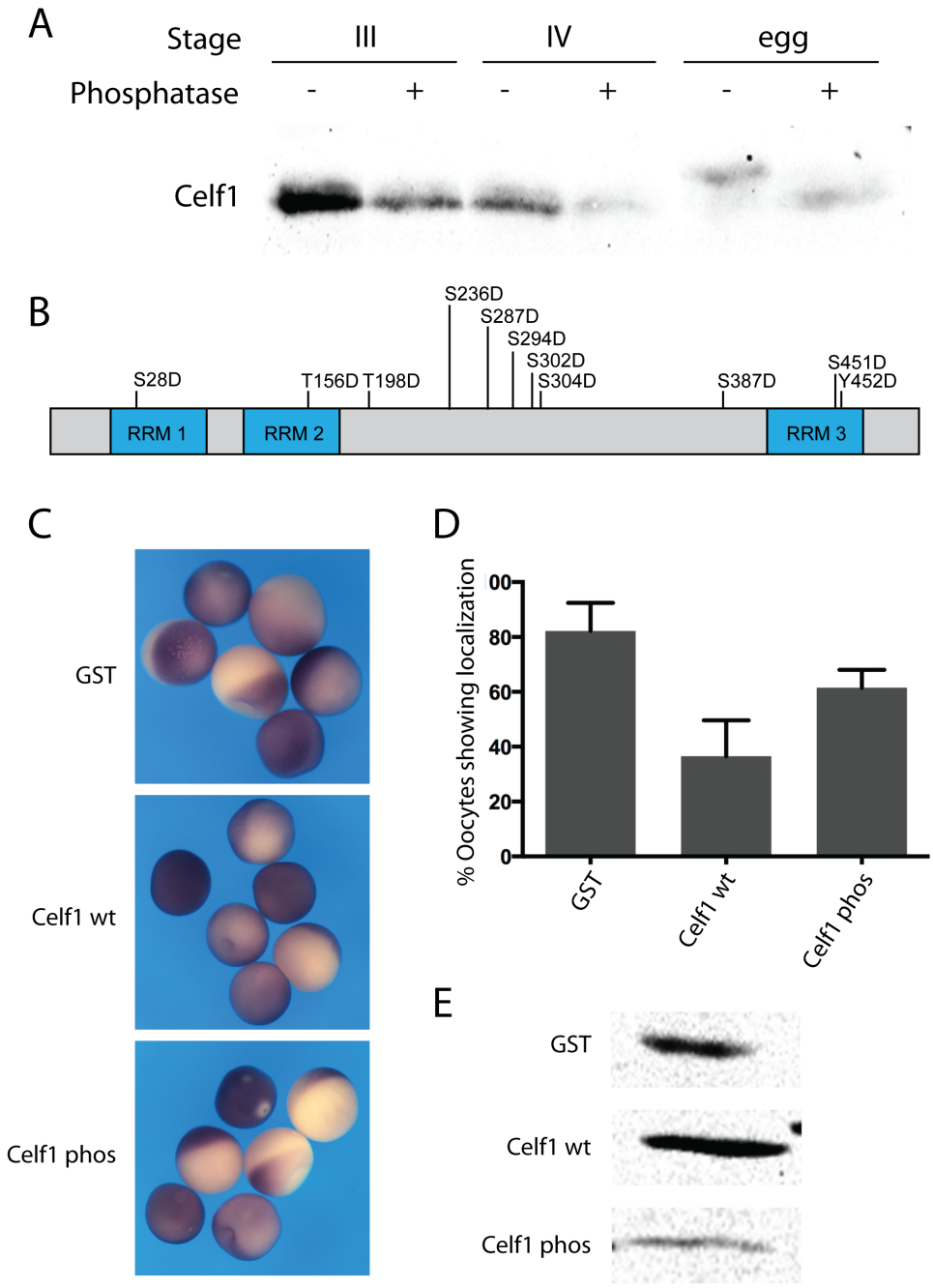

Figure S5. **A phospho-mimetic Celf1 mutant does not affect vegetal localization of *dnd1*-LE.** A) Comparison of endogenous Celf1 electrophoretic mobility in untreated and phosphatase treated oocytes extracts. Celf1 was detected by Western blot using equivalent amounts of oocyte extracts of indicated stages. B) Schematic presentation of the phospho-mimetic Celf1 mutant. Potentially phosphorylated serines (S), threonines (T) or tyrosine (Y) as predicted by the Scansite motif scan program (Obenauer et al., 2003) and the NetPhos 2.0 Server (Blom et al., 1999) were substituted for aspartic acid (D). C) Stage III oocytes pre-injected with RNA encoding Flag-tagged wild-type (wt) Celf1, the phospho-mimetic mutant (Celf1 phos) or GST were injected with *lacZ-dnd1*-LE RNA; localization was detected by whole mount *in situ* hybridization against *lacZ*. D) Quantification of *lacZ-dnd1*-LE localization efficiency. Average values of two independent experiments are shown. Error bars indicate standard error of the mean. E) Expression control of Flag-tagged proteins. Equivalent amounts of respective oocyte extracts were analyzed by anti-Flag Western blotting.

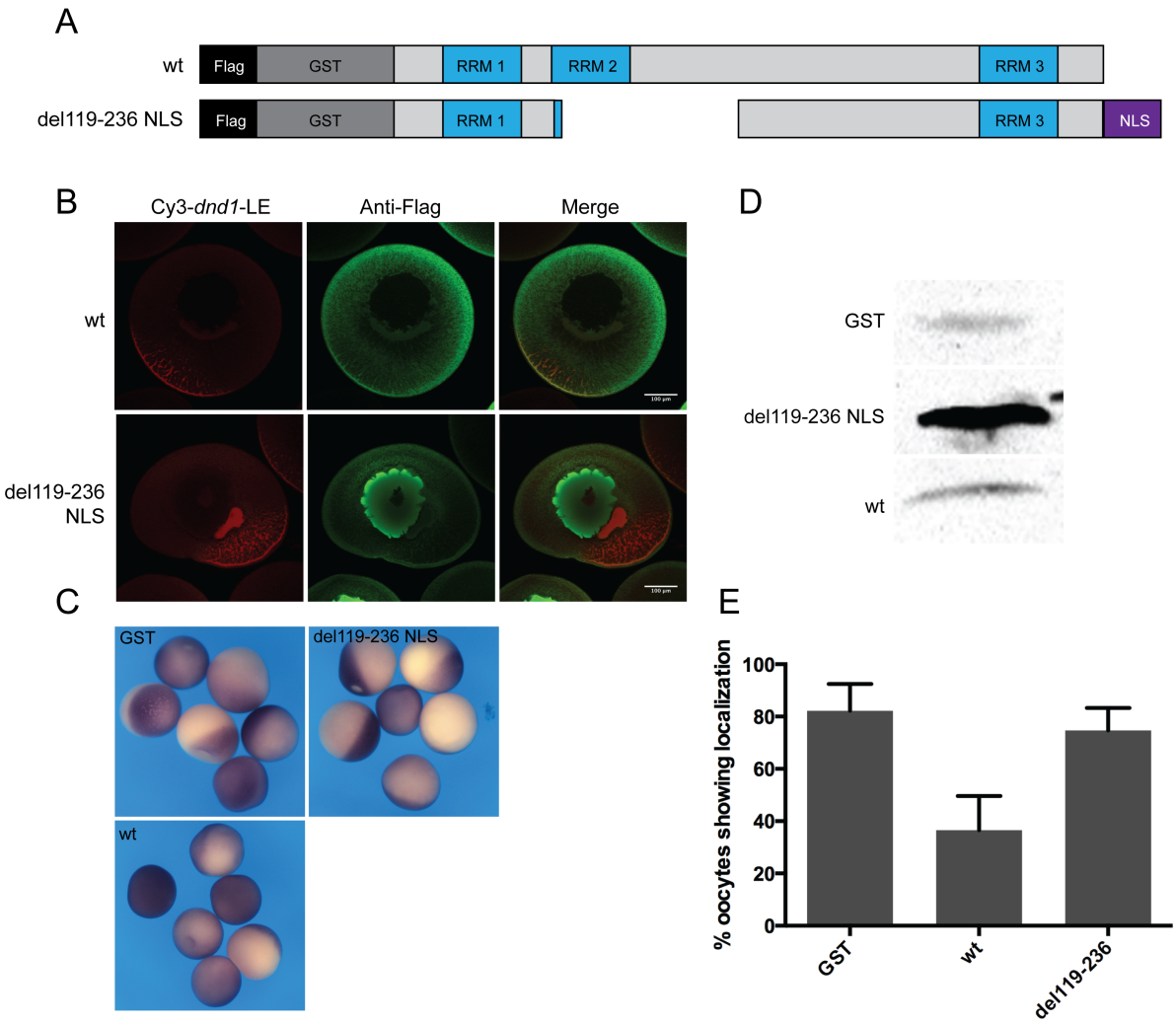

Figure S6. **A mutant version of Celf1 trapped in the nucleus does not affect vegetal localization of *dnd1*-LE.** A) Schematic presentation of wild-type (wt) Celf1 and a mutant version that lacks amino acids 119-236 (del119-236) fused to a nuclear localization signal (NLS). B) Stage III oocytes pre-injected with RNA encoding Flag-tagged wild-type (wt) Celf1 or the mutant version that lacks amino acids 119-236 (del119-236) were injected with Cy3-*dnd1*-LE RNA. After anti-Flag immunostaining of oocytes, RNA and protein signals were detected by confocal imaging. C) Stage IV oocytes pre-injected with RNA encoding Flag-tagged Celf1 wild-type (wt), or the mutant version lacking amino acids 119-236 (del119-236) were injected with *lacZ-dnd1*-LE RNA and RNA localization was detected by whole mount *in situ* hybridization. D) Expression control of Flag-tagged proteins. Equivalent amounts of respective oocyte extracts were analyzed by anti-Flag Western blotting. E) Quantification of *lacZ-dnd1*-LE localization efficiency. Average values of three independent experiments are shown, error bars indicate standard error of the mean.

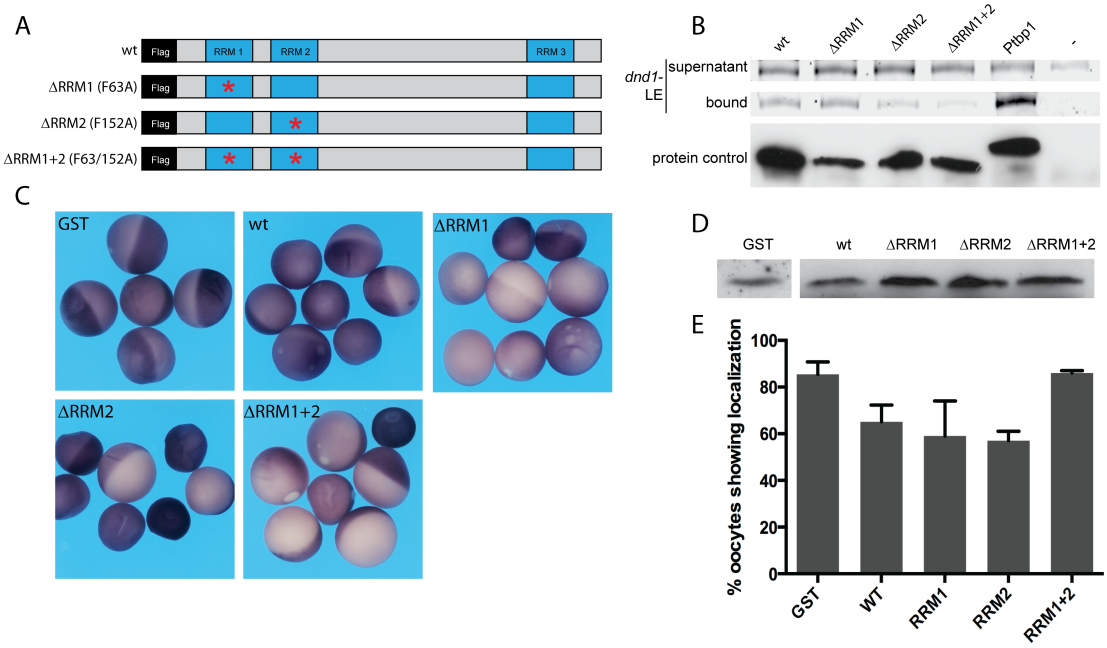

Figure S7. **Mutant versions of Celf1 with reduced RNA affinity moderately affect vegetal localization of *dnd1*-LE.** A) Schematic presentation of wild-type (wt) Celf and mutant versions with point mutations that convert phenylalanine (F) 63 and/or 153 to an alanine (A) in RRM1, RRM2 or RRM1 and 2. B) *In vitro* interaction analysis of wild-type (wt) Celf1, versions with point mutations in RRM1, RRM2 or RRM1 and 2 and Ptbp1 (positive control) with Cy3-*dnd1*-LE. Unprogrammed reticulocyte lysate served as negative control (-). RNAs were separated by urea-PAGE and detected by fluorescence imaging. The expression control for *in vitro* translated Flag-tagged proteins detected by anti-Flag Western blotting is depicted below. C) Stage IV oocytes pre-injected with RNA encoding Flag-tagged Celf1 wild-type (wt), mutant versions with point mutations in RRM1, RRM2 or RRM1 and 2 or GST were injected with *lacZ-dnd1*-LE RNA and RNA localization was detected by whole mount *in situ* hybridization. D) Expression control of Flag-tagged proteins. Equivalent amounts of respective oocyte extracts were analyzed by anti-Flag Western blotting. E) Quantification of *lacZ-dnd1*-LE localization efficiency. Average values of two to three independent experiments are shown. Error bars indicate standard error of the mean.

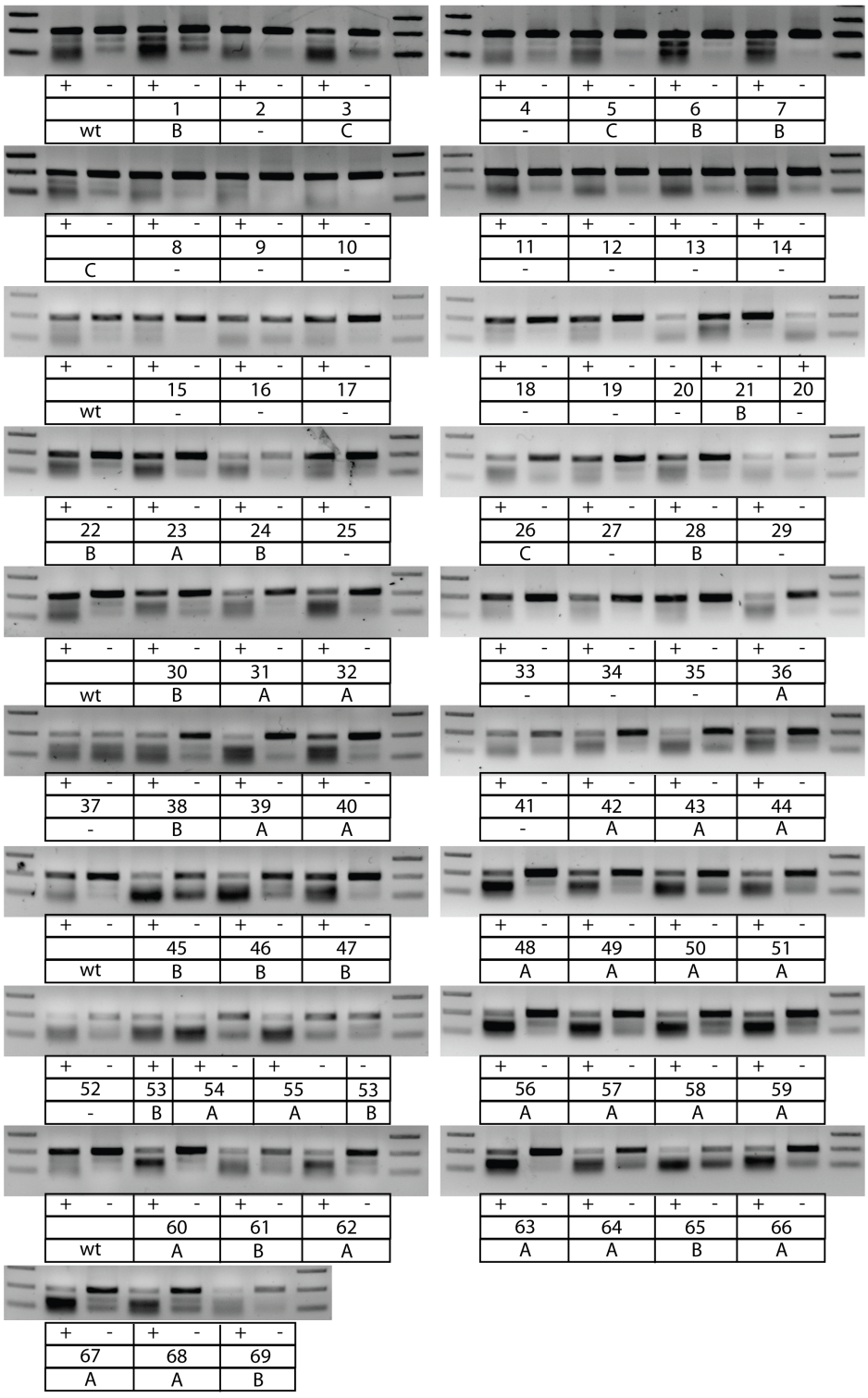

Figure S8. **Identification of somatic mutation rates of CRISPR/Cas treated zebrafish by Endonuclease I assay (batch 1).** The 400 bp CRISPR/Cas target region in the *celf1* gene (exon 4) was amplified from fin DNA of injected zebrafish. PCR products 1-21 were from fish injected with sgRNA against target 1, PCR products 22-47 were from fish injected with sgRNA against target 2, PCR products 48-69 were from fish injected with sgRNA against target 3. PCR products were treated with T7 Endonuclease I and treated (+) as well as untreated (-) DNA fragments were separated by agarose electrophoresis. PCR products of wild-type (wt) zebrafish served as controls. Somatic mutation rates of individual fish were classified as high (A), intermediate (B), low (C) or not detectable (-) by visual inspection of the digested DNA fraction.

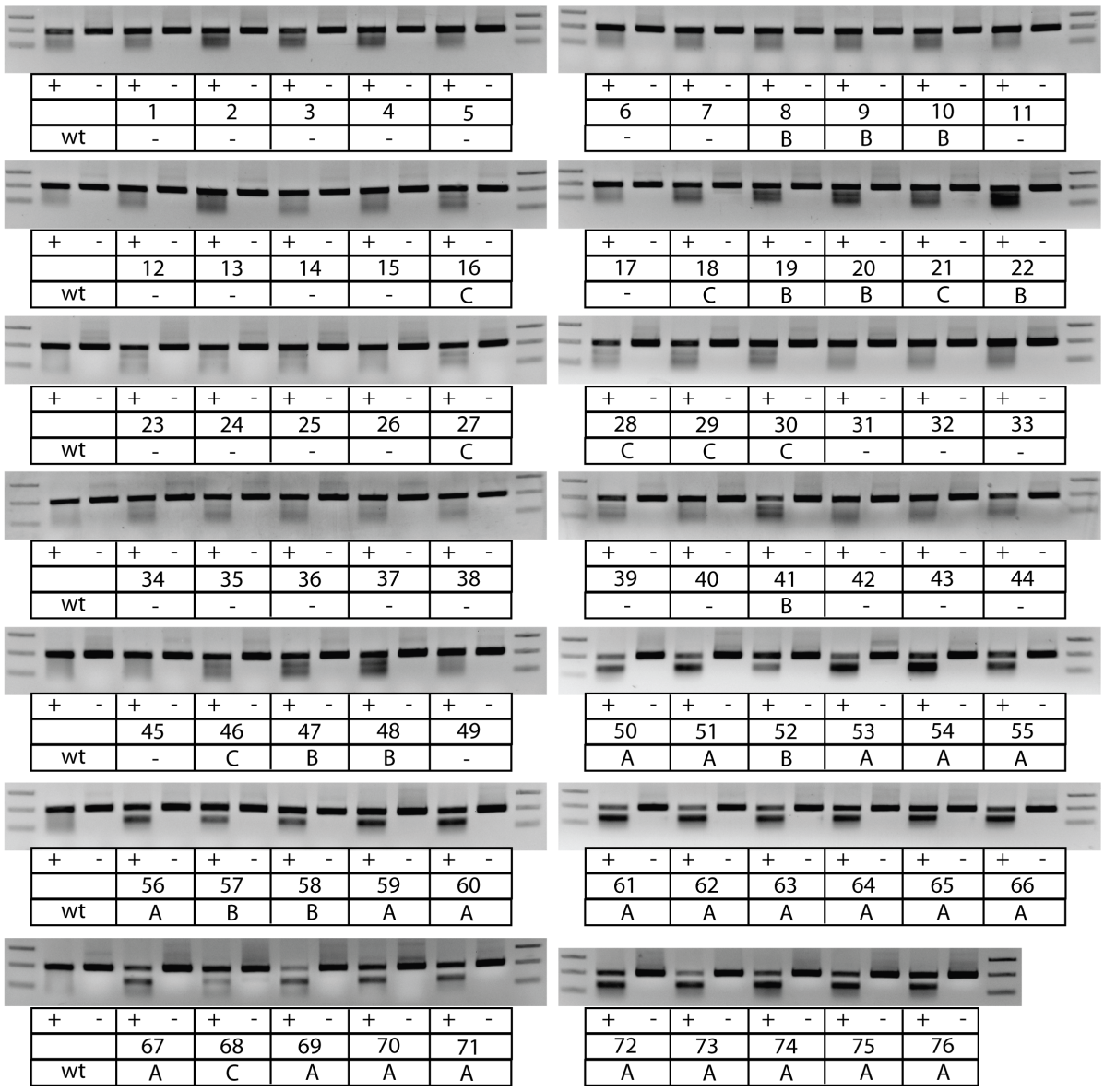

Figure S9. **Identification of somatic mutation rates of CRISPR/Cas treated zebrafish by Endonuclease I assay (batch 2).** The 400 bp CRISPR/Cas target region in the *celf1* gene (exon 4) was amplified from fin DNA of injected zebrafish. PCR products 1-49 were from fish injected with sgRNA against target 1, PCR products 50-76 were from fish injected with sgRNA against target 2. PCR products were treated with T7 Endonuclease I and treated (+) as well as untreated (-) DNA fragments were separated by agarose electrophoresis. PCR products of wild-type (wt) zebrafish served as controls. Somatic mutation rates of individual fish were classified as high (A), intermediate (B), low (C) or not detectable (-) by visual inspection of the digested DNA fraction.

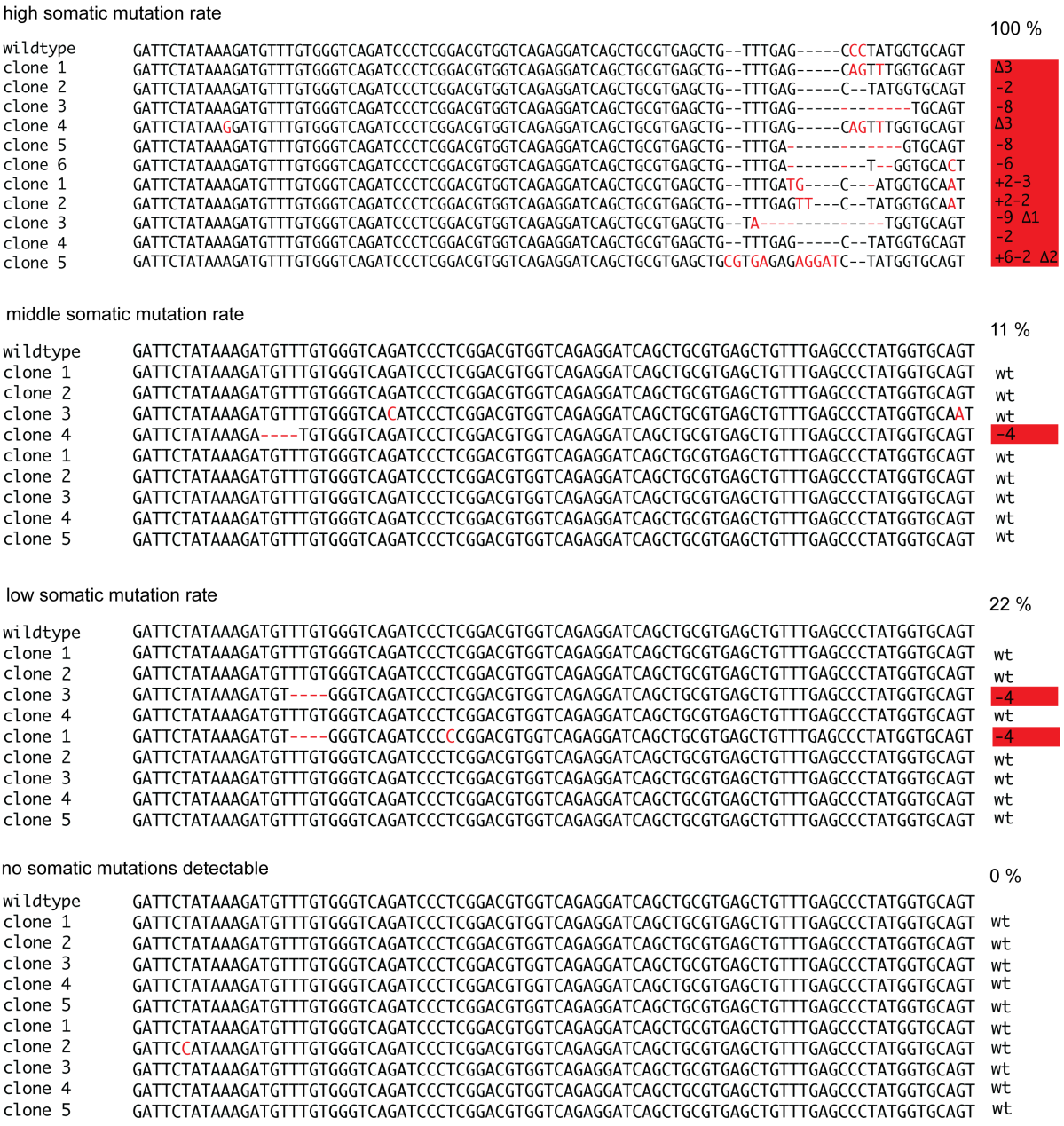

Figure S10. **Verification of somatic mutation rates of CRISPR/Cas injected zebrafish obtained by T7 endonuclease I assay.** The 400 bp CRISPR/Cas target region in the *celf1* gene (exon 4) was amplified from fin DNA of two zebrafish from each category (high, middle, low, no detectable mutation rate). PCR products were cloned and 4-6 clones per fish were sequenced. Sequences corresponding to both fish of each category were aligned with a wild-type sequence on the top. Shown are nucleotides 40-124 of exon 4 covering all three CRISPR/Cas target sites. Deletions are shown as red dashes and base substitutions and insertions are shown as red letters. The change in length caused by mutations is indicated to the right of each sequence (+, insertion; –, deletion; Δ, substitution; wt, no change). Sequences containing mutations are marked by red boxes. Percentages of mutated sequences per category are indicated above.

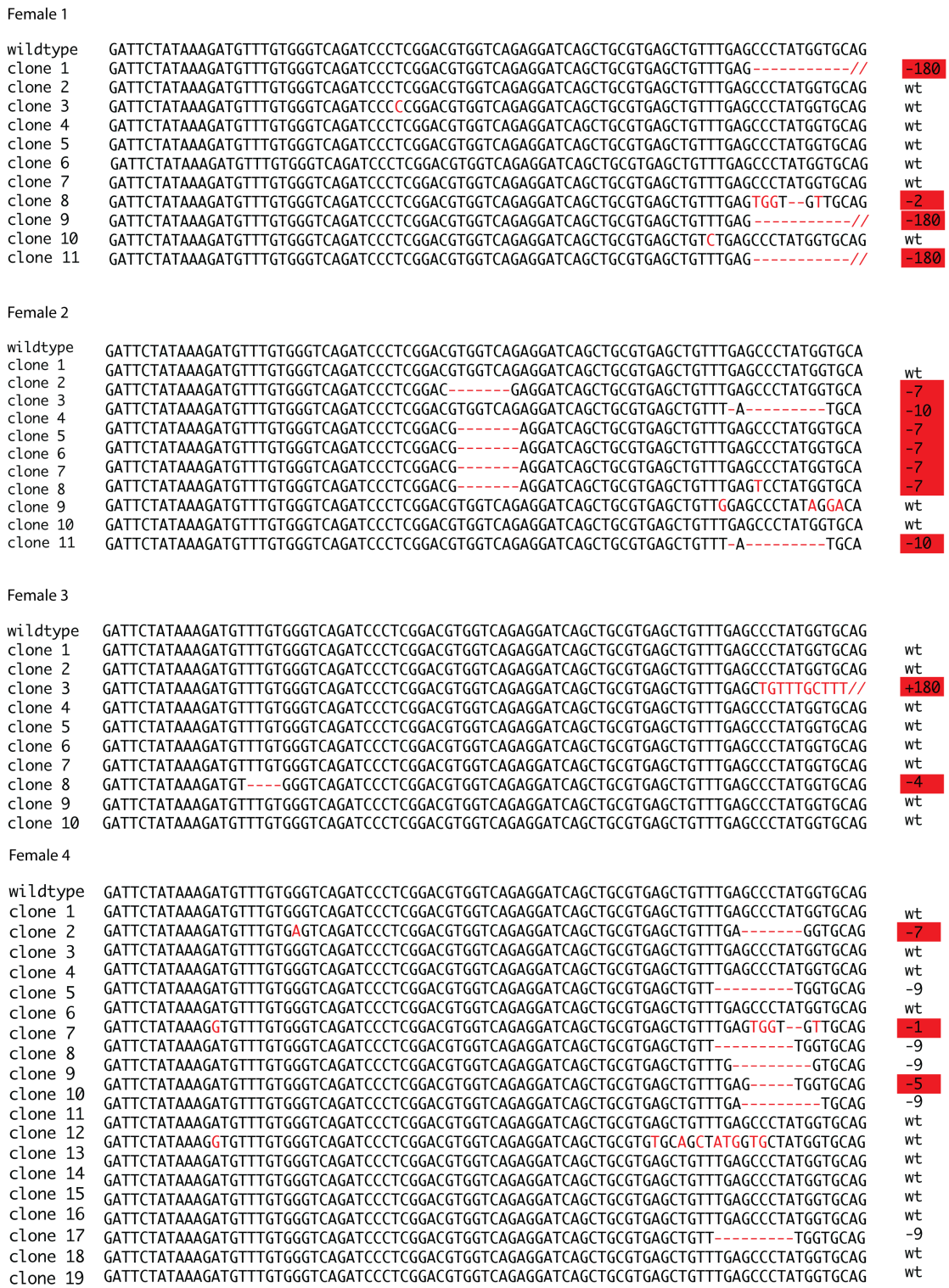

Figure S11. Germline mutations in the *celf1* gene of CRISPR/Cas treated female zebrafish 1-4. The 400 bp CRISPR/Cas target region in the *celf1* gene (exon 4) was amplified from fin DNA of female zebrafish 1-4 showing a high somatic mutation rate. PCR products were cloned and 10-19 clones were sequenced. Sequences corresponding to one fish were aligned with a wild-type sequence on the top. Shown are nucleotides 40-124 of exon 4 covering all three CRISPR/Cas target sites. Deletions are shown as red dashes and base substitutions and insertions are marked by red letters. The change in length caused by mutations is indicated to the right of each sequence (+, insertion; –, deletion; no change in length, wt). Mutations that cause non-sense or miss-sense mutations are boxed in red.

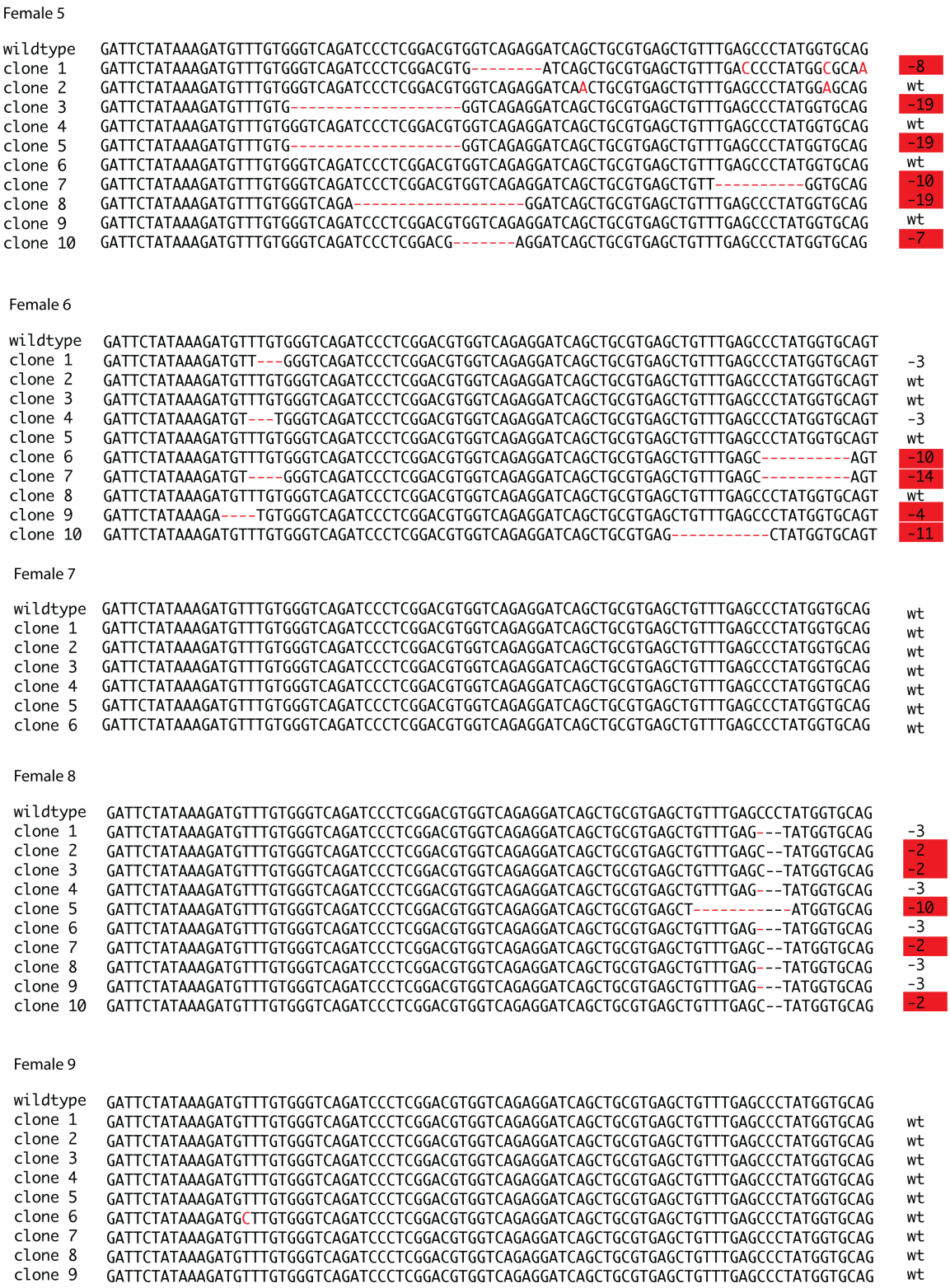

Figure S12. Germline mutations in the *celf1* gene of CRISPR/Cas treated female zebrafish 5-9. see figure S11 legend.

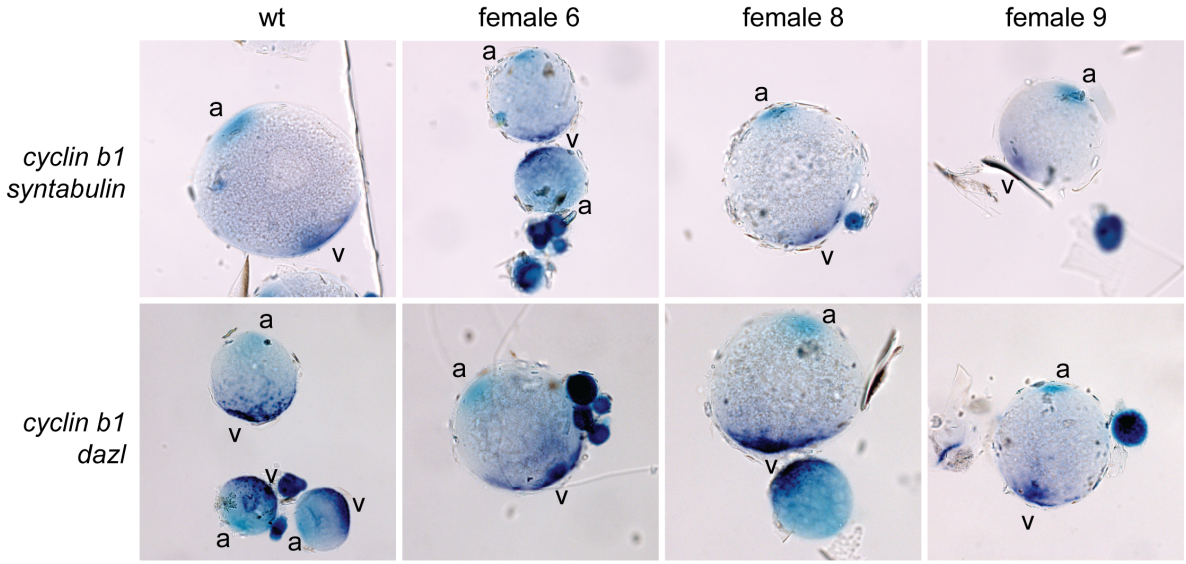

Figure S13. **Moderate *celf1* germline mutation rates do not affect vegetal localization of *syntabulin* and *dazl* mRNAs in zebrafish oocytes.** Stage I-III oocytes of wild-type (wt) and CRISPR/Cas treated zebrafish showing *celf1* germline mutations (female 6, 8) or showing no *celf1* germline mutations (female 9) were analyzed for vegetal localization of *dazl* or *syntabulin* (dark blue) by WMISH. Co-staining of animal localizing *cyclin b1* (light blue) served as marker for the animal pole. Animal (a) and vegetal (v) poles of oocytes are indicated in stage II-III oocytes.

Table S1. Genes, accession numbers, target regions and target sequences for all genes analyzed by Nanostring nCounter analyses

Gene symbol	former gene name	Accession No	Target Region	Target Sequence
actb	b-actin	NM_001088953.1	1179-1279	ATGCTTCTAAAGGACAGACCCTTTCAACATGAACAAATGTA CCTGTGCAGGAAGATCACATTGGCATGGCTTTACTCTTTTG TTGGCGCTTGGCTCAGAA
adap1	ArfGAP	NM_001094747.1	567-667	AACCTTTTAAAGCGAGGGAGAGATAATGGACAGTACCTGCC TAGAAAGTTTGTCCTGTCCGAAATAGATGGCACCTTAAAATA CTTCACAAAGCCTGATG
bicc1	Bic-c	NM_001088527.1	30-130	GGGACACTAGCGGCGCGCGCAGGCGGAGAGGAGTCAGT CGGTGAGTGAGTGCGCGGGGCAGGGAGTGAGTTGGACTT GCGCTTCTCTCCCGACTCTGAGC
ccna1	Cyclin A1	NM_001094201.1	1528-1628	GCTTGCTGTGGGATCAATAGTCTGCAAGCACTTTAGTTAGA TGTACTACTACAAATCGGAACCCTGTGATCAGAGCTGATTT GCACTGACTAACTGACAC
ccnb2	Cyclin B2	NM_001087799.1	228-328	CAGTCTTCCAATGCTGTGGCAAAGCCTTCAAAGATGGCAG CAACTAAAGTGGCAAATGTTAAGACTAAGCATGTACCTGTG AAACCAGTTGTAGCTGAAG
cdh1	xE-cadherin	NM_001172232.1	1029-1129	GGAGAATTTGGGAAAGATCGCACAACAACTGCTACAGCTTT AATCGTTGTGATGGACACTAACGATAATCCTCCAGTGTTTG ACCCCACACAATACACGG
cdh3	xC-cadherin	U04707.1	3324-3424	TGCTGAGTGATGCAACGCCTCTGTACGTTTTTGGAAATAAA AATTGTGGAATACGGTGGGTCAGCAAAACGCCTCTTTGCT GTCTGCATCAGCGTTTATT
cdk5r2	Cdk5r2	NM_001095906.1	94-194	CCGACCTGCTCAACATACATCGATTCCTTCGTACGTCTTGC GCACAGTGAACTGTCTGACGCAGTCATTTAACGCAGGTAAT AACGAGGGGTTGCTTTAT
chek1	Chk1	NM_001088570.1	335-435	AGATTTTATGGACATCGAAGGGAAGGCAACATTCAGTACCT CTTTCTGGAGTATTGTCGAGGTGGTGAGCTCTTTGATCGCA TAGAGCCTGATGTTGGAA
cpeb1-a	CPEB1a	NM_001090603.1	1704-1804	GCAGCACTCTATGGAAATCCTGCGCCACCACCGCCCTCTC ATGCGTAATCAGAAAAGTCGTGACTCCAGCTAAAGACATTG GAACAACATTGGTCCAAAA
dazap2	DAZAP2	NM_001092534.1	3296-3396	TGGCCACTAATAGGTGGCTATAAGGCATTACGCTAATGACCT CATTTGCAGAATCTAAAGTTTGAACCTGCACAGGGCTTGCC AATTCACATGTAACCAT
dazl	Dazl	NM_001088303.1	722-822	CCTATTGATCAGACAGTGTCTGCTTCTGGAGCCAATCCACA GAAGAGATATGTGGAAATGAGTACCCAGACTATTGTATCCT GCTTGTTTGATCCAGCAA
ddx25	Dead South	NM_001088548.1	541-641	TATCCACAGTGCATCTGTCTTAGTCCTACATTTGAACTGGCT TTGCAGACTGGGAAAGTCGTTGAAGAGATGGGGAAGTTCT GTGCTGGAATTGAAGTCA
ddx4	XVLG1	NM_001088259.1	1912-2012	TACCGGTCGCTGTGGTAACACCGGAAAGGCAACATCATTTT TCAATGTTCAGGATGACCATGTGATTGCTCGTCCCCTTGTG AAAATTCTTACCGATGCT
dnd1	Xdead end	AY971581.1	324-424	TGATGATGACATTTAGTGGCCTGAATCGAGGGTTCGCTTAT GCTCGCTATATAAGCAGACGGCAGGCTATCAGCGCTATTAT GTCTCTTAACGGTTTTGA
flrt1	fibronectin receptor	NM_001092942.1	1089-1189	CAGCGAATTGCAGATGATACATTTAGCCGTCTCCAAAACCTA TCCGAGCTTTCCTTGGTCCGAAATTCGTTGGCTGCCCCTC CAGTCAATCTGCCCAGTG
fn1	Fibronectin 1	NM_001087801.1	3973-4073	CCCCAACTGACTGACATAAAGTATGATGATGTAACTGACAC GAGCATTGACCTGAGGTGGACGCCCCTTAATTCCTCCAACA TTATTGGCTACCGAATCA
fyn	Fyn	NM_001085608.1	649-749	ATTGCTCTCTTTTGGGAACCCAAGGGGTACTTATCTAATACG TGAAAGTGAAACAACCAAAGGTGCCTATTCCTTGTCTATTC GTGACTGGGATGATATG
g6pd	G6PDH	NM_001086550.1	862-962	GTGGAGGATACTTTGACGAATTTGGCATCATCCGGGATGTC ATGCAAAATCACTTGCTCCAAATGATGTGTTTGATGGCTATG GAGAAGCCGGTCTCCAC
gapdh	GapDH	NM_001087098.1	773-873	ACCTGCCGCCTGCAGAAGCCGGCCAAGTACGATGACATCA AGGCCGCCATTAAGACTGCATCAGAGGGCCCAATGAAGGG AATCCTGGGATACACACAAG

gdf1	Vg1	NM_001095591.1	459-559	TCTGCGTCTCTATCGCACATTACAGATCACGCTTAAAGGGA TGGGAAGAAGCAAAACAAGCAGAAAGCTGTTGGTGGCCCA AACTTTCCGTCTTCTGCAT
germes	germes	NM_001089043.1	1791-1891	GCCCATAGGTGCACAAGTTTGGATTCATCTAGTCAACCAAG TAACTACTTTCCTGTTGATTCTGTAATGAAGCTAGAAAGCTG TGAACTTGGCATGTCTG
gk	GK	NM_001087171.1	1244-1344	TTGAAGCTGTGTGTTTCCAGACTAGAGAGATTCTGGATGCT ATGAACCAAGATTGTGGCATTCCTCTCAATCAACTTCAGGT TGATGGGGGTATGACAAG
grip2	Grip2	NM_001097913.1	4644-4744	CATTGCCCAAGAACCTTTGTAGGAGCTGTAGATATGTTACAT CTGAAGAGTCACATGTTGGGGAACCCTTATCTTTAAGTTAA GGCACATAGCCCTTCTA
gs17	GS17	NM_001088064.1	71-171	GGATTTCTTGGCCTTGGCTGGCCGTGGAGGTCCTCATTAT GCCAGTCCAACTTCAAGGCATCCCTCACCAAAGGTTTGGA ATTCAACACCACCTTCCCTT
hist1h4a	H4	NM_001094457.1	129-229	GGAGAGGGGGAGTCAAGCGCATCTCTGGCCTCATCTATGA GGAGACTCGTGGGGTCCTCAAGGTTTTCCTGGAGAATGTC ATCCGGGACGCCGTCACCTA
hprt1	HPRT	NM_001096766.1	233-333	CTGTGTGTCCTGAAGGGTGGCTATAAGTTCTTTGCTGATCT ACTTGACTACATTAAAGCACTTAACCGCAACAGTGACAAGT CTATCCCTATGACAGTAG
kif13b	Kif13b	NM_001145074.1	2780-2880	AGTGCATGGTGGTTTTTGACCACTGCAAAGAGTTTGCTGTG AACATTACAGAAGACTTCTTAGAATATCTTTCTGAGGGGGC CCTGGCCATTGAGGTTTA
lefty-a	Lefty A	NM_001085745.1	1371-1471	TGTGTGCCCTACTATCACCATCTTGCCTTACTGACAAGTGTT ACTACTATAGGTGCTGCTGCACATTAAAAAAAGTTGCCTTCC CCAGACTTTATCTGCT
lefty-b	Lefty B	NM_001088574.1	1084-1184	TGGCGGAGTTCCCTAATATGATTGTCGAAAAATGCGGTTGC ACAATGGACAATATCGCTATCATATGACAGATGGCAGCACTA AGTTCATGCAGATCCGG
lmnb1	laminB1	NM_001086584.1	2140-2240	CAGGTCCTGGAGTGAAATATCTCTGCGATTGCTTCTCCACT TGTCTCACTTCAGACACCTTACCCCGAGGTGCTTCACCTTC TCCATTTCCCTCGCTTCC
nanos1	Xcat2	NM_001088034.1	627-727	CCCGGGGCCAAGCGGTGCCCATCCCCATGTACCGGACATT CCAGCTCTCCAGAGACGCTCCAGCCTGGGCCCGCCCGCC CTCTAATTATTTTATTTACTG
nek2	Nek2b	AB019557.1	1143-1243	CAAGCCGCCCTAGAAAATGGCATAGGTATGAGAGCCAACA GAAGGCCTTTGGAGCCCCGGAATGAATGGAGCAAATTCTA ATGTTTTTTGTTTCTGTGGG
nif	XNIF	NM_001090817.1	701-801	AGTCCAGACAGCACTACGTACCCTTCCTGCCCATAACATTG GATGCTTTCACCGTACAGCGTTCTTTACTGGCGGCACCAAT TCCGCAAAGTATAGAGCA
odc1	ODC	NM_001086698.1	855-955	GGATATAATTGGTGTGAGTTTCCATGTTGGCAGTGGCTGCA CTGATCCACAGACTTATGTACAAGCTGTCTCAGATGCACGA TGTGTCTTTGACATGGGG
pgam1	Pgam1	NM_001093340.1	1263-1363	AATTTGACACTCTGGGTTAGTACTGTATGATATATCTGGGAT TTCAAGGGTAAGTTAGGTCAGTTGCCAGTGTGTGGAGATGT AATGGTTTGAGGATCAA
pgat	Xpat	NM_001087463.1	1209-1309	ACTGATCTGTAGCATGCACTAATGTGTTGAGGAGTGATAAG ACTTTCACGCACTGGGTGTTGTATCACATAACAAAGCAGAT TGCGAGGAATGGTTTCAT
plin2	fatvg	NM_001088491.1	1272-1372	TGCAAGACTTTTCCCGTTTGAATGGCAGAGTAGTAAACAGG GACATAAGTTAGTAACAGACTGAACATTTCTTCTCCCTCCCT TGGGTGTTAACTATACC
plk3	plk3	AF357841.1	535-635	CTGGAAAGCTCGGCACACACTACTAGAACCAGAAGTGCGG TATTTTTTGAAACAGATCATTTCTGGATTGAAGCATTTGCAC CTTAAAGGCATCCTGCAC
prdm1	PRDM1	NM_001087104.1	3748-3848	CCTTCCTCTAAACCCATGCCGAAATAACCAGGAAAGGTACA AACTTTACAGCTTTAAAAGATCCATGTAGTCCACACGCAGG CCATGGTCTGACTTTATG
ldlrap1	PTB	NM_001089091.1	2818-2918	TACCAATGGCTTCATAAATAAATATGGTTTAAAAGCCACAGG TAAACAGATGGAGGCTACAGATTGACTATCCTTCATGTATTA GTTCAGTTTGGGAAAC
rtn3	Rtn3	NM_001094076.1	1306-1406	TTTTAGGGACACAAAGTTGCACTCTCTCTCCGTGTGCCTCA CGTTCTGTCTCCTCTACTTGCACCATGAAGAGTCTACACAA GAGTCCCCAAAATTCTGT

spire1	Eg6/Spire2	NM_001093074.1	406-506	ACATGGAACGCGTCTTAAGTGAGCCCCTAGATAAACTTCTG TACGGAATGCTGGGCCTCCATGACATCACTATGGACTACAA CCTACATTTTCAGTGTCC
sybu	Syntabulin	NM_001093953.1	2645-2745	AGCTTGTGTATTCTCGGCTTGAAGTTGTGTGAGCGCTATCT GTGATTCCCTGTGTGAACTGTCTTGTTTCCTTGGCAACCCG CGTACGTTACAGCATGTC
trim36	Trim36/Haprin	NM_001091117.1	2663-2763	ATGGCTGCTGTGTTGGTTCTAAAGCAACGTTTGCAGCTGG ACTATGTGATGCTCTGGGCAATAGTCTGAGGCCTATGAGCT GCTCTTATCAAATATTCTA
vegt	VegT	NM_001088196.1	1789-1889	AGAAGAGAACCCGGGAAAGCAGTTATGGATTTATAGAACAA AGTAATGGGGCCATGAACAGAAGCAGTTTTCTCTTGACTTT AAGTGGTGGTACAGCCAT
velo1	Velo1	NM_001089216.1	406-506	GAATGTGCTTCTAAAAAGCAACATAGTTCAGACGGTAAAGG CTGTGATGGAGGAAATGTAGTCTATCTTTCTTCTGGCATTAG CAGCACCGGAAACGAAA
velo1 isoform	Velo1 isoform	AY280865.1	601-701	GCCCAATACAGAAACATGCCTCCAGGAAGCTATGCATATGA GAAAGAGGAGGAAAAGCTCAAAAGAAAACCCCTGGGACA GCTGTTGAAGAATACTGGGT
wasl	NWASP	NM_001091383.1	140-240	AGAGATCCCCTGCCAACACTAATCATGAGTAACAATATCGG CCCTCACAACAACAACAACAGGCCGACTAAAAGACTGTCA AACAGCGGCTCCATACTGC
wnt11b	Xwnt11	NM_001090858.1	768-868	TACGGCCTTAACATGGGCTCTGCTTTTGTTGACGCTCCAAT GAAGTCAAGCAAGTCTGCTGGGACCCAGGCCACTAAAATT ATGAATCTACACAACAATG
wnt8a	Wnt8	NM_001088168.1	125-225	GTCAGTCAATAACTTTCTGATGACAGGACCCAAGGCATATC TGACATACTCAGCGAGTGTTGCCGTGGGTGCGCAGAATGG AATTGAGGAGTGTAAATAT

Table S2. Raw expression data (counts) for all RNAs analyzed by Nanostring nCounter in experiment 1

	Experiment 1								
Stage	8	8	8	11	11	11	14	14	14
***tia1* RNA (pg)**	-	200	400	-	200	400	-	200	400
actb	18.613	22.123	21.346	20.471	20.371	17.296	45.774	50.681	63.634
adap1	188	165	141	355	443	331	1.428	1.583	1.726
bicc1	540	601	646	439	448	498	115	119	134
ccna1	6.939	7.022	7.079	2.398	2.512	2.709	41	75	63
ccnb2	10.027	10.196	9.638	4.962	5.212	5.358	1.247	1.328	1.606
cdh1	101	29	103	1.789	2.004	1.643	4.127	4.835	5.231
cdh3	1.881	2.121	2.090	1.900	2.012	1.691	1.217	1.379	1.609
cdk5r2	1.948	2.037	2.018	818	702	935	17	56	72
chek1	6.509	5.711	5.515	2.033	1.859	2.171	796	807	998
cpeb1-a	5.550	6.337	6.314	1.342	1.446	1.770	29	73	158
dazap2	378	375	370	390	381	324	705	709	671
dazl	1.395	1.235	1.339	565	581	727	110	171	271
ddx25	3.767	2.828	3.093	2.018	1.846	2.099	433	473	724
ddx4	1.758	1.530	1.499	1.303	1.281	1.184	1.590	1.480	1.801
dnd1	3.801	2.944	3.109	868	1.038	1.678	57	244	895
fn1	1.583	2.584	2.271	2.168	2.348	1.558	2.290	2.208	2.614
fyn	403	459	434	219	255	214	142	151	174
g6pd	1.027	1.132	1.186	859	851	829	332	369	455
gapdh	550	627	583	312	283	329	179	202	158
gdf1	12.904	10.497	11.394	5.345	5.055	6.397	264	668	1.547
germes	1.668	1.104	1.339	328	474	689	52	117	293
gk	826	744	726	326	294	361	152	157	152

grip2	1.379	1.211	1.311	862	746	883	74	102	200
gs17	232	119	227	981	1.008	925	139	137	196
hist1h4a	102.120	82.587	87.865	161.607	168.810	172.856	112.154	96.823	106.821
hprt1	2.374	2.101	2.032	896	891	1.140	668	661	706
kif13b	509	486	516	387	331	361	94	111	155
lefty-a	149	55	173	878	658	866	96	93	75
lefty-b	125	91	187	654	586	620	83	108	83
lmnb1	1.064	1.157	1.159	1.049	1.110	1.049	1.355	1.421	1.458
nanos1	175	172	196	122	116	168	39	25	67
nek2	2.456	2.740	2.475	638	639	719	90	86	120
nif	2.194	2.799	2.829	2.264	2.237	1.838	540	638	881
odc1	12.012	11.983	12.082	13.562	13.554	12.049	26.404	25.825	29.150
pgam1	3.713	3.460	3.458	1.880	1.611	1.896	127	153	249
pgat	3.001	2.583	3.089	2.536	1.863	2.265	987	958	1.315
plin2	2.094	1.977	2.010	898	1.001	938	608	337	577
plk3	7.942	9.425	9.327	4.550	4.675	4.775	1.054	1.698	2.494
prdm1	51	31	62	855	950	798	437	550	510
ldlrap1	7.219	6.021	5.965	3.550	3.382	3.440	933	870	936
rtn3	779	956	1.070	839	727	764	402	380	514
spire1	1.739	2.093	2.174	734	688	749	31	56	85
sybu	900	811	828	278	234	311	40	54	58
trim36	565	502	592	205	181	235	84	90	86
vegt	5.231	5.799	6.155	11.165	11.784	10.519	931	1.370	2.228
velo1	4.392	5.049	4.826	1.868	1.572	1.847	79	118	125
velo1 isoform	2.053	2.189	2.137	751	664	694	27	32	54
wasl	1.389	1.581	1.522	1.150	1.204	1.034	612	680	821
wnt11b	1.793	1.703	1.985	2.261	2.706	2.291	1.315	2.299	3.720
wnt8a	166	78	131	1.742	1.644	1.633	772	737	1.057
NEG_A	4	5	5	11	8	4	4	2	5
NEG_B	5	5	2	3	3	1	5	4	3
NEG_C	7	7	1	2	1	3	5	6	5
NEG_D	2	2	4	4	9	3	7	3	8
NEG_E	3	4	4	3	3	5	7	6	7
NEG_F	10	10	6	3	4	7	5	8	7
NEG_G	2	3	2	1	2	2	1	1	1
NEG_H	3	1	1	1	3	3	1	2	1
POS_A	11.146	13.686	13.245	12.890	13.175	13.037	12.934	16.216	13.215
POS_B	4.862	5.972	5.905	5.650	5.609	5.311	5.500	6.475	5.590
POS_C	1.474	1.772	1.743	1.656	1.645	1.568	1.587	1.861	1.682
POS_D	319	391	356	358	366	344	387	426	390
POS_E	45	53	51	39	48	44	52	60	48
POS_F	21	29	40	39	42	30	34	33	34

Table S3. Raw expression data (counts) for all RNAs analyzed by Nanostring nCounter in experiment 2

	Experiment 2								
Stage	8	8	8	11	11	11	14	14	14
***tia1* RNA (pg)**	-	200	400	-	200	400	-	200	400
actb	20.290	20.278	20.591	17.201	16.969	17.219	37.386	47.625	57.648
adap1	22	35	36	156	124	160	921	1.036	958
bicc1	517	558	454	415	499	499	82	97	89
ccna1	6.757	6.975	7.036	1.660	1.882	1.421	31	29	32
ccnb2	8.997	9.250	9.290	3.512	3.745	3.554	1.160	970	1.118
cdh1	35	69	53	1.407	1.420	1.480	3.228	4.703	4.082
cdh3	1.827	1.779	1.777	1.840	1.801	1.842	1.272	1.285	1.515
cdk5r2	1.864	1.692	1.660	542	620	506	16	14	27
chek1	4.633	4.446	4.432	1.160	1.278	1.069	639	729	685
cpeb1-a	5.639	5.799	5.725	982	999	1.017	30	49	110
dazap2	382	358	373	361	391	362	561	606	557
dazl	903	793	654	425	439	385	134	135	154
ddx25	3.203	2.648	2.320	1.985	1.551	1.588	651	565	578
ddx4	1.645	1.652	1.622	1.176	1.090	1.218	1.339	1.331	1.324
dnd1	3.358	3.137	2.811	981	1.331	1.497	105	479	670
fn1	1.712	1.728	1.773	2.075	1.782	2.195	3.106	2.965	3.034
fyn	359	359	389	173	183	200	143	143	159
g6pd	1.038	1.062	1.048	840	756	825	316	344	424
gapdh	595	522	522	307	292	303	180	209	172
gdf1	4.919	4.517	4.179	1.458	1.966	1.584	139	192	259
germes	2.273	1.869	1.648	679	628	713	97	209	302
gk	440	394	322	191	173	159	187	204	154
grip2	1.471	1.064	801	852	747	708	142	166	214
gs17	162	242	197	958	1.035	930	82	37	54
hist1h4a	95.988	112.163	108.857	170.659	175.508	176.211	107.944	77.763	86.788
hprt1	2.646	2.643	2.750	1.005	1.013	1.069	492	588	571
kif13b	441	452	340	390	390	338	120	105	118
lefty-a	103	213	143	827	650	608	150	91	82
lefty-b	140	170	133	506	493	438	102	92	78
lmnb1	1.143	1.107	1.124	1.110	1.163	1.087	1.403	1.530	1.593
nanos1	238	205	160	193	160	163	69	87	89
nek2	2.223	2.304	2.191	370	436	406	89	106	137
nif	1.895	2.057	2.022	1.722	1.826	1.803	560	616	715
odc1	10.996	11.068	11.235	12.335	12.039	12.359	26.343	28.919	30.210
pgam1	3.893	3.818	3.612	1.268	1.319	1.041	82	110	124
pgat	4.172	3.295	2.561	2.840	2.160	2.280	1.589	1.199	1.132
plin2	2.586	2.659	2.760	1.111	1.233	937	404	372	465
plk3	6.514	6.707	6.384	2.745	2.892	3.055	920	1.504	2.247
prdm1	26	47	41	833	754	813	541	565	579
ldlrap1	5.924	5.987	5.695	2.933	3.005	2.432	787	587	582
rtn3	794	739	605	665	608	624	325	400	335
spire1	1.868	1.845	1.636	668	592	448	45	25	53
sybu	825	736	621	256	239	186	29	36	50
trim36	517	522	439	201	194	146	88	81	101
vegt	6.023	6.393	5.321	10.123	11.232	10.072	1.001	916	1.505
velo1	5.627	5.255	5.051	1.863	1.739	1.501	90	88	97

velo1 isoform	2.189	2.131	2.007	633	632	505	26	33	31
wasl	1.075	1.106	1.177	765	756	810	525	552	584
wnt11b	1.430	1.616	1.241	2.066	2.182	2.355	1.393	2.217	3.075
wnt8a	158	187	116	1.862	1.696	1.738	833	911	1.107

Table S4. Average fold changes over uninjected controls of two experiments

	Average fold changes over uninjected controls									Standard deviation								
Stage	8	8	8	11	11	11	14	14	14	8	8	8	11	11	11	14	14	14
***tia1* RNA (pg)**	-	200	400	-	200	400	-	200	400	-	200	400	-	200	400	-	200	400
actb	1,0	1,1	1,1	1,0	1,0	0,9	1,0	1,2	1,5	0,0	0,1	0,1	0,0	0,0	0,1	0,0	0,1	0,1
adap1	1,0	1,5	1,5	1,0	1,0	1,0	1,0	1,1	1,1	0,0	0,9	1,1	0,0	0,3	0,1	0,0	0,0	0,1
bicc1	1,0	1,1	1,0	1,0	1,1	1,2	1,0	1,1	1,2	0,0	0,0	0,2	0,0	0,1	0,0	0,0	0,1	0,0
ccna1	1,0	1,0	1,0	1,0	1,1	1,0	1,0	1,4	1,4	0,0	0,0	0,0	0,0	0,1	0,2	0,0	1,0	0,4
ccnb2	1,0	1,0	1,0	1,0	1,1	1,0	1,0	0,9	1,1	0,0	0,0	0,1	0,0	0,0	0,0	0,0	0,2	0,2
cdh1	1,0	1,3	1,4	1,0	1,1	1,0	1,0	1,3	1,3	0,0	1,5	0,5	0,0	0,1	0,1	0,0	0,2	0,0
cdh3	1,0	1,1	1,0	1,0	1,0	0,9	1,0	1,1	1,3	0,0	0,1	0,1	0,0	0,1	0,1	0,0	0,1	0,1
cdk5r2	1,0	1,0	1,0	1,0	1,0	1,0	1,0	3,3	7,0	0,0	0,1	0,1	0,0	0,2	0,1	0,0	4,7	2,7
chek1	1,0	0,9	0,9	1,0	1,0	1,0	1,0	1,1	1,2	0,0	0,1	0,1	0,0	0,1	0,1	0,0	0,1	0,1
cpeb1-a	1,0	1,1	1,1	1,0	1,0	1,2	1,0	2,7	6,9	0,0	0,1	0,1	0,0	0,0	0,2	0,0	0,9	1,3
dazap2	1,0	1,0	1,0	1,0	1,0	0,9	1,0	1,0	1,0	0,0	0,0	0,0	0,0	0,1	0,1	0,0	0,1	0,0
dazl	1,0	0,9	0,8	1,0	1,0	1,1	1,0	1,3	1,9	0,0	0,0	0,2	0,0	0,0	0,3	0,0	0,4	1,0
ddx25	1,0	0,8	0,8	1,0	0,8	0,9	1,0	1,0	1,3	0,0	0,1	0,1	0,0	0,1	0,2	0,0	0,2	0,6
ddx4	1,0	0,9	0,9	1,0	1,0	1,0	1,0	1,0	1,1	0,0	0,1	0,1	0,0	0,0	0,1	0,0	0,0	0,1
dnd1	1,0	0,9	0,8	1,0	1,3	1,7	1,0	5,0	13,1	0,0	0,1	0,0	0,0	0,1	0,3	0,0	0,0	8,4
fn1	1,0	1,3	1,2	1,0	1,0	0,9	1,0	1,0	1,1	0,0	0,4	0,3	0,0	0,2	0,2	0,0	0,0	0,1
fyn	1,0	1,1	1,1	1,0	1,1	1,1	1,0	1,0	1,2	0,0	0,1	0,0	0,0	0,1	0,1	0,0	0,1	0,1
g6pd	1,0	1,1	1,1	1,0	0,9	1,0	1,0	1,1	1,4	0,0	0,1	0,1	0,0	0,1	0,0	0,0	0,0	0,0
gapdh	1,0	1,0	1,0	1,0	0,9	1,0	1,0	1,1	0,9	0,0	0,2	0,1	0,0	0,0	0,0	0,0	0,0	0,1
gdf1	1,0	0,9	0,9	1,0	1,1	1,1	1,0	2,0	4,0	0,0	0,1	0,0	0,0	0,3	0,1	0,0	0,8	2,9
germes	1,0	0,7	0,8	1,0	1,2	1,6	1,0	2,4	5,1	0,0	0,1	0,1	0,0	0,4	0,8	0,0	0,2	2,4
gk	1,0	0,9	0,8	1,0	0,9	1,0	1,0	1,1	0,9	0,0	0,0	0,1	0,0	0,0	0,2	0,0	0,0	0,1
grip2	1,0	0,8	0,7	1,0	0,9	0,9	1,0	1,3	2,3	0,0	0,1	0,3	0,0	0,0	0,1	0,0	0,2	1,0
gs17	1,0	1,0	1,1	1,0	1,1	1,0	1,0	0,7	1,0	0,0	0,7	0,2	0,0	0,0	0,0	0,0	0,5	0,6
hist1h4a	1,0	1,0	1,0	1,0	1,0	1,1	1,0	0,8	0,9	0,0	0,3	0,2	0,0	0,0	0,0	0,0	0,1	0,1
hprt1	1,0	0,9	0,9	1,0	1,0	1,2	1,0	1,1	1,1	0,0	0,1	0,1	0,0	0,0	0,1	0,0	0,1	0,1
kif13b	1,0	1,0	0,9	1,0	0,9	0,9	1,0	1,0	1,4	0,0	0,1	0,2	0,0	0,1	0,1	0,0	0,3	0,5
lefty-a	1,0	1,3	1,3	1,0	0,8	0,9	1,0	0,8	0,6	0,0	1,3	0,2	0,0	0,0	0,2	0,0	0,3	0,2
lefty-b	1,0	1,0	1,2	1,0	0,9	0,9	1,0	1,1	0,9	0,0	0,4	0,4	0,0	0,1	0,1	0,0	0,3	0,2
lmnb1	1,0	1,0	1,0	1,0	1,1	1,0	1,0	1,1	1,1	0,0	0,1	0,1	0,0	0,0	0,0	0,0	0,0	0,0
nanos1	1,0	0,9	0,9	1,0	0,9	1,1	1,0	0,9	1,7	0,0	0,1	0,3	0,0	0,1	0,4	0,0	0,5	0,4
nek2	1,0	1,1	1,0	1,0	1,1	1,1	1,0	1,1	1,5	0,0	0,1	0,0	0,0	0,1	0,0	0,0	0,2	0,2
nif	1,0	1,2	1,2	1,0	1,0	0,9	1,0	1,1	1,5	0,0	0,1	0,2	0,0	0,1	0,2	0,0	0,1	0,3
odc1	1,0	1,0	1,0	1,0	1,0	0,9	1,0	1,0	1,1	0,0	0,0	0,0	0,0	0,0	0,1	0,0	0,1	0,0
pgam1	1,0	1,0	0,9	1,0	0,9	0,9	1,0	1,3	1,8	0,0	0,0	0,0	0,0	0,1	0,1	0,0	0,1	0,3
pgat	1,0	0,8	0,8	1,0	0,7	0,8	1,0	0,9	1,0	0,0	0,1	0,3	0,0	0,0	0,1	0,0	0,2	0,4
plin2	1,0	1,0	1,0	1,0	1,1	0,9	1,0	0,7	1,1	0,0	0,1	0,1	0,0	0,0	0,1	0,0	0,3	0,2
plk3	1,0	1,1	1,1	1,0	1,0	1,1	1,0	1,6	2,4	0,0	0,1	0,1	0,0	0,0	0,0	0,0	0,0	0,1
prdm1	1,0	1,4	1,6	1,0	1,0	1,0	1,0	1,2	1,1	0,0	1,3	0,5	0,0	0,1	0,0	0,0	0,2	0,1

ldlrap1	1,0	0,9	0,9	1,0	1,0	0,9	1,0	0,8	0,9	0,0	0,1	0,1	0,0	0,1	0,1	0,0	0,1	0,2
rtn3	1,0	1,1	1,1	1,0	0,9	0,9	1,0	1,1	1,2	0,0	0,2	0,4	0,0	0,0	0,0	0,0	0,2	0,2
spire1	1,0	1,1	1,1	1,0	0,9	0,8	1,0	1,3	2,5	0,0	0,2	0,3	0,0	0,0	0,3	0,0	1,4	1,6
sybu	1,0	0,9	0,8	1,0	0,9	0,9	1,0	1,4	2,0	0,0	0,0	0,1	0,0	0,1	0,3	0,0	0,1	0,7
trim36	1,0	0,9	0,9	1,0	0,9	0,9	1,0	1,0	1,1	0,0	0,1	0,1	0,0	0,1	0,3	0,0	0,1	0,1
vegt	1,0	1,1	1,0	1,0	1,1	1,0	1,0	1,2	2,0	0,0	0,0	0,2	0,0	0,0	0,0	0,0	0,4	0,6
velo1	1,0	1,0	1,0	1,0	0,9	0,9	1,0	1,3	1,4	0,0	0,2	0,1	0,0	0,1	0,1	0,0	0,4	0,4
velo1 isoform	1,0	1,0	1,0	1,0	0,9	0,9	1,0	1,4	2,1	0,0	0,1	0,1	0,0	0,1	0,1	0,0	0,1	0,7
wasl	1,0	1,1	1,1	1,0	1,0	1,0	1,0	1,1	1,2	0,0	0,1	0,0	0,0	0,0	0,1	0,0	0,0	0,2
wnt11b	1,0	1,0	1,0	1,0	1,1	1,1	1,0	1,7	2,5	0,0	0,1	0,2	0,0	0,1	0,1	0,0	0,1	0,4
wnt8a	1,0	0,8	0,7	1,0	0,9	0,9	1,0	1,0	1,4	0,0	0,5	0,0	0,0	0,0	0,0	0,0	0,1	0,0

List of figures

List of tables

Publications

Bauermeister, D., Claussen, M., Pieler, T., 2014. Biochemical Aspects of Subcellular RNA Transport and Localization, in: V.A. Erdmann, W.T. Markiewicz, J. Barciszewski (Eds.), Chemical Biology of Nucleic Acids. Springer Berlin Heidelberg, pp. 293-308.